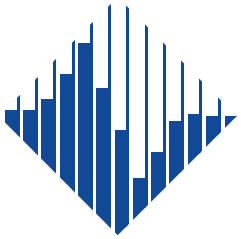

PACIFIC EARTHQUAKE ENGINEERING
RESEARCH CENTER

Development of NGA-Sub Ground-Motion Model of 5%-Damped Pseudo-Spectral Acceleration Based on Database for Subduction Earthquakes in Japan

Hongjun Si
Seismological Research Institute Inc.
Tokyo, Japan

Saburoh Midorikawa
Tokyo Institute of Technology
Tokyo, Japan

Tadahiro Kishida
Civil Infrastructure and Environmental Engineering
Khalifa University
Abu Dhabi, UAE

PEER Report No. 2020/06

Pacific Earthquake Engineering Research Center
Headquarters at the University of California, Berkeley
December 2020

PEER 2020/06
December 2020

Development of NGA-Sub Ground-Motion Model of 5%-Damped Pseudo-Spectral Acceleration Based on Database for Subduction Earthquakes in Japan

Hongjun Si
Seismological Research Institute Inc.
Tokyo, Japan

Saburoh Midorikawa
Tokyo Institute of Technology
Tokyo, Japan

Tadahiro Kishida
Civil Infrastructure and Environmental Engineering
Khalifa University
Abu Dhabi, UAE

PEER Report No. 2020/06

Pacific Earthquake Engineering Research Center
Headquarters at the University of California, Berkeley
December 2020

ABSTRACT

Presented within is an empirical ground-motion model (GMM) for subduction-zone earthquakes in Japan. The model is based on the extensive and comprehensive subduction database of Japanese earthquakes by the Pacific Engineering Research Center (PEER). It considers RotD50 horizontal components of peak ground acceleration (PGA), peak ground velocity (PGV), and 5%-damped elastic pseudo-absolute acceleration response spectral ordinates (PSA) at the selected periods ranging from 0.01 to 10 sec. The model includes terms and predictor variables considering tectonic setting (i.e., interplate and intraslab), hypocentral depths (D), magnitude scaling, distance attenuation, and site response. The magnitude scaling derived in this study is well constrained by the data observed during the large-magnitude interface events in Japan (i.e., the 2003 Tokachi-Oki and 2011 Tohoku earthquakes) for different periods. The developed ground-motion prediction equation (GMPE) covers subduction-zone earthquakes that have occurred in Japan for magnitudes ranging from 5.5 to as large as 9.1, with distances less than 300 km from the source.

ACKNOWLEDGMENTS

NGA-Sub was supported by FM Global, the U.S. Geological Survey, the California Department of Transportation, and the Pacific Gas and Electric Company. This support is gratefully acknowledged. The opinions, findings, conclusions or recommendations expressed in this publication are those of the authors and do not necessarily reflect the views of the sponsors

Any opinions, findings, and conclusions or recommendations expressed in this material are those of the authors and do not necessarily reflect those of PEER or the Regents of the University of California.

CONTENTS

LIST OF TABLES

LIST OF FIGURES

1 Overview

Ground-motion prediction equations (GMPEs) are widely used because they are simple and practical for seismic hazard assessment. In Japan, the pioneering work on GMPEs was conducted by Kanai [1961]. Since then, many GMPEs have been developed whenever strong-motion records from large earthquakes have been obtained. The initial generation of GMPEs consisted simple equations with parameters of magnitude, hypocentral distance, and soil type. Recent GMPEs adopt additional parameters such as earthquake type, focal depth, and physical site parameters. By incorporating updated seismological knowledge and strong-motion records, continuous refinement of GMPEs is an on-going effort.

Presented within is a GMPE of peak ground acceleration (PGA), peak ground velocity (PGV), and pseudo-spectral acceleration (PSA) for subduction-zone earthquakes in Japan. The model is based on the NGA-sub database by the Pacific Engineering Research Center (PEER), which is currently the most extensive and comprehensive subduction database of Japanese earthquakes [Kishida et al. 2018]. Construction of the model entailed a three-step approach.

First, the site effects were eliminated from the records. Shallow-soil amplifications were obtained using a semi-empirical model developed by Seyhan and Stewart [2014], with modification of nonlinear terms. This modification is based on amplification models from strong-motion records in Japan [Midorikawa and Hori 2018]. Basin amplifications were derived from strong-motion records. Ground-motion parameters at reference-rock sites were calculated by dividing the PSA at ground surface by the shallow soil and basin amplifications.

Second, path effects were eliminated from ground-motion parameters at reference-rock sites. Per Midorikawa and Ohtake [2004], different attenuation models were used for shallow- versus deep-focus earthquakes.

Third, source effects were examined using ground-motion parameters at reference-rock sites where path effects had been removed. Based on findings by Si et al. [2016] and Ibrahim et al. [2016], a piecewise linear model was used for magnitude scaling. Dependences of earthquake type and of focal depth were also evaluated. Finally, this GMPE was constructed by combining the site terms in Step 1, the path terms in Step 2, and the source terms in Step 3.

2 Analyzed Ground-Motion Data

This study analyzed the NGA-Sub Database for Japan. The database covers a wide range of Japanese subduction-zone earthquakes. Moment magnitude (**M**) ranged from 3.9 to 9.1. The closest distance from the rupture to the station (*ClstD*) ranged from 8 to 2300 km. The database includes RotD50 values of the PGA, PGV, and PSA from 0.01 sec to 10 sec at 108 periods. This study selected those earthquake events that met the general selection criteria and project requirements.

- The event had a **M** greater than 5.5, with records from obtained from at least three stations within *ClstD* that were less than 100 km (backarc counts) from the epicenter.
- When the event was recorded as an aftershock, the **M** should be at least smaller by 2.0 compared to the mainshock.

Figure 2.1 shows the epicenter locations of the events analyzed in this study. In addition, this study collected the depth of the Mohorovičić discontinuity (Moho) at hypocenter locations from J-SHIS website (*http://www.j-shis.bosai.go.jp/map/*). These data were used to judge whether the hypocenter was located below the Moho or not. Past studies have demonstrated that the upward seismic wave shows transmission loss at the Moho [Midorikawa and Ohtake 2004, Joshi and Midorikawa 2005]. The GMPE developed in this study considered this effect.

After selecting the events meeting the above criteria, the time series were selected based on the following conditions:

- The time series were recorded in the forearc regions when the hypocenter was located in the forearc region;
- All time series were considered when hypocenter was located in the backarc region; and
- The *ClstD* is less than the specified values in Table 2.1.

The criteria in Table 2.1 were designed to eliminate the influence of long-distance data on the regression parameters. If the criteria in Table 2.1 is not applied, the weight of the data within the specified distance becomes smaller since the number of records rapidly increases with distance.

The application of the above criteria resulted in 4038 recordings from 71 earthquakes, with the *ClstD* ranging from 13 to 300 km, and the **M** ranging from 5.5 to 9.1; see Figure 2.2. By using these data, this study developed the GMPEs for PGA, PGV, and 5%-damped PSA for periods of 0.01, 0.02, 0.03, 0.05, 0.075, 0.1, 0.15, 0.2, 0.25, 0.3, 0.4, 0.5, 0.75, 1, 1.5, 2, 3, 4, 5, 7.5, and 10 sec for RotD50 values.

Table 2.1 **Time series selection criteria for distance cutoff depending on M.**

M	*ClstD* (km)
M > 7.0	< 300
6.5 < **M** < 7.0	< 200
6.3 < **M** < 6.5	< 150
M < 6.3	< 100

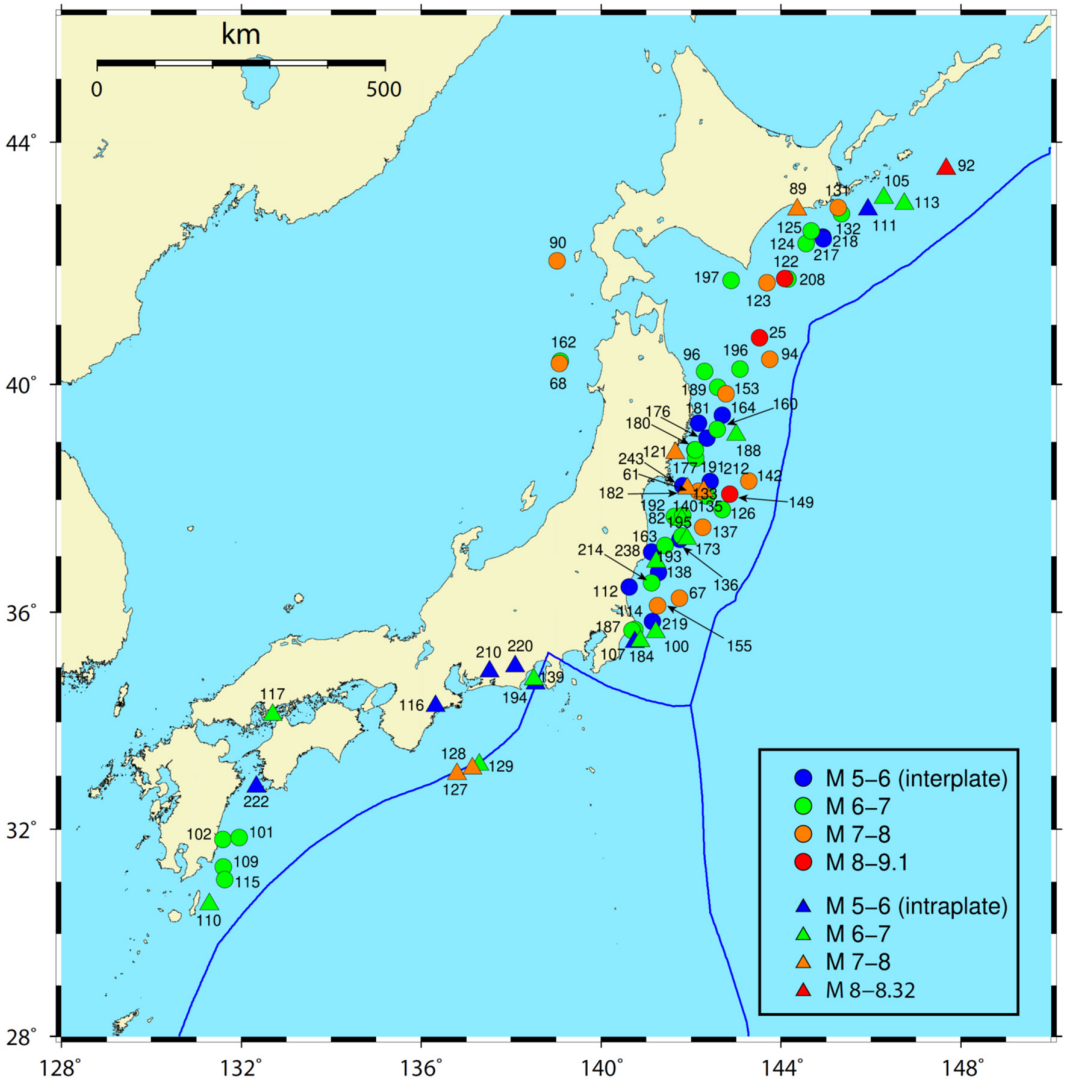

Figure 2.1 **Epicenter locations of the analyzed events. Old event IDs in NGA-Sub flatfile are listed next to the epicenter locations.**

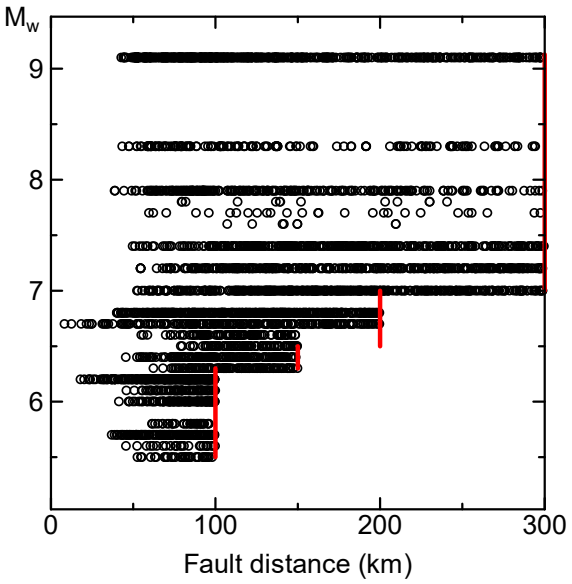

Figure 2.2 **Distribution of the fault distance and M for the analyzed ground-motion recordings.**

3 Ground-Motion Model

This section describes the development of the GMM. The functional forms used in the NGA-Sub GMPE were originally developed by Si and Midorikawa [2000]. Site effects were calculated by using the model by Seyhan and Stewart [2014] after adjusting the parameters for nonlinear soil behaviors [Midorikawa and Hori 2018].

3.1 REGRESSION ANALYSIS APPROACH

Development of this model was done in three phases. In the first phase, strong-motion data were converted to the reference site by eliminating the site effects. In the second phase, ground-motion attenuations were fitted by the functional form, where the parameters related to the distance attenuation were fixed, based on the past studies [Midorikawa and Ohtake 2004] to obtain the parameters related to source characteristics. In the third phase, these parameters were regressed against **M**, earthquake type, and hypocentral depth (D) by assigning different weights depending on the number of recordings for each event. By smoothing the regression results among different periods, the GMPE was developed.

3.2 SITE RESPONSE EFFECTS

First, the site response effects were removed from strong ground-motion recordings. The reference site condition was selected at "engineering bedrock," which has the shear-wave velocity (V_s) of 760 m/sec (V_{ref}). By expressing site response effect as $G(T)$, its effects can be split into two parts:

$$G(T) = G_s(T) + G_d(T) \tag{3.1}$$

where $G_s(T)$ and $G_d(T)$ are shallow-soil response and basin response terms, respectively.

3.2.1 Shallow-Soil Response Term

Seyhan and Stewart [2014] developed the model for $G_s(T)$; see reference for more detail. The model was adopted in the GMPE by Boore et al. [2014]. The following equation shows the shallow-soil response model.

$$G_s(T) = \ln\left[F_{lin}(T)\right] + \ln\left[F_{nl}(T)\right] \tag{3.2}$$

where F_{lin} and F_{nl} represent the linear and nonlinear site amplifications, respectively, defined by the following equations:

$$\ln\left[F_{lin}\left(T\right)\right]=\begin{cases} c(T)\ln\left(\dfrac{V_{s30}}{V_{\text{ref}}}\right) & V_{s30}\le V_c(T) \\ c(T)\ln\left[\dfrac{V_c(T)}{V_{\text{ref}}}\right] & V_{s30}>V_c(T) \end{cases} \tag{3.3}$$

$$\ln\left[F_{nl}\left(T\right)\right]=f_1+f_2(T)\ln\left[\frac{\text{PGA}_r(T)+f_3}{f_3}\right] \tag{3.4}$$

$$f_2(T)=0.5f_4\left[\exp\left\{f_5(T)\cdot\left[\min\left(V_{s30},760\right)-360\right]\right\}-\exp\left\{f_5(T)\cdot\left(760-360\right)\right\}\right] \tag{3.5}$$

The c in Equation (3.3) determines the linear shallow-soil response with V_{s30} referenced to V_{ref} = 760 m/sec. When the V_{s30} is greater than V_c, the F_{lin} becomes constant, where the V_c is the period-dependent variable. Equation (3.4) determines the nonlinear site response depending on the PGA at V_{ref} (PGA$_r$). The f_1 and f_3 are constant values of 0 and 0.1g, respectively. The f_2 in Equations (3.4) and (3.5) controls the nonlinear effects of shallow-soil responses in which the f_4 and f_5 are parameters.

Midorikawa and Hori [2018] suggested using the model of $G_s(T)$ in a similar functional form for strong-motion records in Japan. Figure 3.1(a) and (b) compare these models at short and intermediate periods. The model by Midorikawa and Hori [2018] shows smaller soil nonlinear effects compared to those in Seyhan and Stewart [2014] for these period ranges. Based on these comparisons, this study adopted the model by Seyhan and Stewart [2014] but reduced the parameter f_4 in Equation (3.5) by half from the original model to match the observations by Midorikawa and Hori [2018]. Herein, the adjusted model for shallow-soil response by Seyhan and Stewart [2014] is called the "Modified Seyhan and Stewart Model."

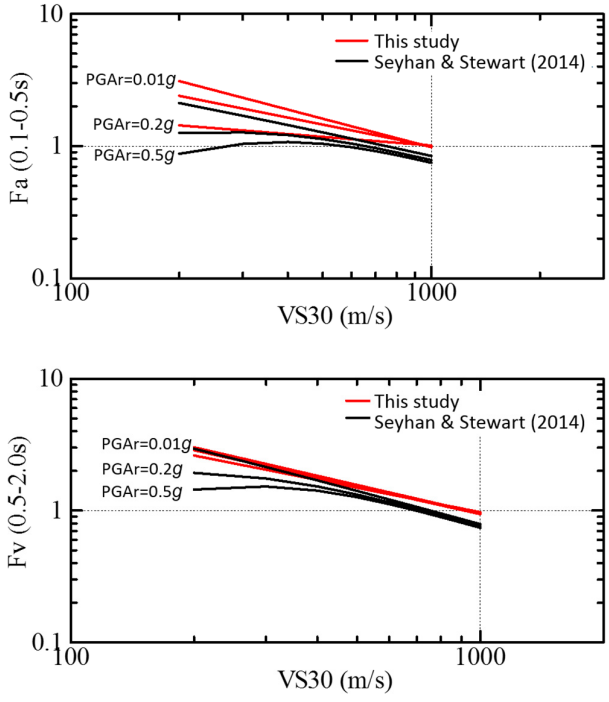

Figure 3.1 **Comparison of shallow soil response models by Midorikawa and Hori [2018] and Seyhan and Stewart [2014] for period ranges of (a) 0.1–0.5 sec, and (b) 0.5–2.0 sec.**

3.2.2 Basin Response Term

Figure 3.2 shows a flowchart of the model $G_d(T)$ in Equation (3.1). First, the $G_s(T)$ was removed from all the recorded PSA(T) for $T \geq 1.0$ sec. The $G_s(T)$ was calculated from Equations (3.2)–(3.4) by using the PGA_r approximated by the recorded PGA divided by the F_{lin}. Second, these data were fitted by the following equation for each earthquake to remove the path effects.

$$\log_{10} A(T) = b(T) + g(T, X) - k(T)X \tag{3.6}$$

where

$$g(T,X) = \begin{cases} -\log_{10}\left[X + C(T)\right] & D \leq \text{Moho depth or } X < 1.7D \\ 0.6\log_{10}[1.7D + C(T)] - 1.6\log_{10}[X + C(T)] & D > \text{Moho depth and } X \geq 1.7D \end{cases} \tag{3.7}$$

$$C(T) = \begin{cases} 0.0055 \cdot 10^{0.5M} & T < 0.3\,\text{sec} \\ [0.000810 - 0.00897\log_{10}(T)] \cdot 10^{0.5M} & 0.3\,\text{sec} \leq T \leq 0.6\,\text{sec} \\ 0.0028 \cdot 10^{0.5M} & T > 0.6\,\text{sec} \end{cases} \tag{3.8}$$

$$k(T) = \begin{cases} 0.003 & T < 0.3\,\text{sec} \\ 0.00126 - 0.00332\log_{10}(T) & 0.3\,\text{sec} \leq T \leq 0.6\,\text{sec} \\ 0.002 & T > 0.6\,\text{sec} \end{cases} \tag{3.9}$$

Equations (3.8) and (3.9) are from Si and Midorikawa [1999]. The details of Equation (3.6) are presented in the following section.

The A and X in Equation (3.6) are the amplitude of PSA(T) and the *ClstD*, respectively. Figure 3.3 shows the residuals against $Z_{2.5}$ for different periods, where $Z_{2.5}$ is defined as the depth to the top of the layer with $V_s = 2.5$ km/sec. The red closed circles and error bars represent the means and standard deviations of residuals, respectively. These values were calculated for each 0.5 km interval of $Z_{2.5}$. Finally, the means were regressed by the following equation to obtain the basin response term of the GMPE.

$$G_d(T) = C_d(T) + D_d(T)Z_{2.5} \tag{3.10}$$

where C_d and D_d are regression parameters. Table 3.1 shows the regression results obtained by Equation (3.10). Figure 3.4 shows the proposed basin effects for $Z_{2.5}$ =1.0, 2.0, and 3.0 km. The basin effects saturate above $T > 5.0$ sec. These residuals were similarly reviewed against $Z_{1.0}$; however, a clear trend was not apparent.

Table 3.1 Coefficients of the basin effect model with $Z_{2.5}$.

T	C_d	D_d
1.0	0.008	0.056
1.5	0.030	0.067
2.0	0.037	0.081
3.0	0.022	0.108
4.0	-0.021	0.142
5.0	-0.072	0.181
7.0	-0.114	0.198
10.0	-0.133	0.190

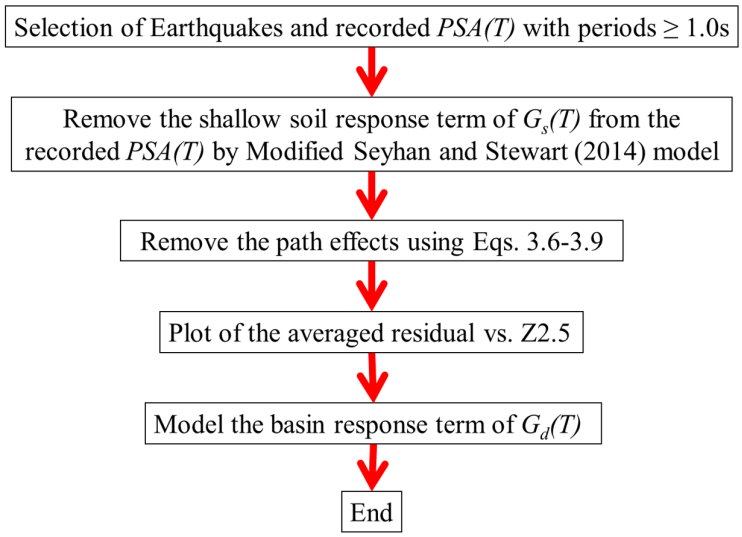

Figure 3.2 **Methodology used to obtain basin response model.**

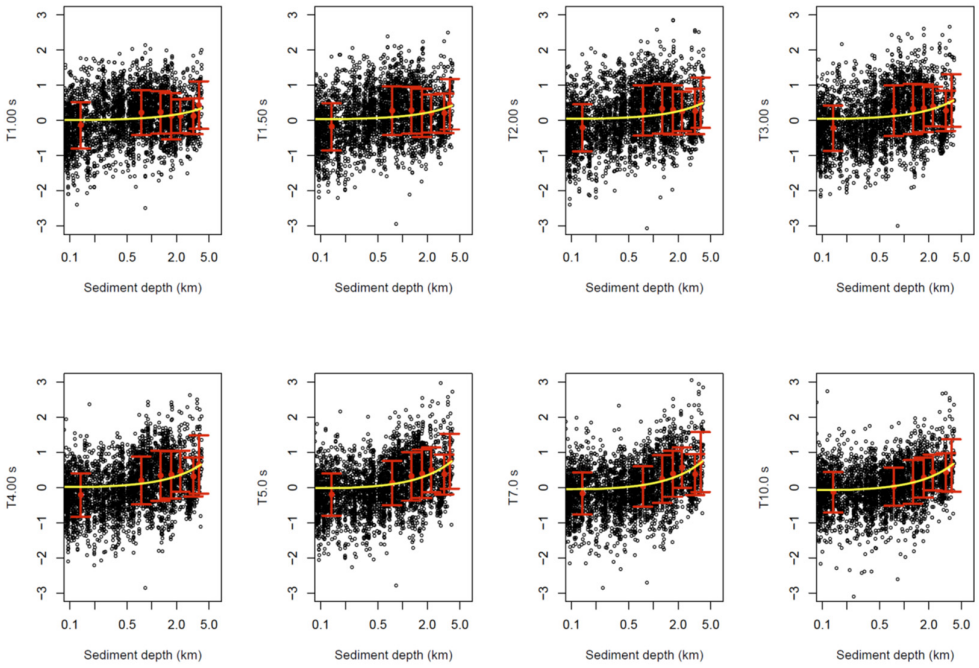

Figure 3.3 **Residuals of PSA vs. $Z_{2.5}$ for periods of 1.0, 1.5, 2.0, 3.0, 4.0, 5.0, 7.0, and 10.0 sec. The residuals were calculated by removing shallow-soil and distance effects. Black circles show the residuals. Red circles and error bars show the means and standard deviations of the residuals, respectively. Yellow solid lines show the regression lines for the basin model.**

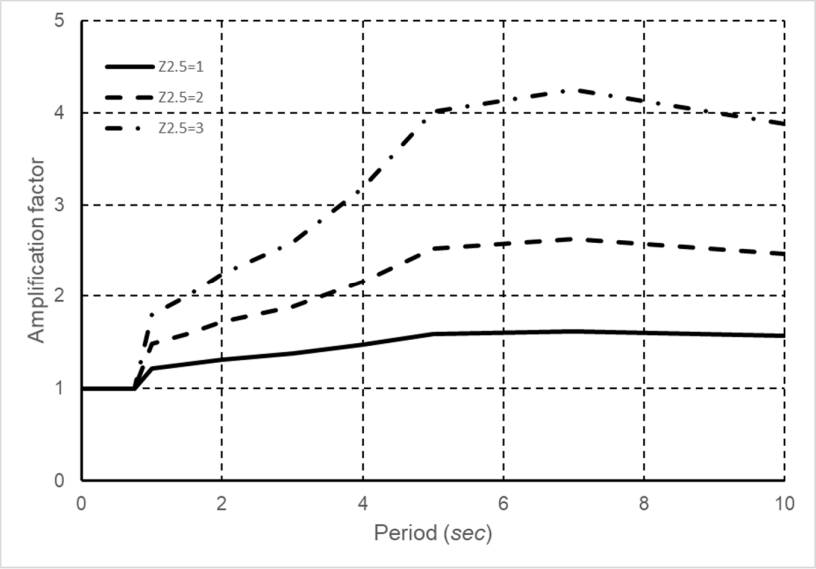

Figure 3.4 Proposed basin effects for $Z_{2.5}$ =1.0, 2.0, and 3.0 km.

3.3 PATH EFFECTS

Path effects were modeled at the referenced site condition of V_{ref} = 760 m/sec. Attenuations of ground motion amplitude were generally modeled using the following equation.

$$\log_{10} A(T) = b(T) - n\log_{10}\left[X + C(T)\right] - k(T)X \tag{3.11}$$

where, A and X are the ground-motion amplitude and the source-to-site distance, respectively; b represents the source term; C controls the saturation of ground-motion amplitude near fault ruptures; and n and k represent the geometric and anelastic attenuation terms, respectively.

Past studies have often selected n = 1.0 (e.g., Douglas [2003]). This value is consistent to the theoretical decay of body-wave amplitudes proportional to the inverse of distances at infinite medium and fits the ground-motion observations reasonably well. When the D is deeper than 30 km, then n becomes 1.6—on average—demonstrating higher attenuation compared to shallow earthquakes [Midorikawa and Ohtake 2004]. This observation is explained by noting that seismic waves propagated from the source are reflected at the Moho, thus ground-motion attenuation becomes higher at the ground surface. [Joshi and Midorikawa 2005].

Figure 3.5 shows the simulated PGA attenuation with *ClstD* given D = 40 km [Midorikawa and Ohtake 2004]. The solid line shows the results when the Moho exists at the depth of 30 km; the dashed line shows when there is no layered structure. The simulation results show that the slope becomes -1.6 at longer distances—the solid line—which is consistent with field observations. Midorikawa and Ohtake [2004] performed similar simulations by ranging D with and without considering the Moho structure. The results show that these attenuation curves generally cross at $X = 1.7D$; see Figure 3.5. Based on these observations, the following model for path effects was proposed herein.

$$\log_{10} A(T) = b(T) + g(T, X) - k(T)X \tag{3.12}$$

where

$$g(T,X)=\begin{cases}-\log_{10}\left[X+C(T)\right] & D \le \text{Moho depth or } X<1.7D \\ 0.6\log_{10}[1.7D+C(T)]-1.6\log_{10}[X+C(T)] & D>\text{Moho depth and } X\ge 1.7D\end{cases} \tag{3.13}$$

$$C(T)=\begin{cases}0.0055\cdot 10^{0.5\min(\mathbf{M}8.3)} & T<0.3\,\text{sec} \\ [0.000810-0.00897\log_{10}(T)]\cdot 10^{0.5\min(\mathbf{M}8.3)} & 0.3\,\text{sec}\le T\le 0.6\,\text{sec} \\ 0.0028\cdot 10^{0.5\min(\mathbf{M}8.3)} & T>0.6\,\text{sec}\end{cases} \tag{3.14}$$

$$k(T)=\begin{cases}0.003 & T<0.3\,\text{sec} \\ 0.00126-0.00332\log_{10}(T) & 0.3\,\text{sec}\le T\le 0.6\,\text{sec} \\ 0.002 & T>0.6\,\text{sec}\end{cases} \tag{3.15}$$

Equations (3.14) and (3.15) are per the study by Si and Midorikawa [2000].

To obtain *b(T)*, regression analyses were performed using Equation (3.12) by fitting the observed data for each earthquake. As described earlier, the site response effects were removed before the regression analysis. The weighted least square method was adopted, as shown in Table 3.2. The weight increases as distance decreases because the shorter-distance data are more important in determining *b(T)*. The variation in the resulting *b*(*T*) is discussed in Section 3.4. Figure 3.6 shows the regression results, where *ClstD* is used for *X* in Equation (3.12). The regression results capture the observed trend, indicating that the proposed model in Equation (3.12) represents the path effects of these data to a reasonable degree.

Table 3.2 Weights of the data with distances determined by regression analyses using Equation (3.12).

T = 5.0 sec (km)	Weight
0 – 100	3
100 – 150	2
> 150	1

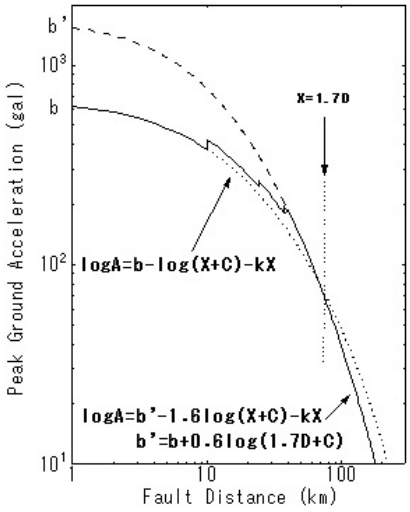

Figure 3.5 Difference in apparent geometric attenuation depending on the existence of Moho structure based on the simulation results [Midorikawa and Ohtake 2004].

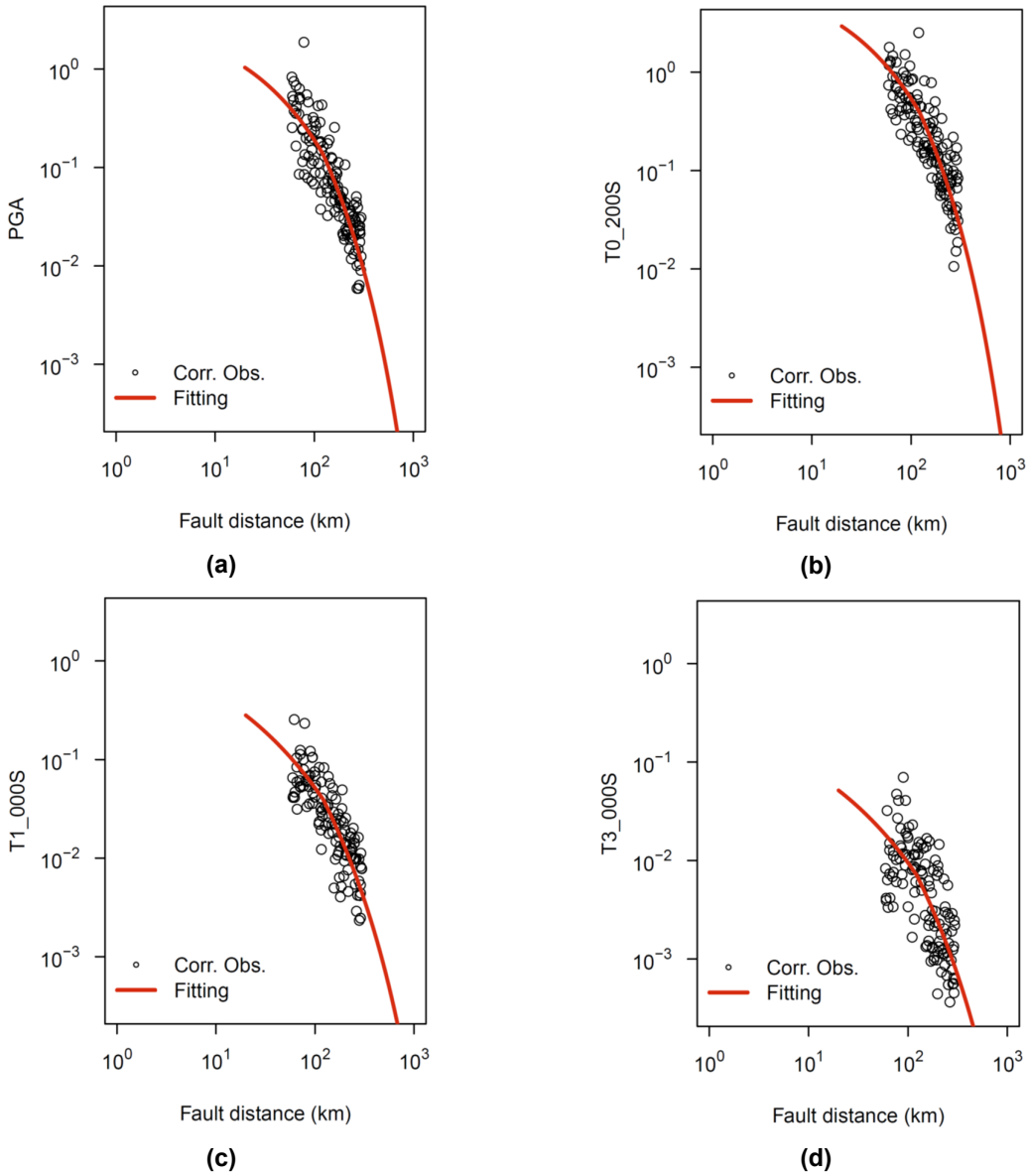

Figure 3.6 **Examples of regression analysis by Equation (3.9) for different periods of PSA for the 2011 Iwate offshore earthquake: (a) PGA, (b) T = 0.2 sec; (c) T = 1.0 sec; and (d) T = 3.0 sec.**

3.4 EARTHQUAKE SOURCE EFFECTS

The $b(T)$ obtained using Equation (3.12) is presented in Figure 3.7, showing the results at T = 0.02 and 2.0 sec, respectively. Red and black circles show the results for interplate and intraplate earthquakes, respectively. The $b(T)$ and **M** are correlated in this figure even though the scatter of the data exists. The $b(T)$ obtained for intraplate earthquakes tend to be larger than those obtained for interplate ones.

In past studies, the trend between $b(T)$ and **M** was expressed by a piecewise linear model by decreasing its slope as **M** increases [Si et al. 2016; Ibrahim et al. 2016]. A similar trend is observed for interplate earthquakes. Figure 3.7 demonstrates that the slope of $b(T)$

decreases when **M** > 8.3 for $T = 0.02$ sec [Figure 3.7(a)] and **M** > 7.5 for $T = 2.0$ sec; see Figure 3.7(b). A review of the data of interplate earthquakes for different periods confirms that the breaking point of **M** decreases as T increases. In contrast, for intraplate earthquakes it was difficult to evaluate these trends because of the limited data where **M** > 8.0. Therefore, the current study adopted the same slopes for the breaking points of **M** for intraplate earthquakes for interplate earthquakes.

Figure 3.8 shows the variation in $b(T)$ with D at $T = 0$, 0.2, 1.0, and 3.0 sec, respectively. Red and black circles show the results for interplate and intraplate earthquakes, respectively. The comparison was made by selecting the data from **M** = 6.6–6.8 for interplate earthquakes, and from **M** = 6.2–6.4 for intraplate earthquakes because of the limited data. The results show that $b(T)$ increases with D for short and intermediate periods; however, $b(T)$ does not increase with D at $T = 3.0$ sec compared to the shorter periods. A review of the data for different periods confirms that the dependency of $b(T)$ on D is strong at shorter periods and weak at longer periods.

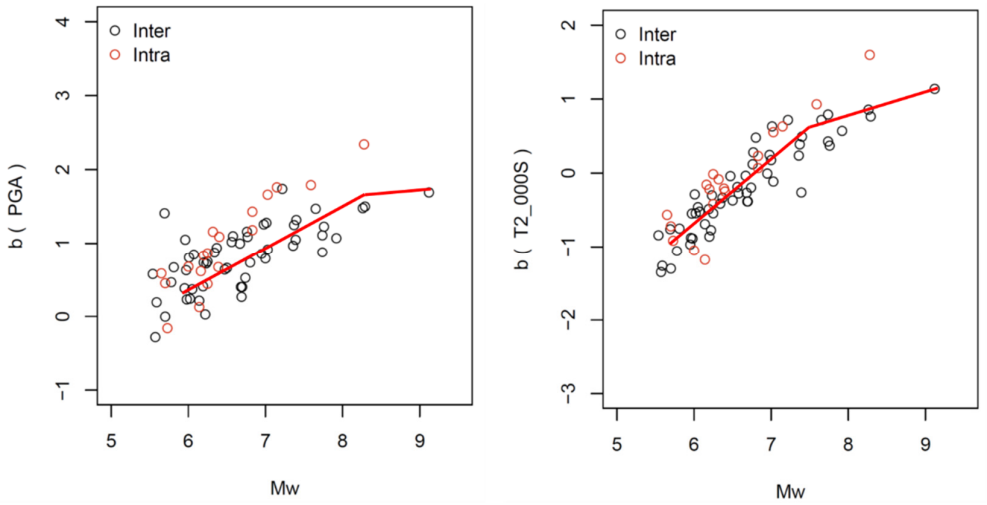

(a) (b)

Figure 3.7 **Variation in $b(T)$ against M for interplate and intraplate earthquakes: (a) T = 0.02 sec; and (b) T = 2.0 sec.**

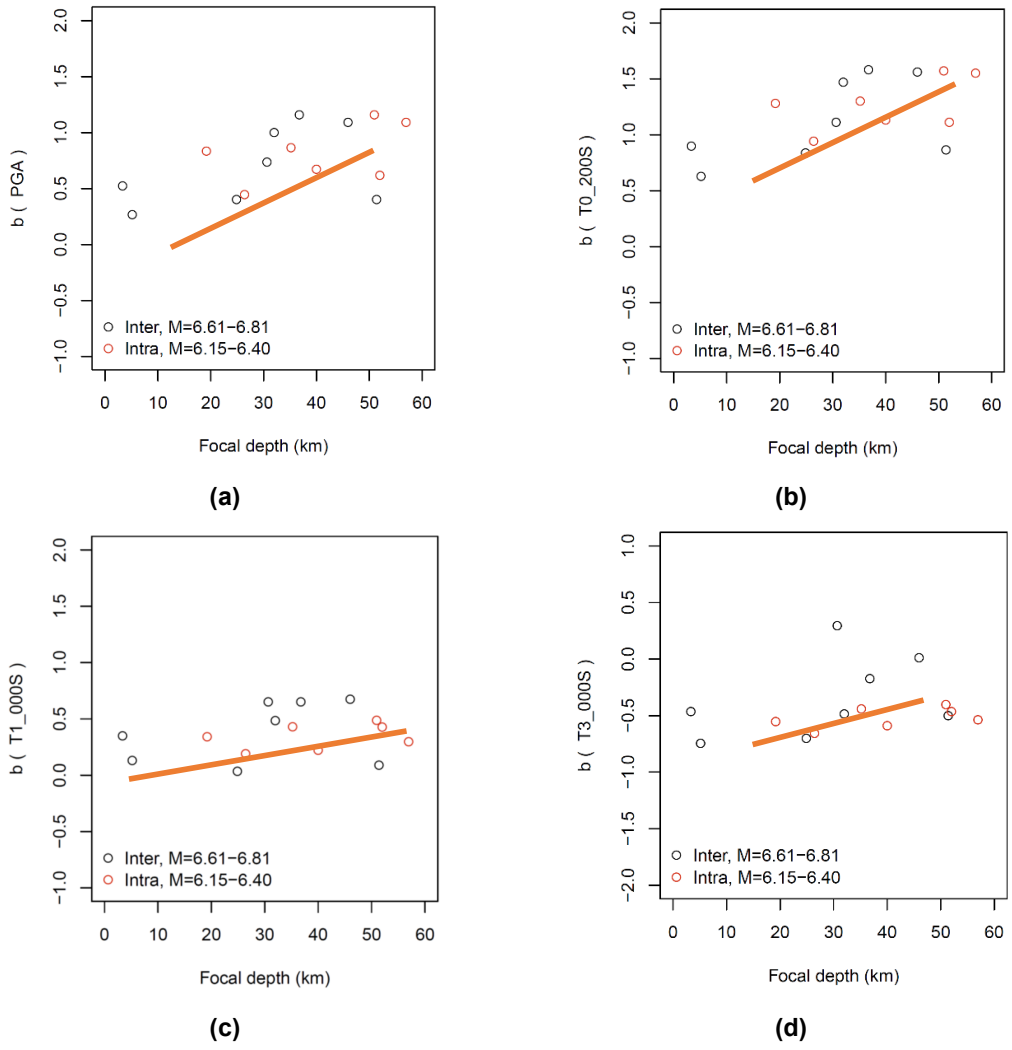

Figure 3.8 **Variation in *b(T)* against *D* for interplate and intraplate earthquakes: (a) PGA; (b) *T* = 0.2 sec; (c) *T* = 1.0 sec; and (d) *T* = 3.0 sec. The data were selected from M = 6.6–6.8 for interplate and M = 6.2–6.4 for intraplate earthquakes.**

Figure 3.9 **Schematic drawing of piecewise linear models of *b*(*T*): (a) *T* < 2.0 sec; and (b) *T* ≥ 2.0 sec.**

Based on these observations, earthquake source effects were modeled using earthquake types and D. Equation (3.16) shows the adopted model of $b(T)$; similar models have been proposed by Si et al. [2016] and Ibrahim et al. [2016].

Presented below is the basic expression except when $T < 2.0$ sec and **M** > 8.3 or when $T \geq 2.0$ sec and **M** > 7.5:

$$b(T) = a_1(T)M + d_0(T)S_0 = d_1(T)S_1 + h(T)D + e \tag{3.16a}$$

When $T < 2.0$ sec and **M** > 8.3:

$$b(T) = a_1(T)M + [a_2(T) - a_1(T)](M - 8.3) + d_0(T)S_0 + d_1(T)S_1 + h(T)D + e \tag{3.16b}$$

When $T \geq 2.0$ sec and **M** > 7.5:

$$b(T) = a_1(T)M + [a_2(T) - a_1(T)](M - 7.5) + d_0(T)S_0 + d_1(T)S_1 + h(T)D + e \tag{3.16c}$$

where

$$S_0 = \begin{cases} 1 & \text{Interplate earthquake} \\ 0 & \text{Intraplate earthquake} \end{cases} \tag{3.17}$$

$$S_1 = \begin{cases} 0 & \text{Interplate earthquake} \\ 1 & \text{Intraplate earthquake} \end{cases} \tag{3.18}$$

Figure 3.9 shows schematic drawings of the piecewise linear model presented in Equation (3.16). The slope of $b(T)$ against **M** changes at the specified **M**, where its breaking point is **M** = 8.3 at $T < 2.0$ sec and **M**=7.5 at $T \geq 2.0$ sec, respectively. The regression parameters in Equation (3.16) were obtained as follows:

- Step 1. $a_1(T)$, $d_0(T)$, and $d_1(T)$ were obtained for Equation (3.16a) by regression analysis depending on the earthquake types using the subset of the data that satisfies the conditions of the equations. $a_1(T)$, $d_0(T)$, and $d_1(T)$ were smoothed using a spline function;
- Step 2. Regression analysis was performed by using the residuals in Step 1 against D to obtain $h(T)$. $h(T)$ was smoothed using a spline function; and
- Step 3. $a_2(T)$ in Equation (3.16b) and (3.16c) were obtained by regression analysis using the subset of data that satisfies the conditions of the equations after removing the influence of $a_1(T)$, $h(T)$, $d_0(T)$, and $d_1(T)$.

During the regression analyses, weights of data were ranged depending on the number of available data in earthquake events shown in Table 3.3. The weight of the data increases as the number of available data increases in the event.

Figure 3.10 shows the regression results of $a_1(T)$, $a_2(T)$, $h(T)$, $d_0(T)$, and $d_1(T)$. Figure 3.10(a) shows that $a_1(T)$ is 0.5 when the T is shorter than 0.3 sec, but increases to 1.0 when the T becomes greater than 3.0 sec. This observation is consistent with past studies. Figure 3.10(b) shows that $a_2(T)$ is 0 when the T is shorter than 0.5 sec, and increases to 0.5 when T becomes greater than 2.0 sec. Figure 3.10(c) shows the variation in d_0 and d_1 with T, where d_1 is about 0.25 when T is shorter than 0.3 sec and decreases to 0.13 as T increases to 10 sec. This indicates that the PSA is larger in intraplate earthquakes compared to interplate earthquakes by a factor of 1.8 and 1.3 for short and long periods, respectively. Figure 3.10(d) shows the variation in

$h(T)$ with T where the $h(T)$ is about 0.075 when T is shorter than 0.2 sec and gradually decreases as T increases. When T is greater than 1.0 sec, $h(T)$ becomes about a constant of 0.04.

Table 3.3 **Weights of the data by regression analyses in Equation (3.13) depending on the numbers of available data in earthquake events.**

Number of records	Weight
< 10	1
10 – 20	2
20 – 30	3
> 30	4

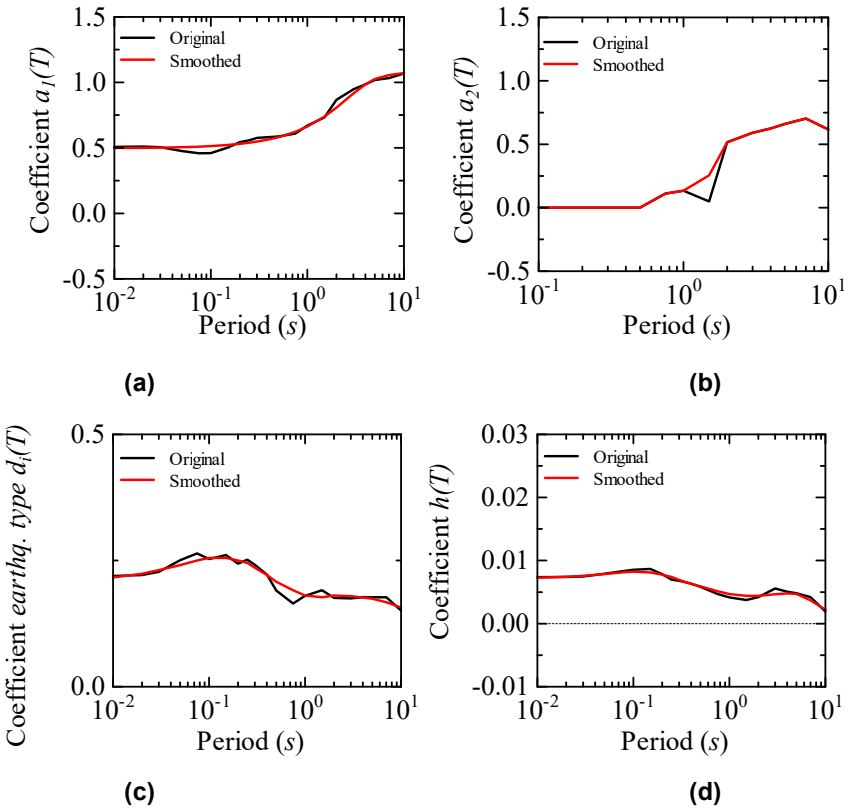

Figure 3.10 **Variation in regression parameters against T: (a) $a_1(T)$; (b) $a_2(T)$; (c) $d_1(T)$: and (d) $h(T)$. Black and red lines show the unsmoothed and smoothed regression parameters, respectively.**

3.5 REGRESSION RESULTS

The proposed GMPE is summarized by following equations.

$$\log_{10} A(T) = b(T) + g(T, R_{rup}) - k(T)R_{rup} + G(T) \tag{3.19}$$

where

$$b(T) = \begin{cases} a_1(T)M + d_0(T)S_0 + d_1(T)S_1 + h(T)D + e & \text{if } T < 2.0\,\text{sec and } M < 8.3 \text{ or } T \geq 2.0\,\text{sec and } M < 7.5 \\ a_1(T)M + [a_2(T) - a_1(T)](M - 8.3) + d_0(T)S_0 + d_1(T)S_1 + h(T)D + e & \text{if } T < 2.0\,\text{sec and } M > 8.3 \\ a_1(T)M + [a_2(T) - a_1(T)](M - 7.5) + d_0(T)S_0 + d_1(T)S_1 + h(T)D + e & \text{if } T \geq 2.0\,\text{sec and } M > 7.5 \end{cases} \tag{3.20}$$

$$S_0 = \begin{cases} 1 & \text{Interplate earthquake} \\ 0 & \text{Intraplate earthquake} \end{cases} \tag{3.21}$$

$$S_1 = \begin{cases} 0 & \text{Interplate earthquake} \\ 1 & \text{Intraplate earthquake} \end{cases} \tag{3.22}$$

$$g(T, X) = \begin{cases} -\log_{10}[X + C(T)] & D \leq \text{Moho depth or } X < 1.7D \\ 0.6\log_{10}[1.7D + C(T)] - 1.6\log_{10}[X + C(T)] & D > \text{Moho depth and } X \geq 1.7D \end{cases} \tag{3.23}$$

$$C(T) = \begin{cases} 0.0055 \cdot 10^{0.5\min(\mathbf{M}8.3)} & \text{if } T < 0.3\,\text{sec} \\ [0.000810 - 0.00897\log_{10}(T)] \cdot 10^{0.5\min(\mathbf{M}8.3)} & \text{if } 0.3\,\text{sec} < T < 0.6\,\text{sec} \\ 0.0028 \cdot 10^{0.5\min(\mathbf{M}8.3)} & \text{if } T > 0.6\,\text{sec} \end{cases} \tag{3.24}$$

$$k(T) = \begin{cases} 0.003 & \text{if } T < 0.3\,\text{sec} \\ 0.000126 - 0.00332\log_{10}(T) & \text{if } 0.3\,\text{sec} < T < 0.6\,\text{sec} \\ 0.002 & \text{if } T < 0.6\,\text{sec} \end{cases} \tag{3.25}$$

$$G(T) = G_s(T) + G_d(T) \tag{3.26}$$

$$G_s(T) = \ln\left[F_{lin}(T)\right] + \ln\left[F_{nl}(T)\right] \tag{3.27}$$

$$\ln\left[F_{lin}(T)\right] = \begin{cases} c(T)\ln\left(\dfrac{V_{s30}}{V_{\text{ref}}}\right) & \text{if } V_{s30} \leq V_c(T) \\ c(T)\ln\left[\dfrac{V_c(T)}{V_{\text{ref}}}\right] & \text{if } V_{s30} > V_c(T) \end{cases} \tag{3.28}$$

$$\ln\left[F_{nl}(T)\right] = f_1 + f_2(T)\ln\left[\frac{\text{PGA}_r(T) + f_3}{f_3}\right] \tag{3.29}$$

$$f_2(T) = 0.5f_4\left[\exp\left\{f_5(T)\cdot\left[\min\left(V_{s30}, 760\right) - 360\right]\right\} - \exp\left\{f_5(T)\cdot\left(760 - 360\right)\right\}\right] \tag{3.30}$$

$$G_d(T) = C_d(T) + D_d(T)Z_{2.5} \tag{3.31}$$

Associated coefficients are presented in an attached excel file (Appendix A).

Figure 3.11 shows the predicted PSA by the proposed regression model for different values of **M** and earthquake types at R_{rup} = 75 km and D = 20 km; a Moho depth of 30 km is used. The figure shows that intraplate earthquakes have larger amplitude than interplate earthquakes, and that the amplitudes tend to saturate when **M** is larger than 8. Figure 3.12 shows the predicted PSA by the proposed regression model for different rupture distances at **M** = 7 and D = 20 km.

Figures 3.13 and 3.14 show the predicted PSA by the proposed regression model for different focal depths at distance of 100 km for an interplate earthquake and intraplate earthquake with M_w = 7, respectively. The figures show larger amplitude for deeper earthquakes and stronger depth dependence at shorter periods.

Figures 3.15–3.18 show the predicted PSA by the proposed regression model vs. fault distance for different magnitudes and earthquake types with a focal depth of 20 km. The figures show nonlinear magnitude dependence at **M** larger than 8 and steeper attenuation decay for smaller magnitudes at shorter distances. The comparison of the PSA for different magnitudes at different periods (Figures 3.16–3.18) shows stronger magnitude dependence at longer periods. Figures 3.19–3.22 show those events with D = 40 km, respectively. The figures show steeper attenuation decay than that for a shallower earthquake, as shown in Figures 3.15–3.18. Thus, the proposed model considers different attenuation decay for both shallower and deeper earthquakes, as well as nonlinear magnitude dependence, depth dependence, and dependence of earthquake type.

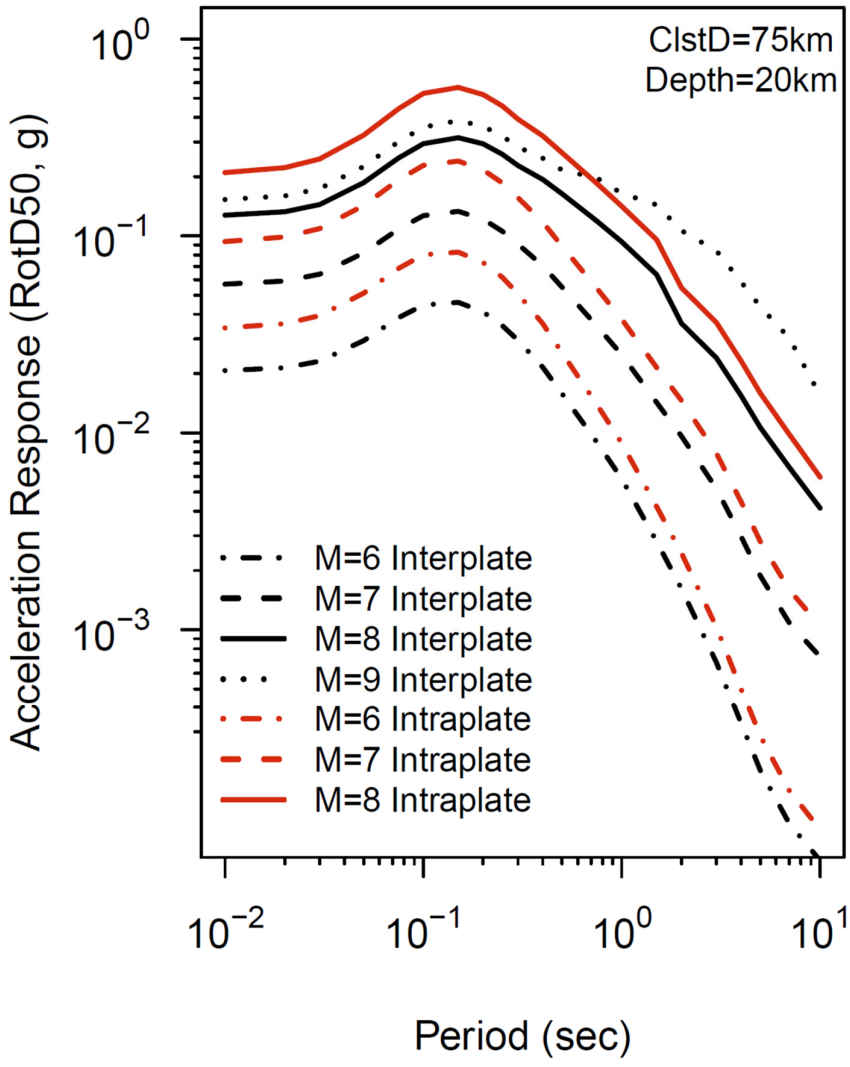

Figure 3.11 **Predicted PSA by the proposed regression model for different M and earthquake types at R_{rup} = 75 km and D = 20 km.**

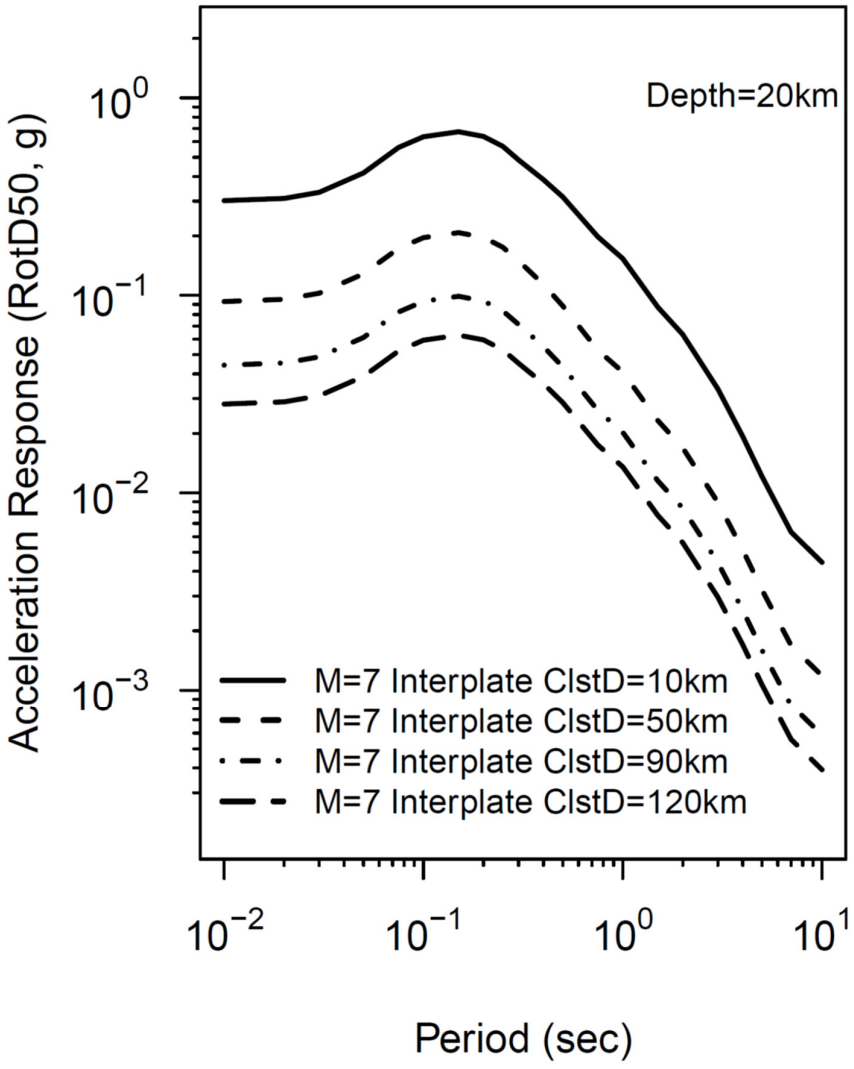

Figure 3.12 **Predicted PSA by the proposed regression model for different rupture distances at M = 7 and *D* = 20 km.**

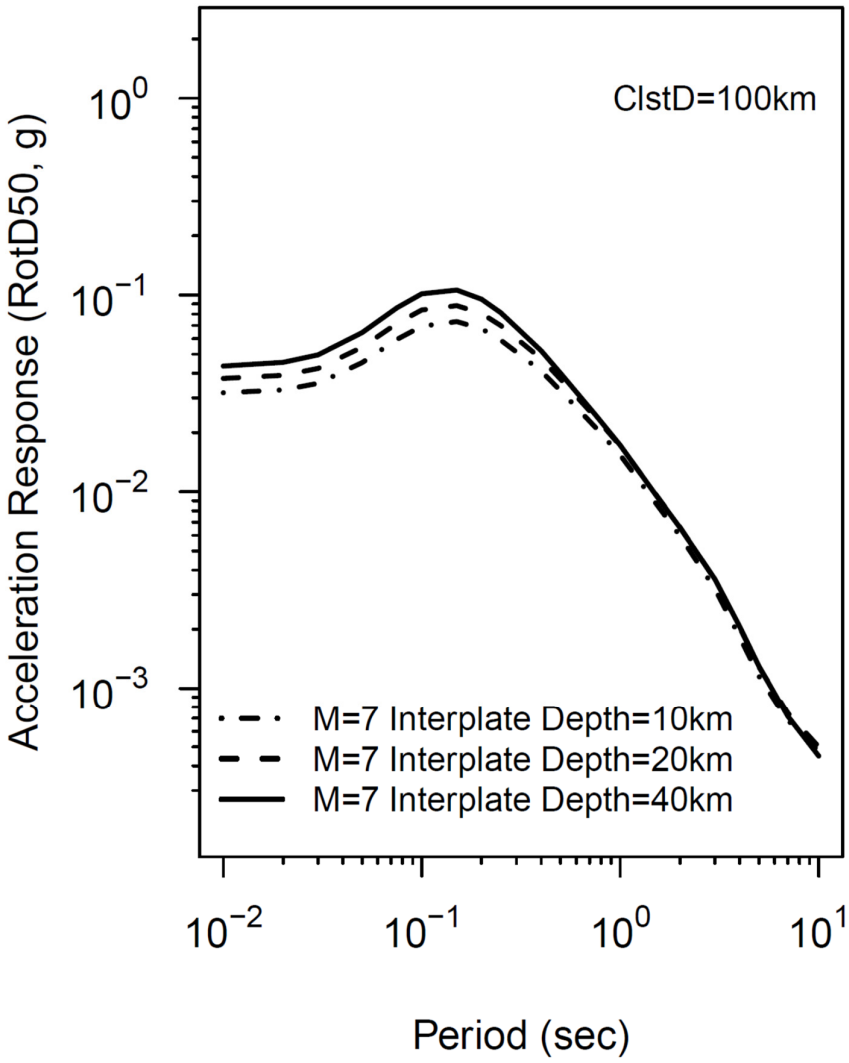

Figure 3.13 **Predicted PSA by the proposed regression model for different focal depths at distance of 100 km for an interplate earthquake with M = 7.**

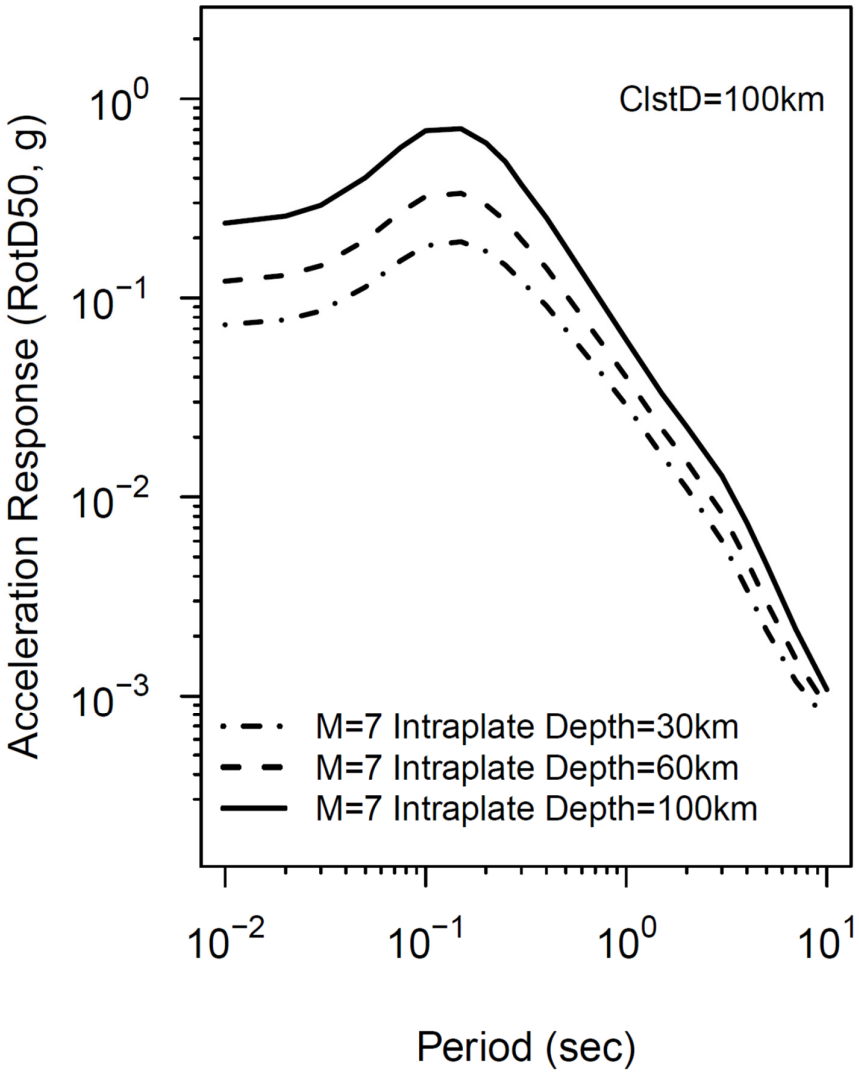

Figure 3.14 **Predicted PSA by the proposed regression model for different focal depths at distance of 100 km for an intraplate earthquake with M = 7.**

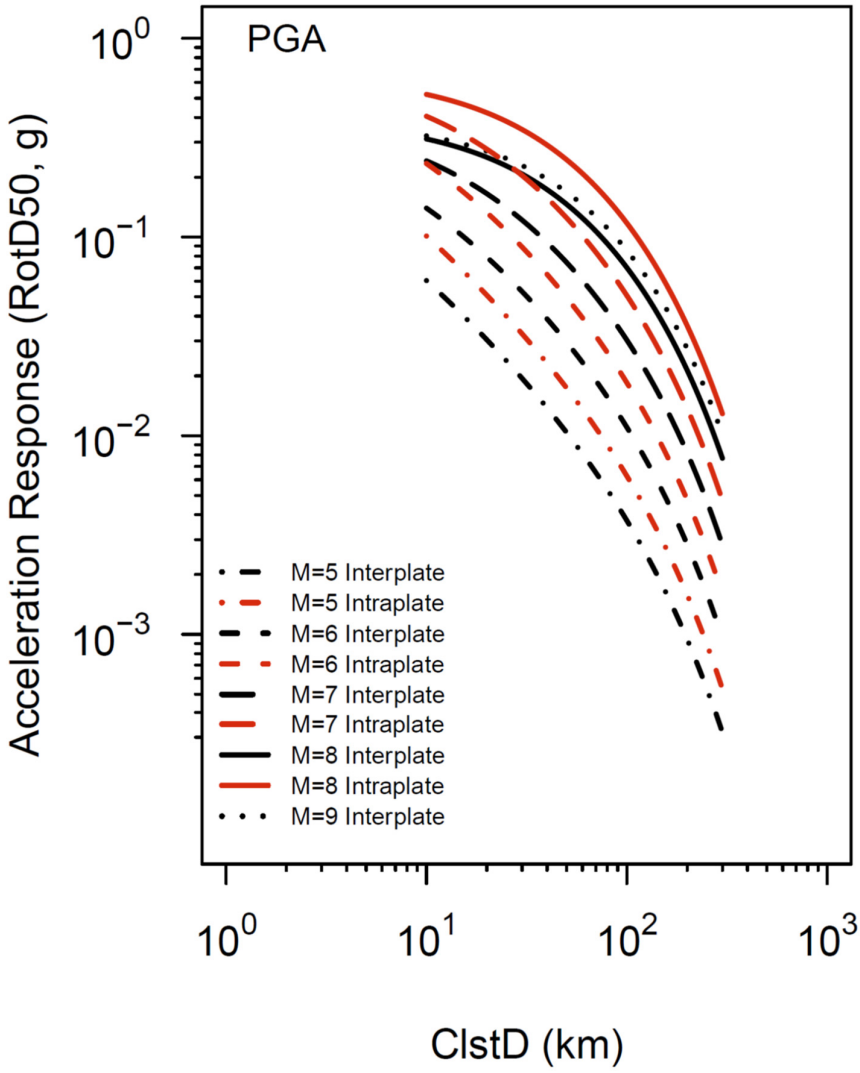

Figure 3.15 **Predicted PGA vs R_{rup} (M5,6,7,8, and 9, V_{s30} = 760 m/sec, $Z_{2.5}$ = 0 km, and D = 20 km).**

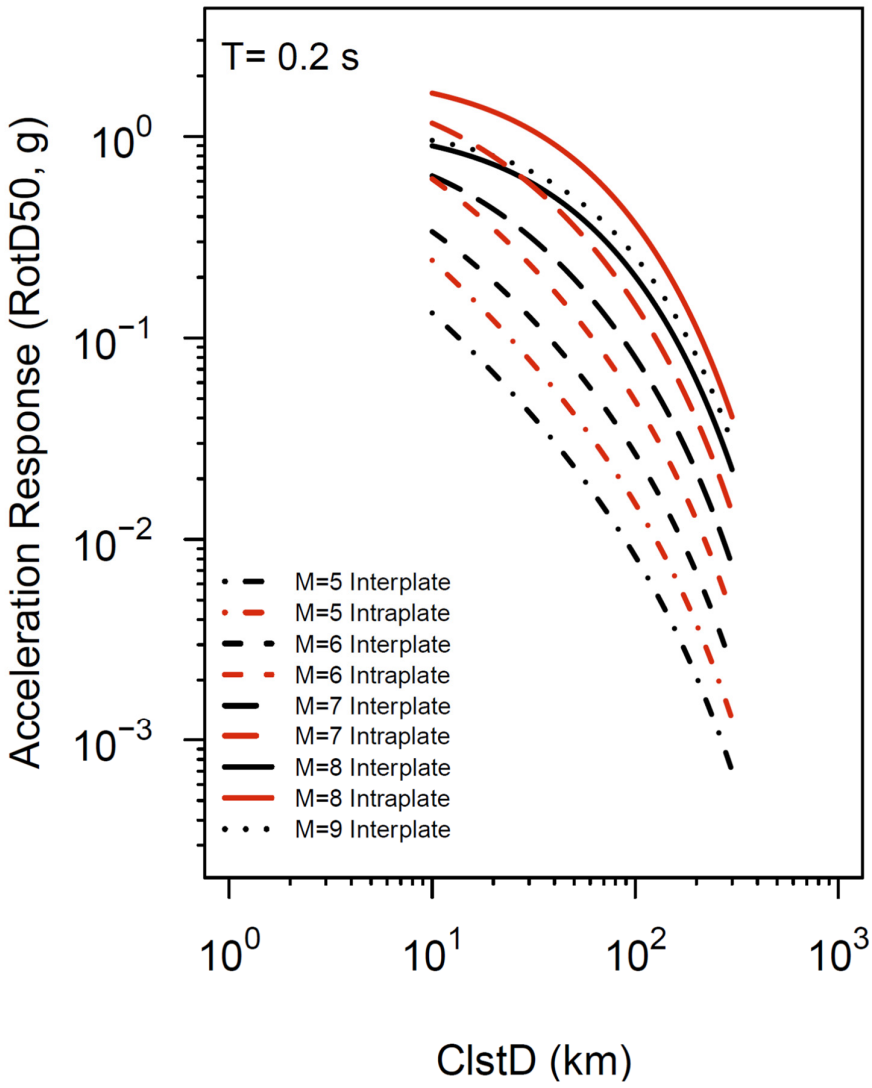

Figure 3.16 **Predicted PSA vs R_{rup} (M5,6,7,8, and 9, V_{s30} = 760 m/sec, $Z_{2.5}$ = 0 km, D = 20 km, and T = 0.2 sec).**

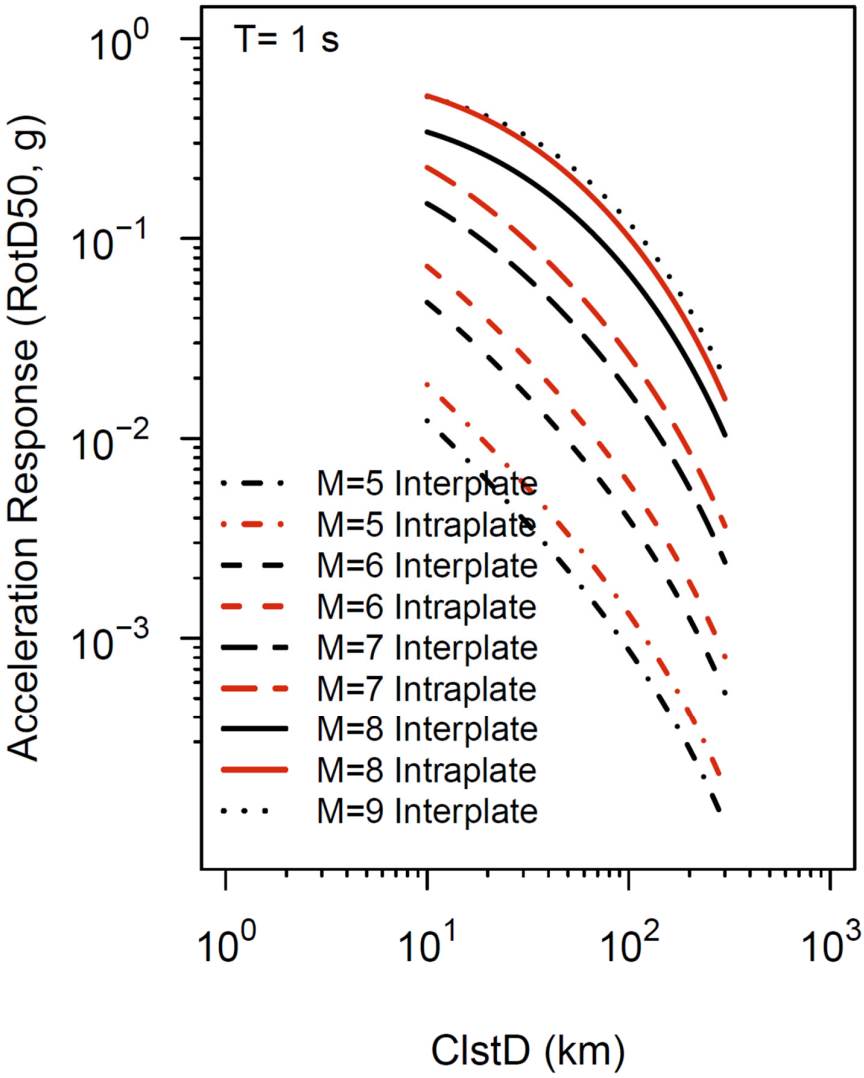

Figure 3.17 **Predicted PSA vs R_{rup} (M5,6,7,8, and 9, V_{s30} = 760 m/sec, $Z_{2.5}$ = 0 km, D = 20 km, and T = 1 sec).**

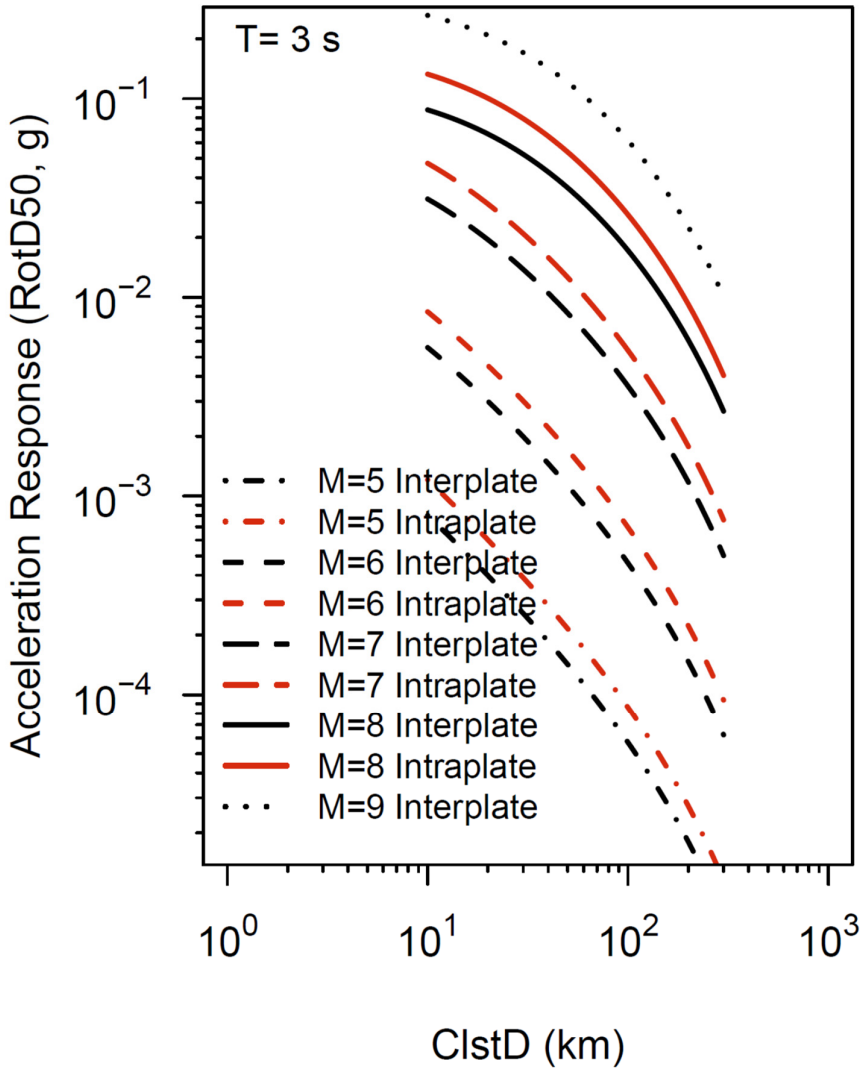

Figure 3.18 **Predicted PSA vs R_{rup} (M5,6,7,8, and 9, V_{s30} = 760 m/sec, $Z_{2.5}$ = 0 km, D = 20 km, and T = 3 sec).**

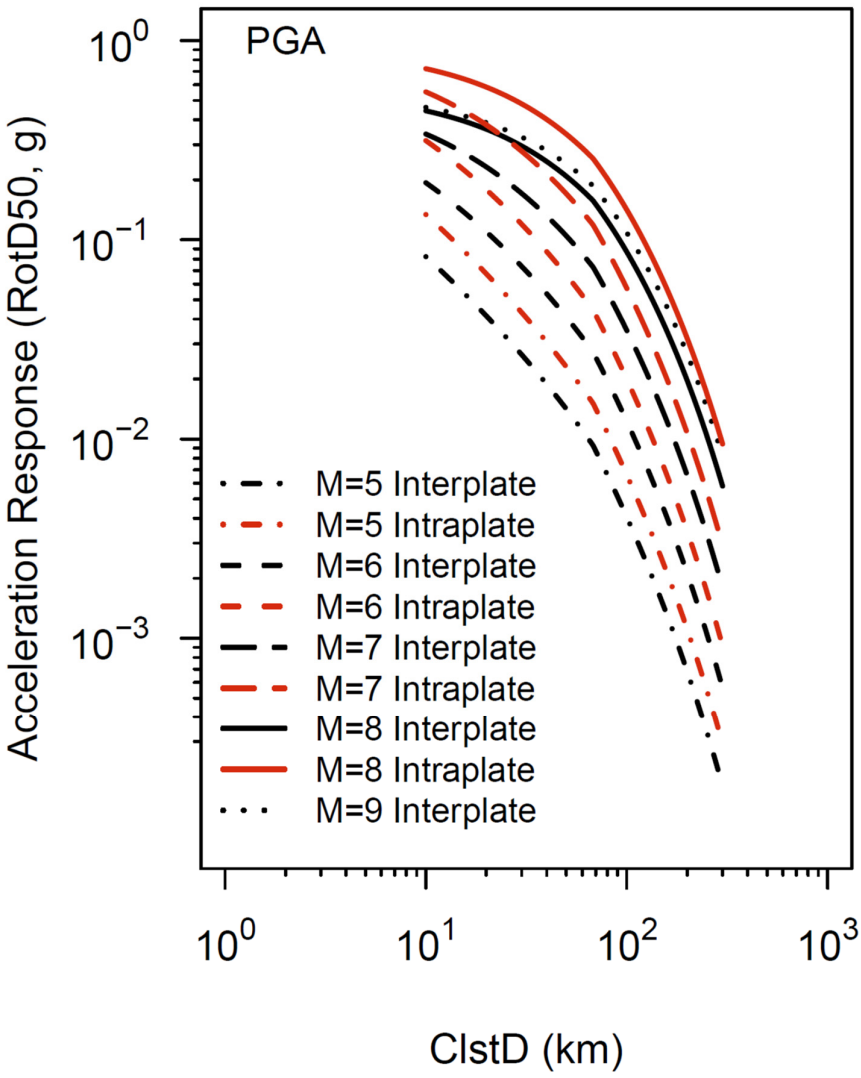

Figure 3.19 **Predicted PGA vs R_{rup} (M5,6,7,8, and 9, V_{s30} = 760 m/sec, $Z_{2.5}$ = 0 km, and D = 40 km).**

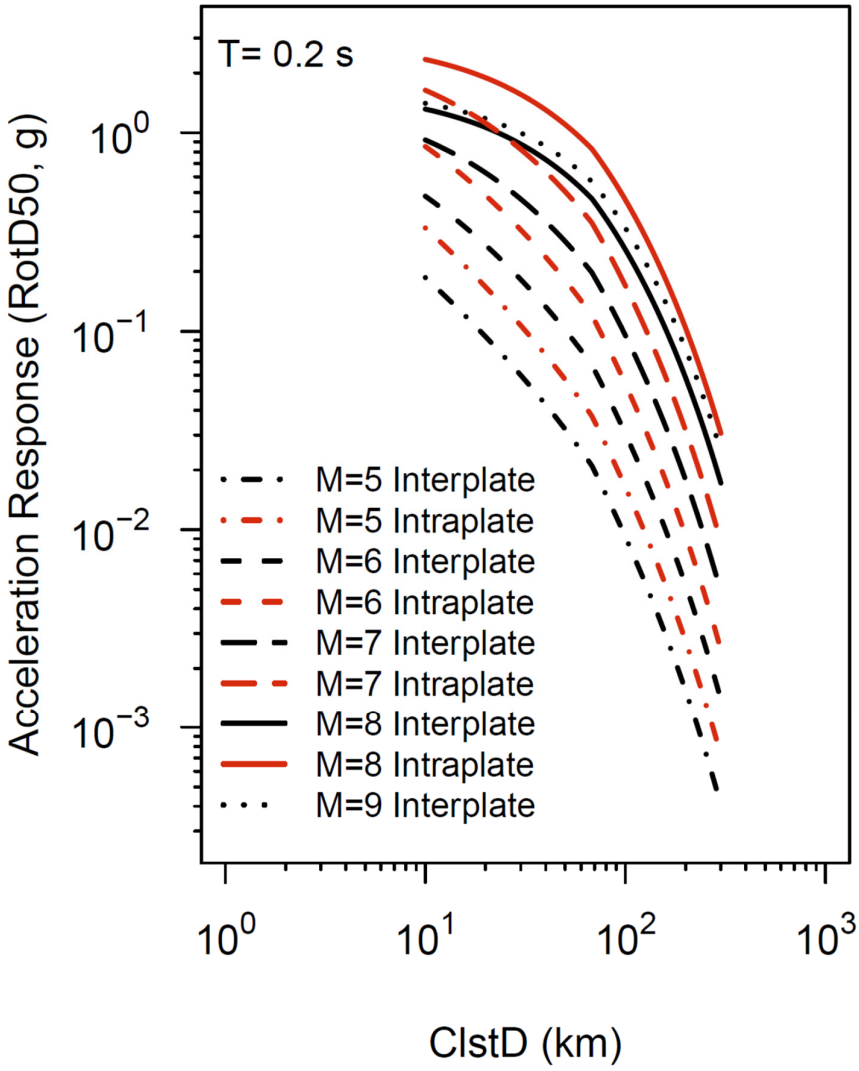

Figure 3.20 **Predicted PSA vs R_{rup} (M5,6,7,8, and 9, V_{s30} = 760 m/sec, $Z_{2.5}$ = 0 km, D = 40 km, and T = 0.2 sec).**

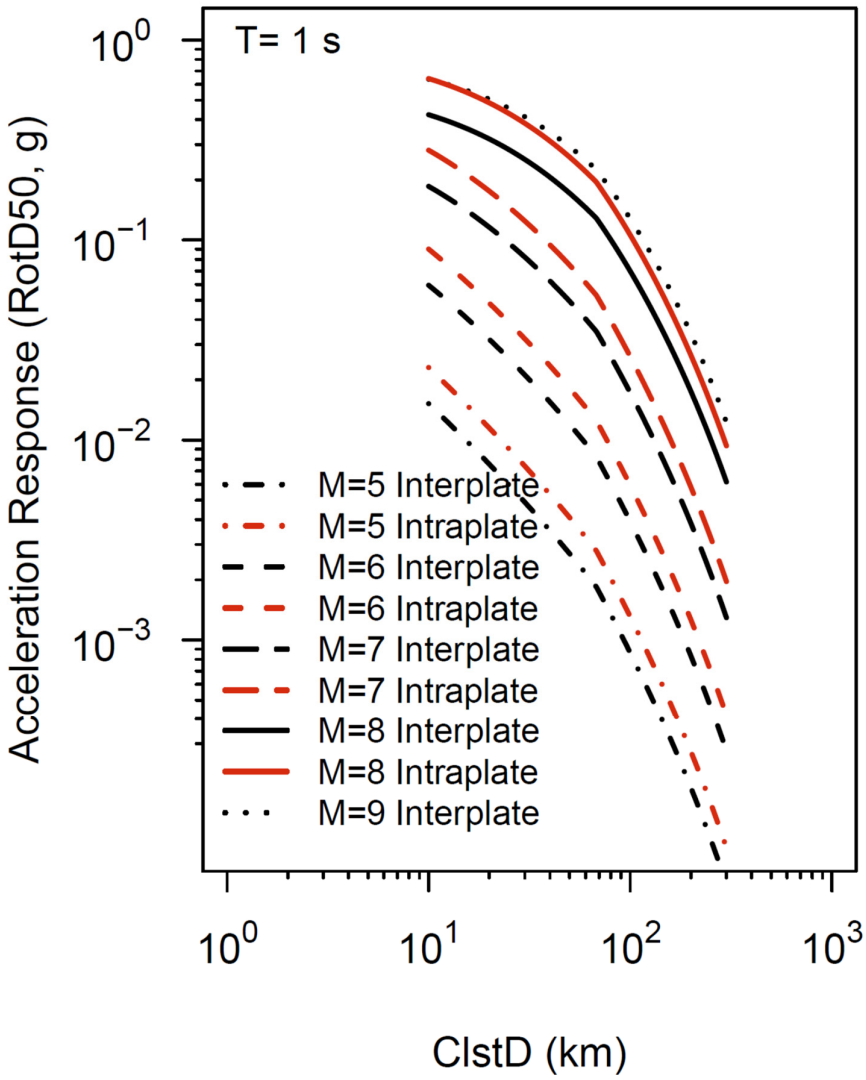

Figure 3.21 **Predicted PSA vs R_{rup} (M5,6,7,8, and 9, V_{s30} = 760 m/sec, $Z_{2.5}$ = 0 km, D = 40 km, and T = 1 sec).**

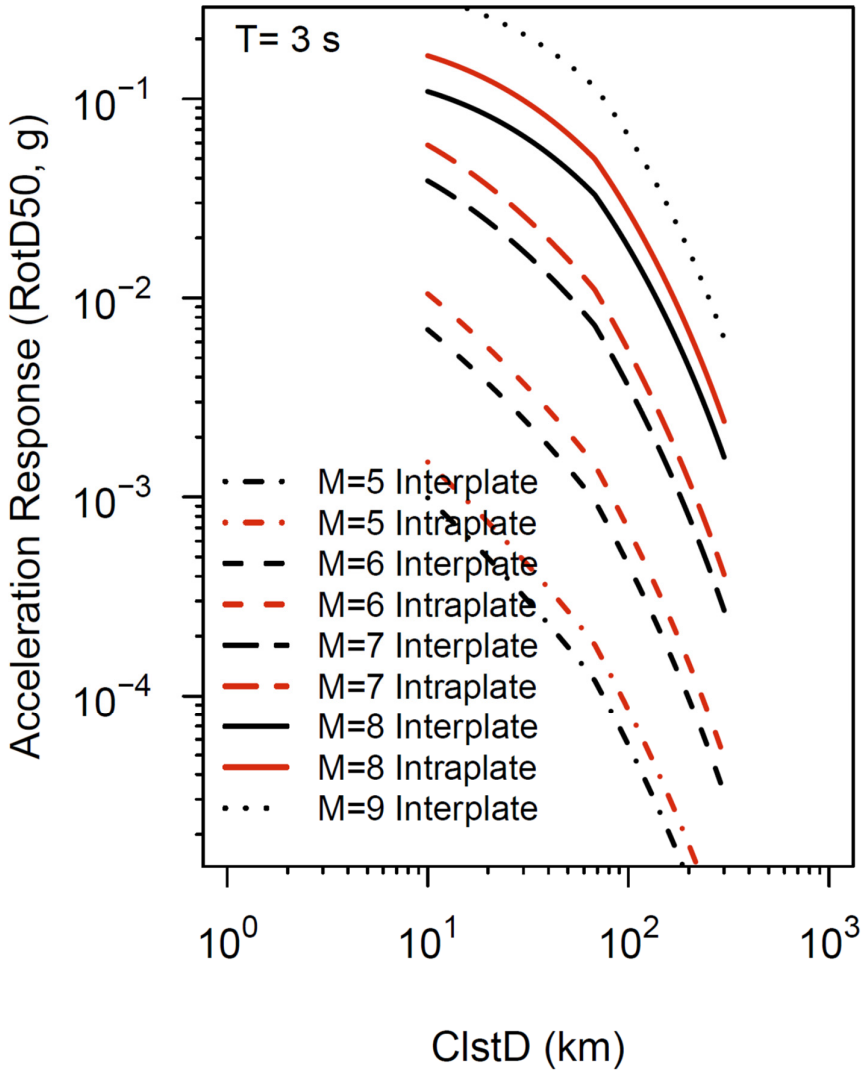

Figure 3.22 **Predicted PSA vs R_{rup} (M5,6,7,8, and 9, V_{s30} = 760 m/sec, $Z_{2.5}$ = 0 km, D = 40 km, and T = 3 sec).**

3.6 RESIDUAL ANALYSIS

The resulting residuals were analyzed against various variables. The total residuals were plotted against *ClstD* in Figure 3.23 from PGA to PSA at T = 5.0 sec. These residuals were sorted into 10 bins, which are equally spaced in log scale of *ClstD*. In addition, the mean and the standard deviation for each bin were plotted at the central *ClstD*. There is no apparent trend in mean data from *ClstD* = 10–300 km and from PGA to PSA at T = 5.0 sec. These observations show that there is no prediction bias in PSA for different T against a range of *ClstD*. Figure 3.23 also shows that the total standard deviations (σ) are approximately constant against *ClstD*, indicating that there is no clear dependency of σ on *ClstD*. Figure 3.24 shows the total residuals against **M**. Similarly, the residuals were sorted into 10 bins, which were equally spaced in **M**. The mean and the standard deviation were plotted for each bin. The figure shows that there is no apparent trend in mean data against **M** from 5.0–9.1 and from PGA to PSA at T = 5.0 sec. These observations indicate that there is no clear prediction bias either in PSA for different T against a range of **M**. Figure 3.24 also shows that the σ are approximately constant against **M**, indicating that there is no clear dependency of σ on **M**.

These residuals are further analyzed by splitting the results into within- and between-event residuals by using mixed-effect models.

$$y_{ij} = \eta_1 + \varepsilon_{ij} \tag{3.32}$$

where y_{ij} is total residual from observed value to predicted value for recording j of event i; η_i is the between-event residual for event i; and ε_{ij} is within-event residual for recording j of event i, respectively. The standard deviation of ε and η are called within-event standard deviation (ϕ) and between-event standard deviation (τ). The ε and η are plotted against various variables.

Figure 3.25 plots ε against *ClstD* for **M** < 7.0 in. The mean and the standard deviation are also plotted for each bin at the central *ClstD* of the bin. There is no apparent trend in mean data from *ClstD* = 10–300 km and from PGA to PSA at T = 5.0 sec. These observations show that there is no prediction bias in PSA for different T against a range of *ClstD* when **M** < 7.0. Figure 3.24 also shows that the standard deviations are approximately constant against *ClstD*, indicating that there is no clear dependency of within-event standard deviation (ϕ) on *ClstD* when **M** < 7.0. Figure 3.26 shows the within-event residuals against *ClstD* for **M** > 7.0. The mean and the standard deviation are plotted for each bin. The figure shows that there is no apparent trend either in mean values against *ClstD* and from PGA to PSA at T = 5.0 sec. These observations indicate that there is no clear prediction bias in PSA for different T against a range of *ClstD* when **M** > 7.0. Figure 3.26 also shows that the ϕ are approximately constant against *ClstD*, indicating that there is no clear dependency of ϕ on *ClstD* when **M** > 7.0. Figure 3.27 shows the ε against V_{s30}. The mean and the standard deviation were plotted for each bin. The figure shows that there is no apparent trend in mean values against V_{s30} from 100 to 2000 m/sec and from PGA to PSA at T = 5.0 sec. These observations indicate that there is no clear prediction bias in PSA for different T against a range of V_{s30}. Figure 3.27 also shows that the ϕ are approximately constant against V_{s30}, indicating that there is no clear dependency of ϕ on V_{s30}.

Figure 3.28 shows the η against **M** from PGA to PSA at T = 5.0 sec. There is no apparent trend in the η against **M** from 5.0–9.1. This observation shows that the **M** dependency of the event term was reasonably removed in the proposed GMPE. Figure 3.28 also shows the standard deviation of the η (τ) in dash lines. The τ is about constant against **M**, indicating that there is no clear dependency of τ on **M**. Figure 3.29 shows the η against D from PGA to PSA

at T = 5.0 sec. There is no apparent trend in the data, indicating that the dependency of the event term on D was reasonably removed in the proposed GMPE. Figure 3.29 also shows the τ in dashed lines. The data variation is roughly constant, indicating that there is no clear dependency of τ on D.

Table 3.4 and Figure 3.30 shows the variation in ϕ, τ, and σ of PSA against T. The σ is large around T = 0.1 sec and small around T = 1.0 sec. τ^2 contributes to the σ^2 from 28 to 50% depending on the period.

Figure 3.31 and Figure 3.32 show the comparison of the proposed model with the observed PSA corrected to engineering bedrock with V_{S30} = 760 m/sec at periods of 0.1, 1.0, and 3.0 sec for two well-recorded interplate and intraplate earthquakes, respectively. The figures present the data beyond the distances of model applicability in Chapter 2. These figures confirm that the SMK model is constrained well within the model applicability of *ClstD* ≤ 300 km when **M** > 7.0. These observations are consistent with the residual plots in Figure 3.23 and Figure 3.26 in which no clear bias was observed within this distance.

Table 3.4 Within-event, between-event, and total standard deviation (ln unit) against *T*.

PSA period (sec)	Within-event standard deviation (ϕ)	Between-event standard deviation (τ)	Total standard deviation (σ)
PGA	0.720	0.485	0.868
0.01	0.698	0.469	0.841
0.02	0.699	0.469	0.841
0.03	0.707	0.482	0.856
0.05	0.745	0.528	0.913
0.075	0.802	0.569	0.983
0.1	0.825	0.561	0.997
0.15	0.811	0.488	0.947
0.2	0.793	0.455	0.914
0.25	0.765	0.434	0.879
0.3	0.742	0.400	0.843
0.4	0.712	0.363	0.799
0.5	0.699	0.338	0.777
0.75	0.707	0.298	0.768
1	0.724	0.296	0.782
1.5	0.764	0.307	0.823
2	0.795	0.267	0.839
3	0.800	0.302	0.855
4	0.796	0.342	0.867
5	0.774	0.355	0.852
7	0.741	0.357	0.823
10	0.700	0.334	0.775
PGV	0.638	0.335	0.721

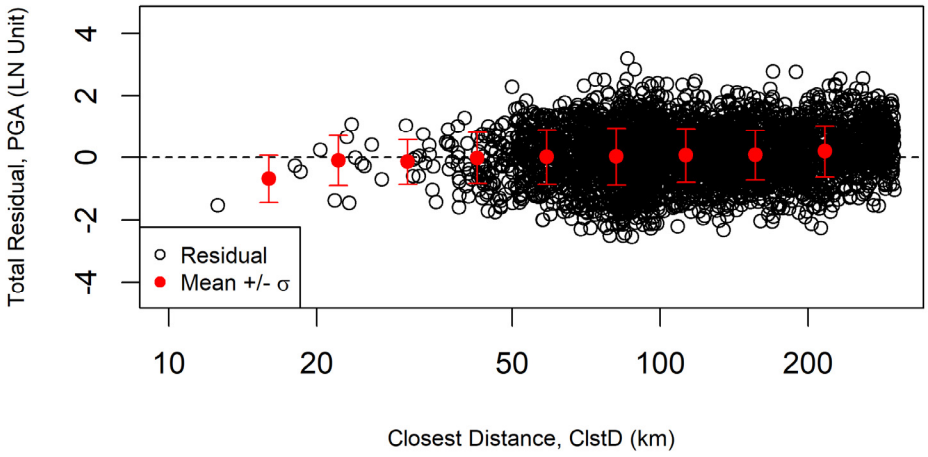

(a)

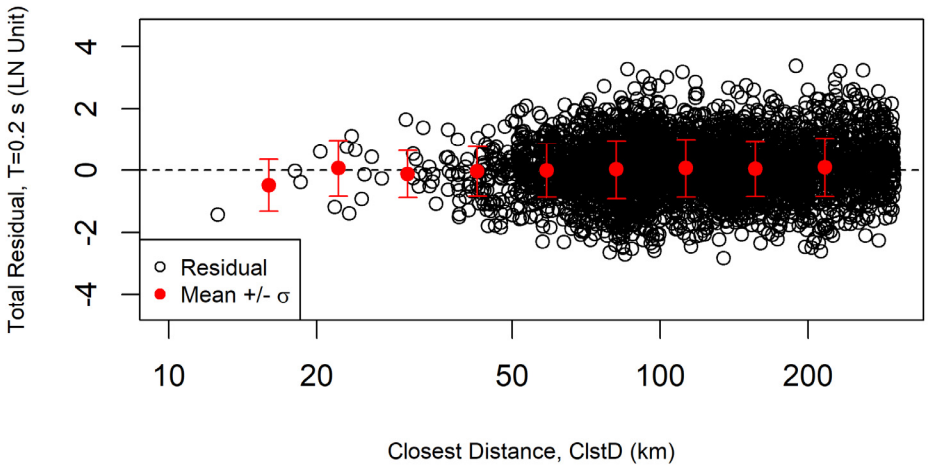

(b)

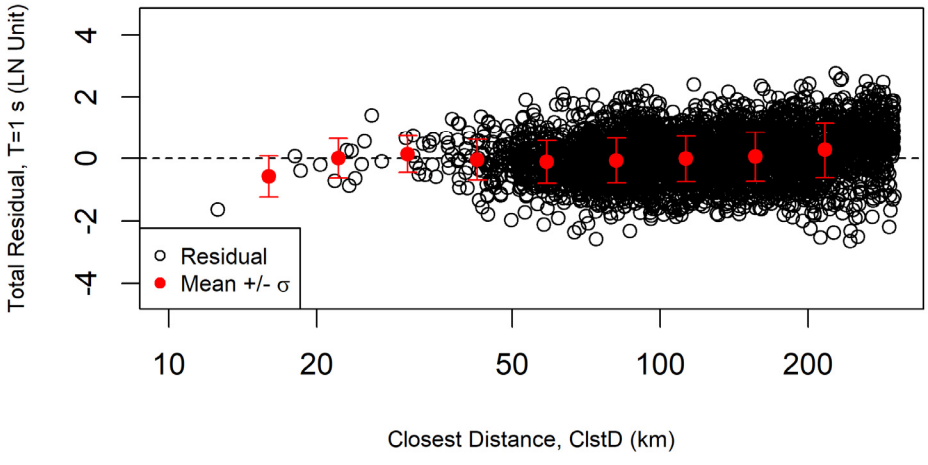

(c)

Figure 3.23 **Total residuals of PSA vs *ClstD*: (a) PGA; (b) *T* = 0.2 sec; (c) *T* = 1.0 sec; (d) *T* = 3.0 sec; and (e) *T* = 5.0 sec.

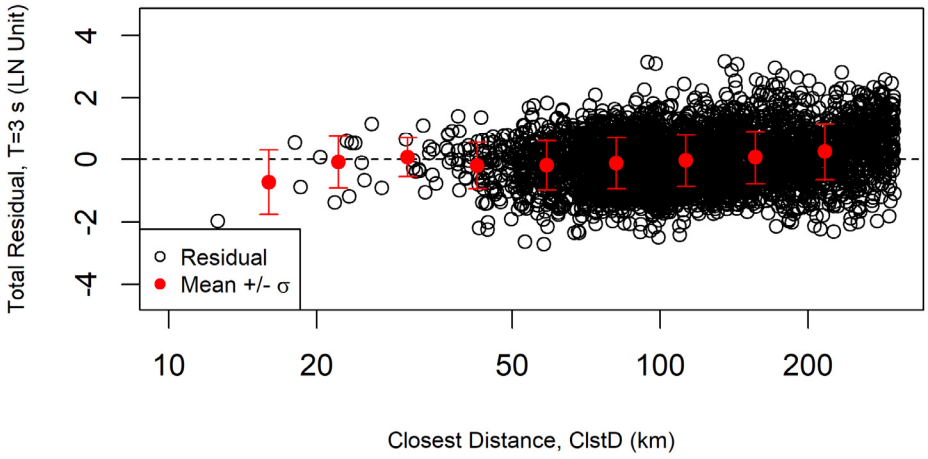

(d)

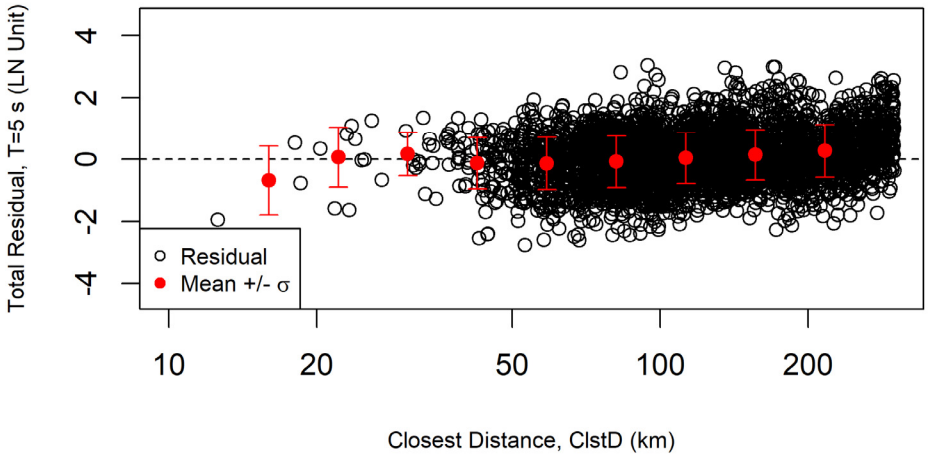

(e)

Figure 3.23 (continued).

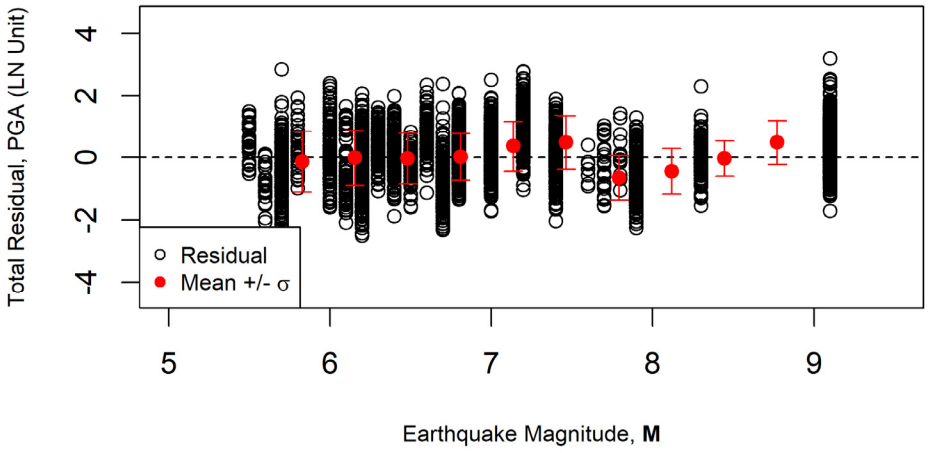

(a)

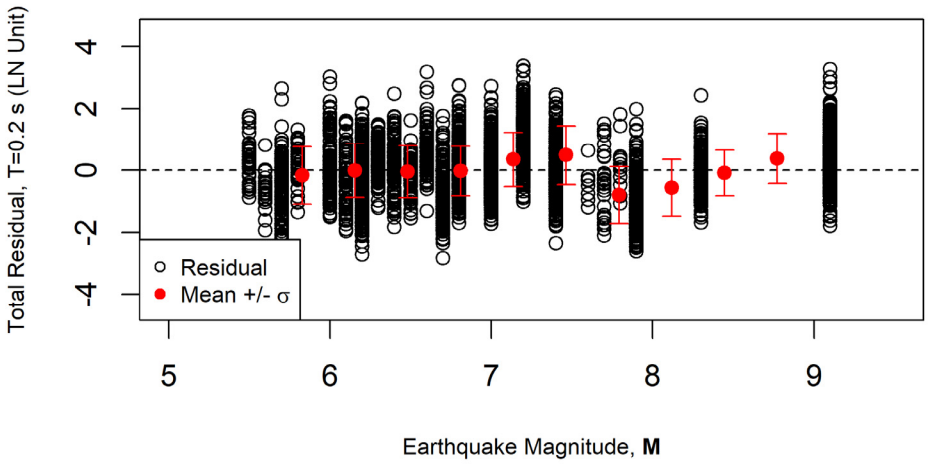

(b)

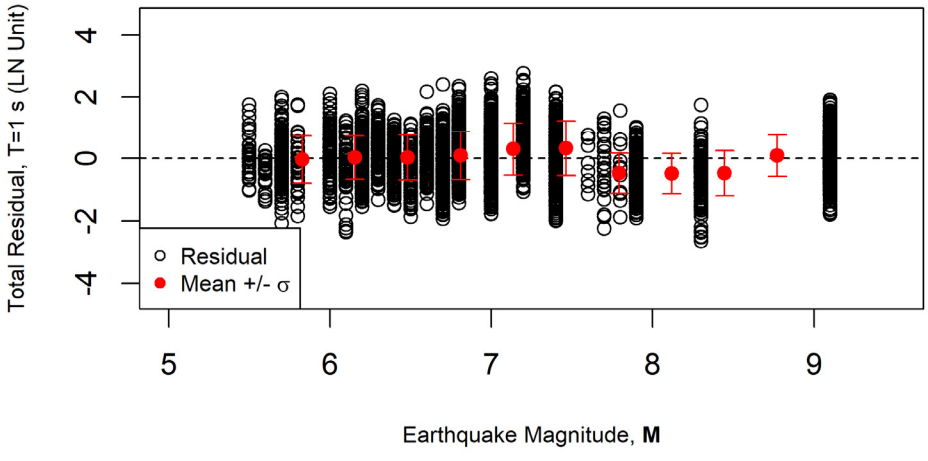

(c)

Figure 3.24 **Total residuals of PSA vs M: (a) PGA, (b) *T* = 0.2 sec, (c) *T* = 1.0 sec; (d) *T* = 3.0 sec; and (e) *T* = 5.0 sec.**

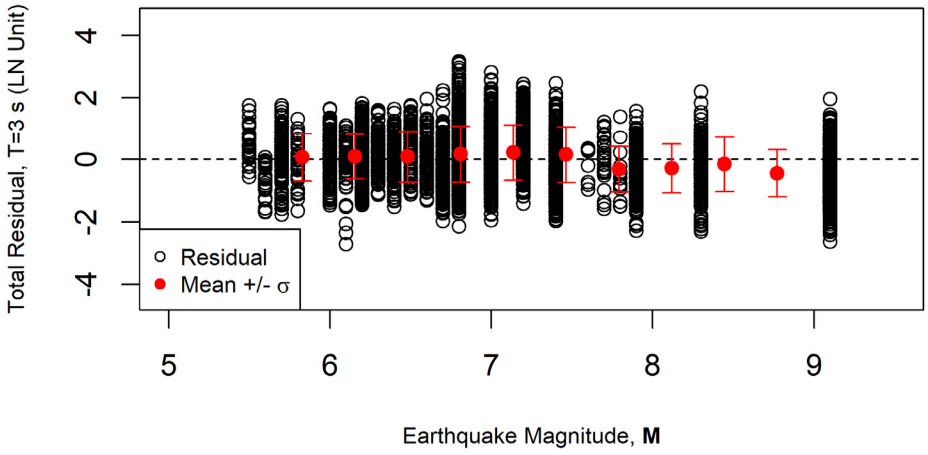

(d)

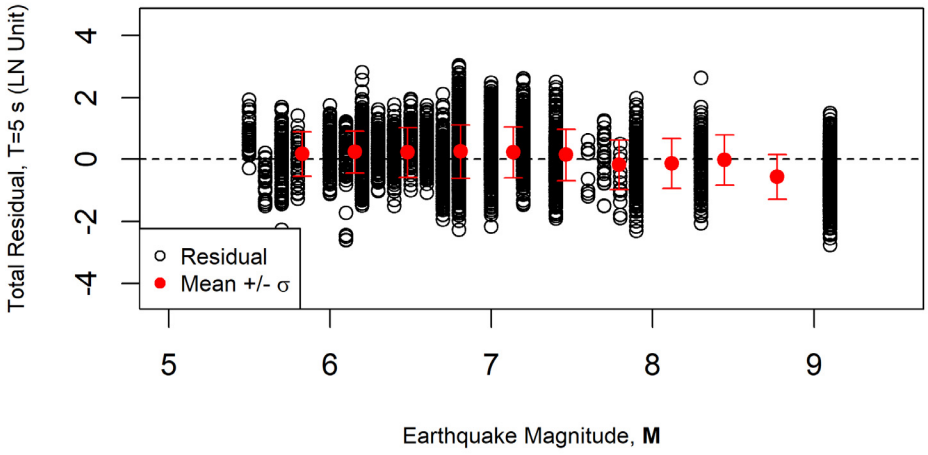

(e)

Figure 3.24 (continued).

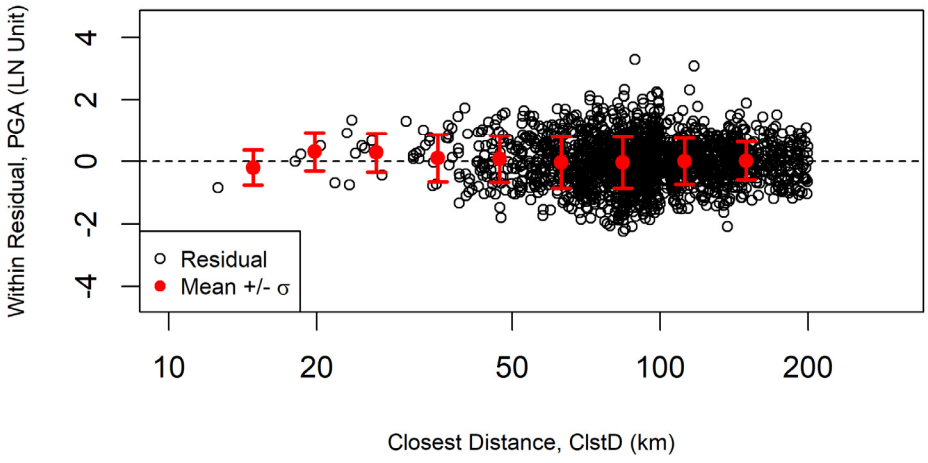

(a)

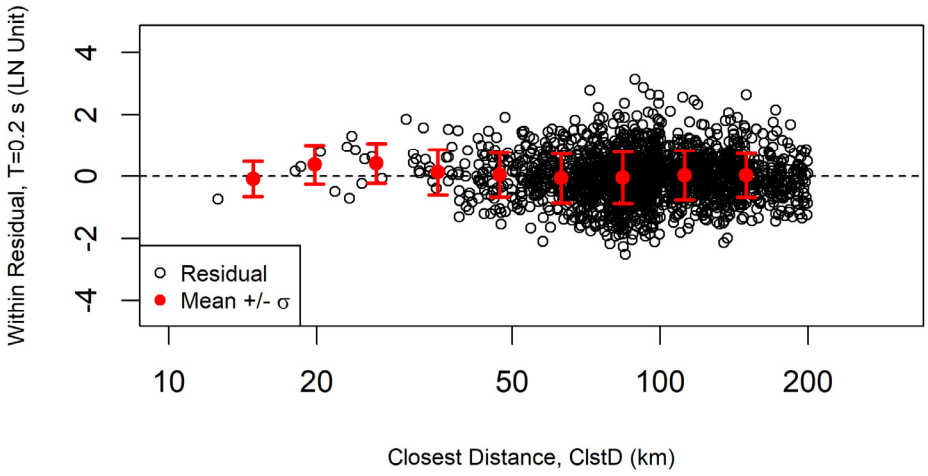

(b)

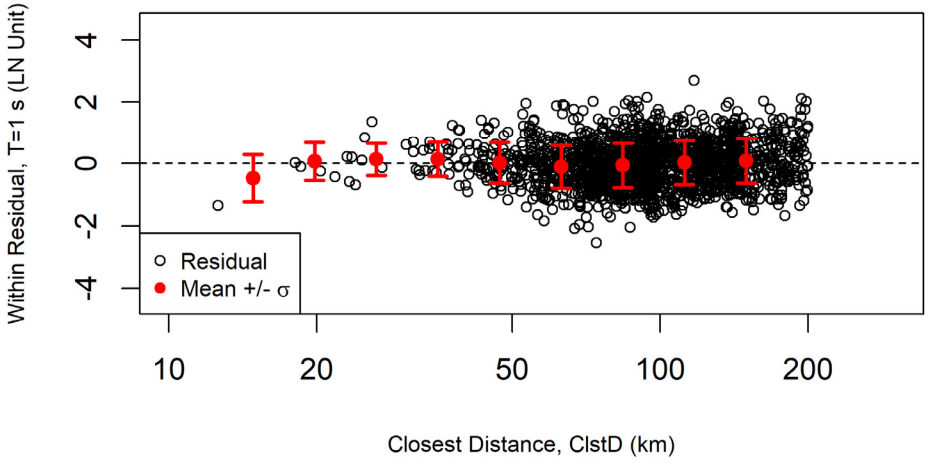

(c)

Figure 3.25 **Within-event residuals of PSA vs *ClstD* for M < 7.0: (a) PGA; (b) *T* = 0.2 sec; (c) *T* = 1.0 sec; (d) *T* = 3.0 sec; and (e) *T* = 5.0 sec.**

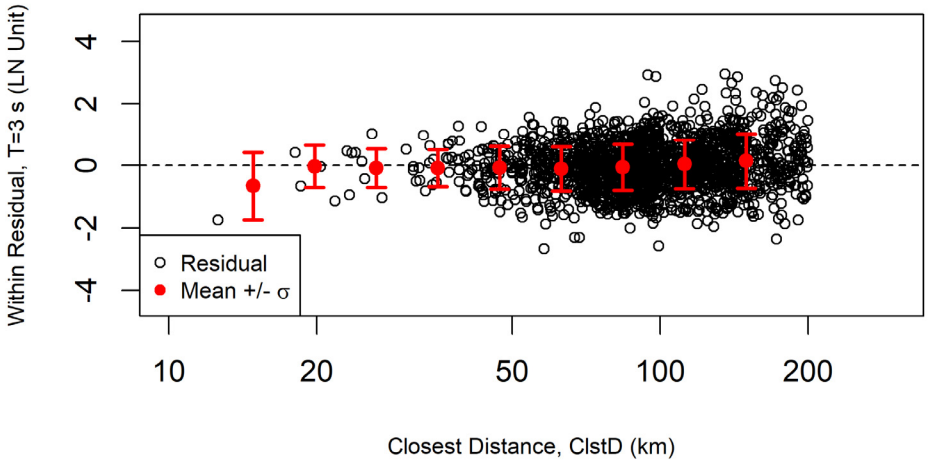

(d)

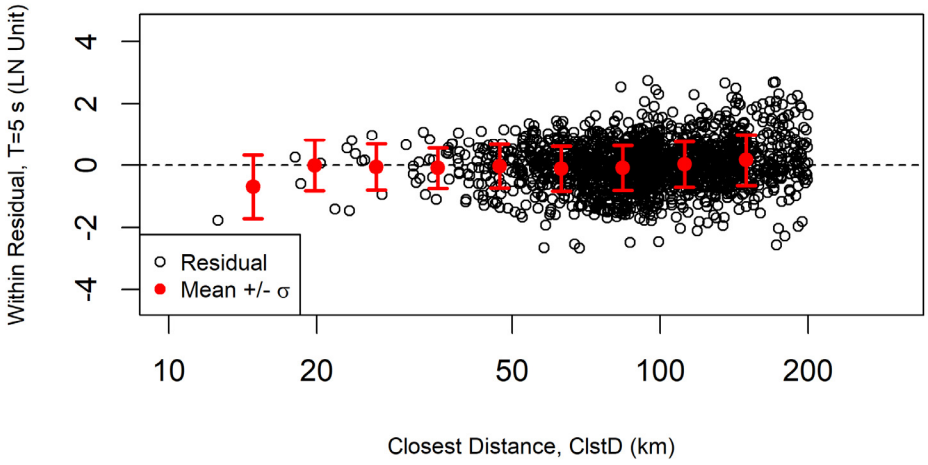

(e)

Figure 3.25 (continued).

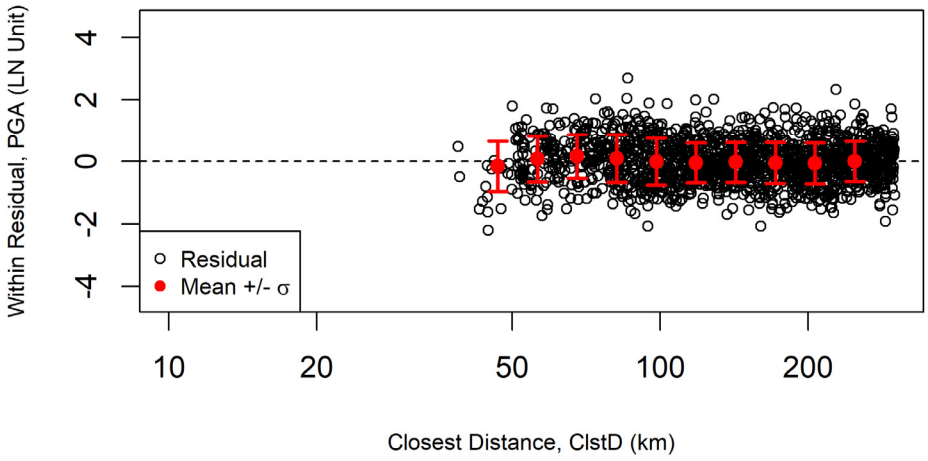

(a)

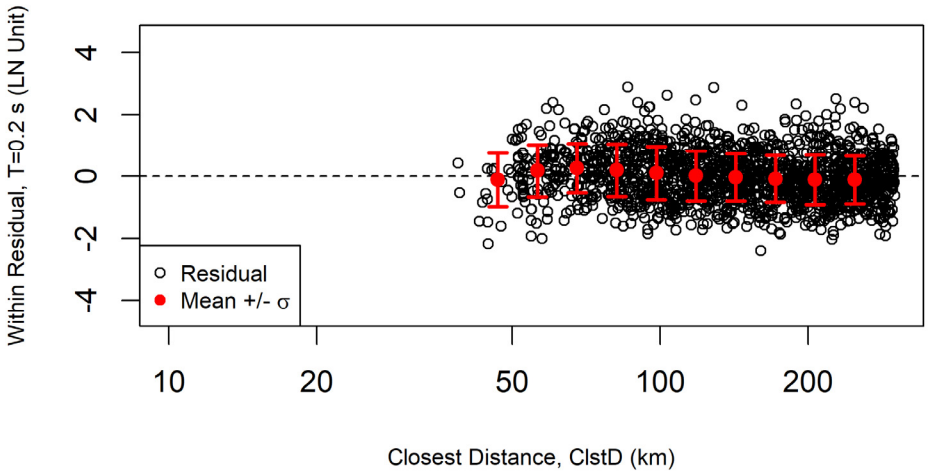

(b)

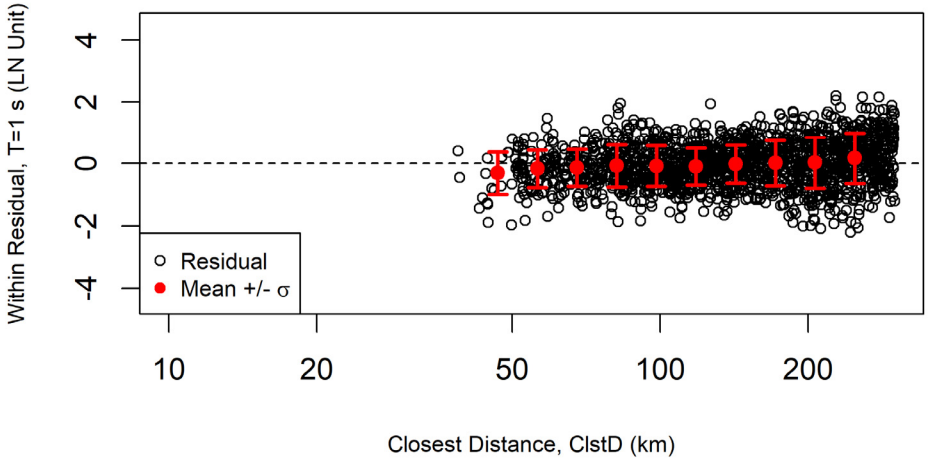

(c)

Figure 3.26 **Within-event residuals of PSA vs *ClstD* for M > 7.0: (a) PGA; (b) *T* = 0.2 sec; (c) *T* = 1.0 sec; (d) *T* = 3.0 sec; and (e) *T* = 5.0 sec.**

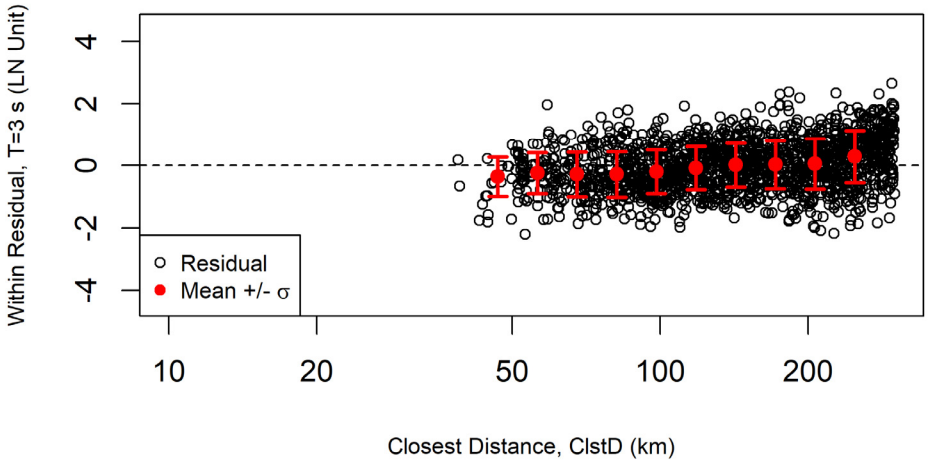

(d)

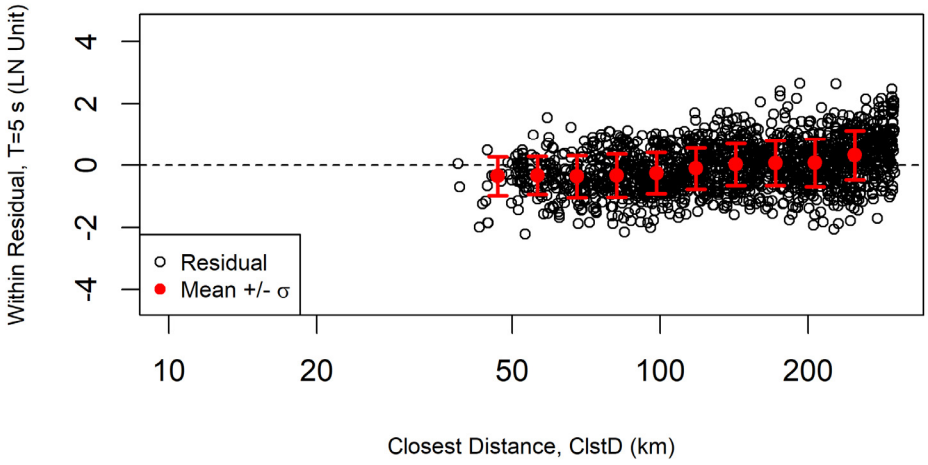

(e)

Figure 3.26 (continued).

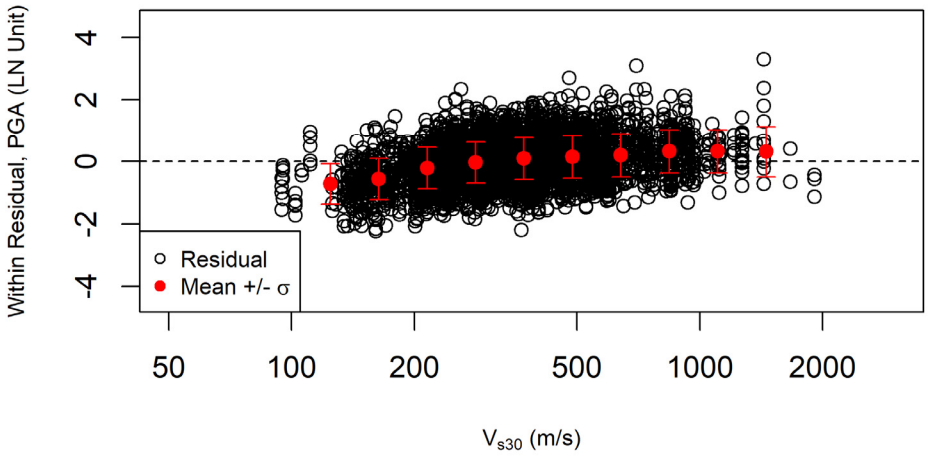

(a)

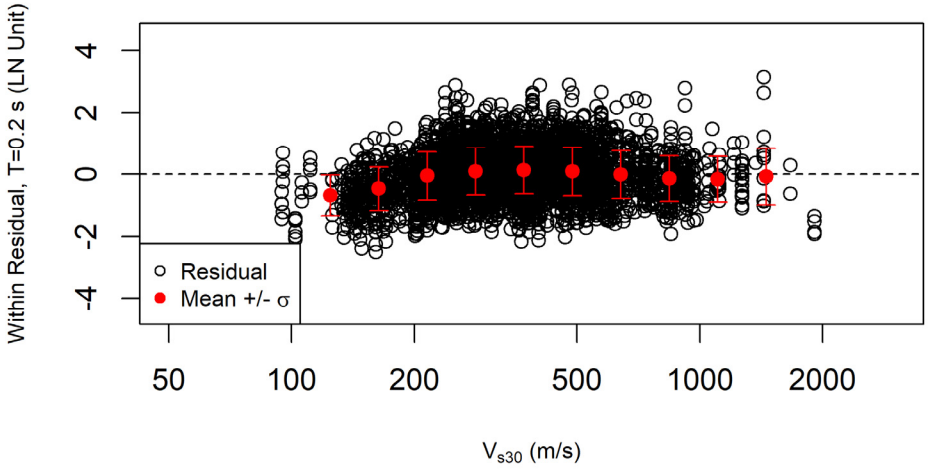

(b)

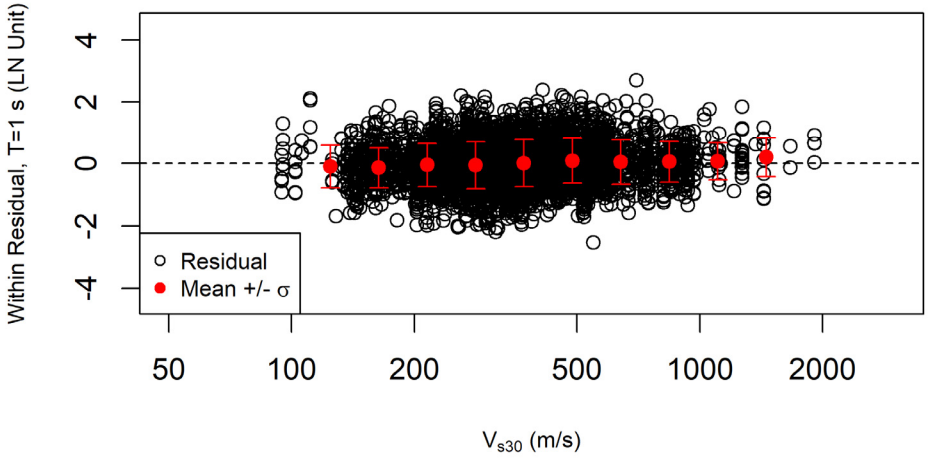

(c)

Figure 3.27 **Within-event residuals of PSA vs V_{s30}: (a) PGA; (b) T = 0.2 sec; (c) T = 1.0 sec; (d) T = 3.0 sec; and (e) T = 5.0 sec.**

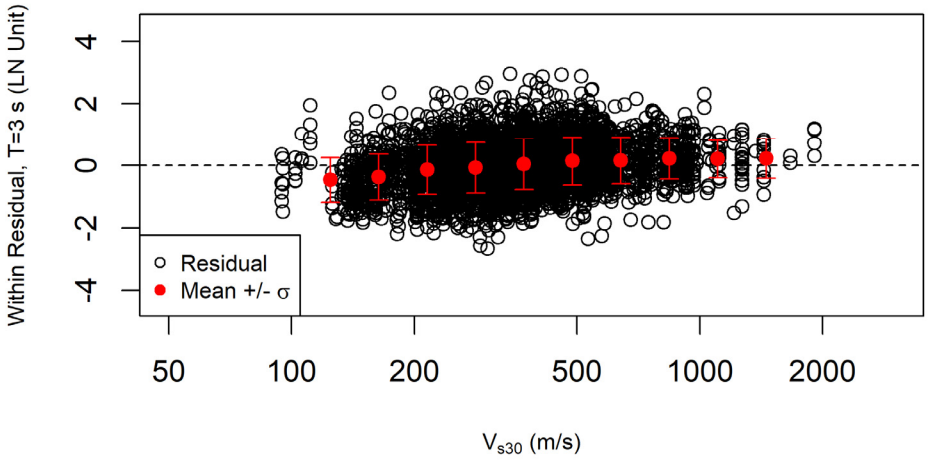

(d)

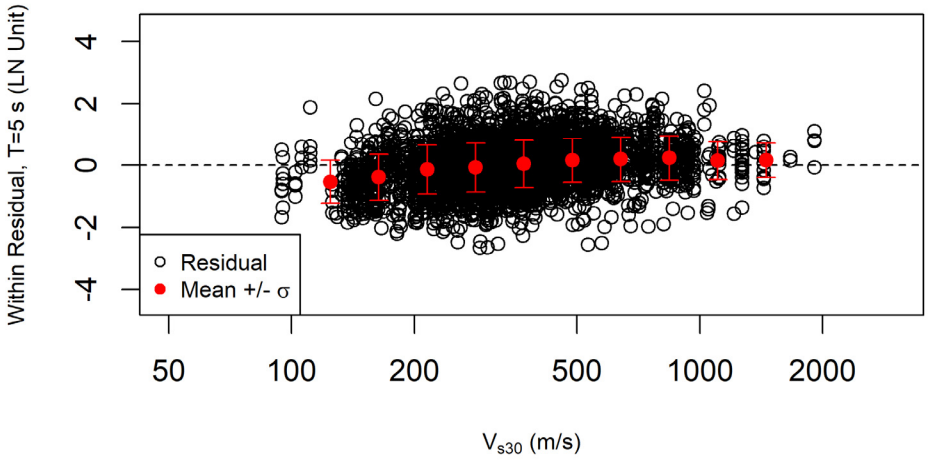

(e)

Figure 3.27 (continued).

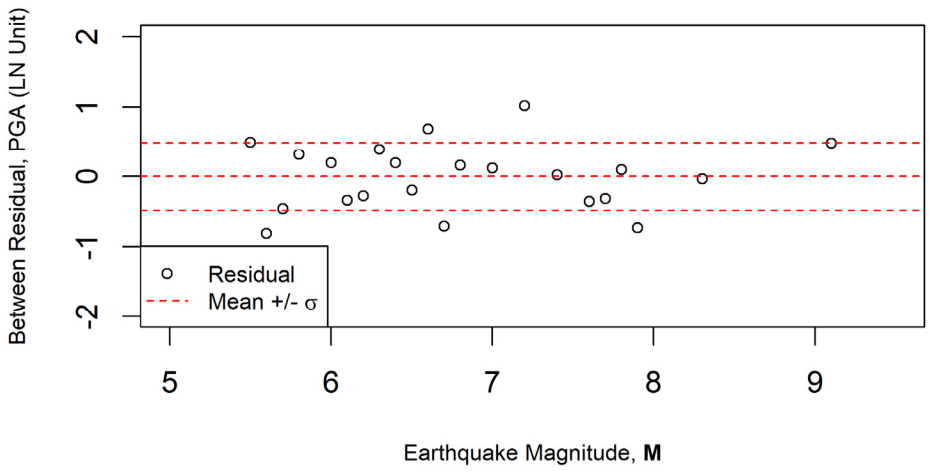

(a)

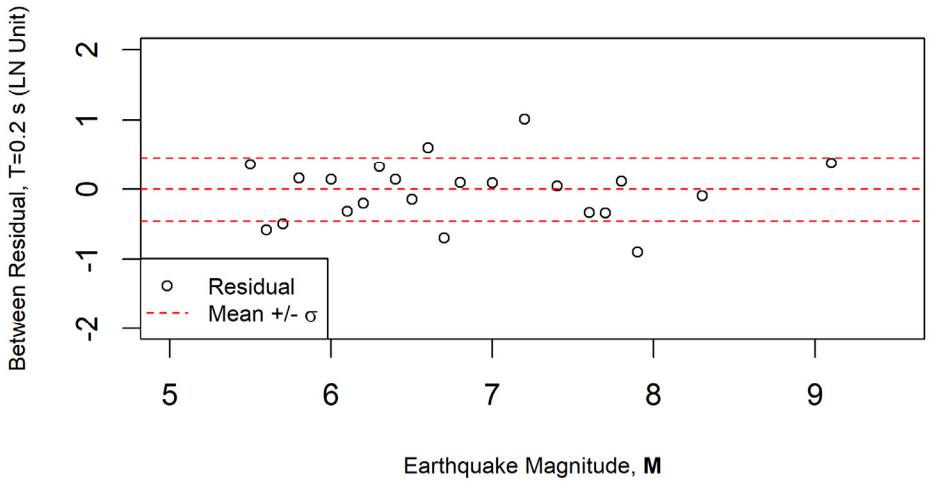

(b)

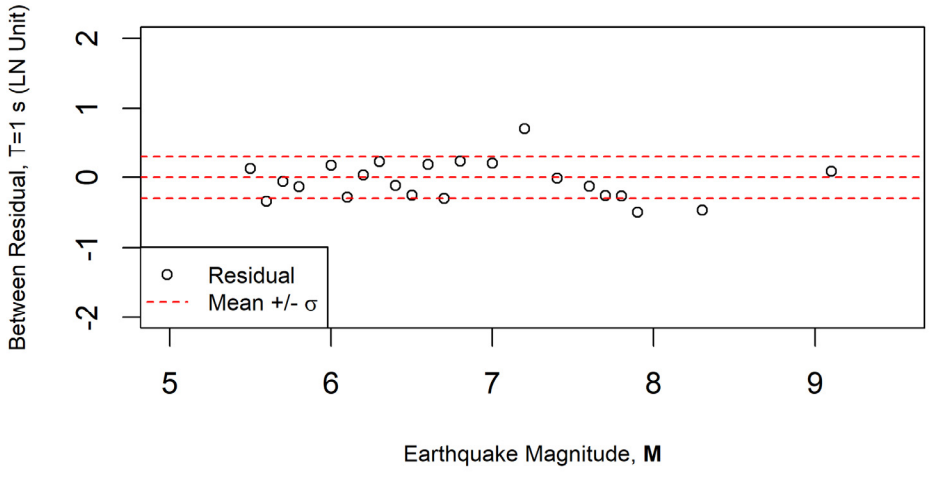

(c)

Figure 3.28 **Between-event residuals of PSA vs M: (a) PGA; (b) *T* = 0.2 sec; (c) *T* = 1.0 sec; (d) *T* = 3.0 sec; and (e) *T* = 5.0 sec.**

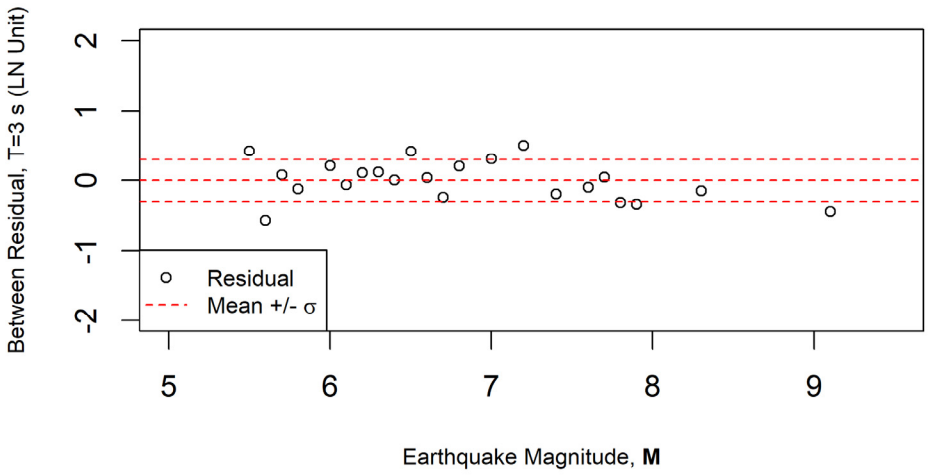

(d)

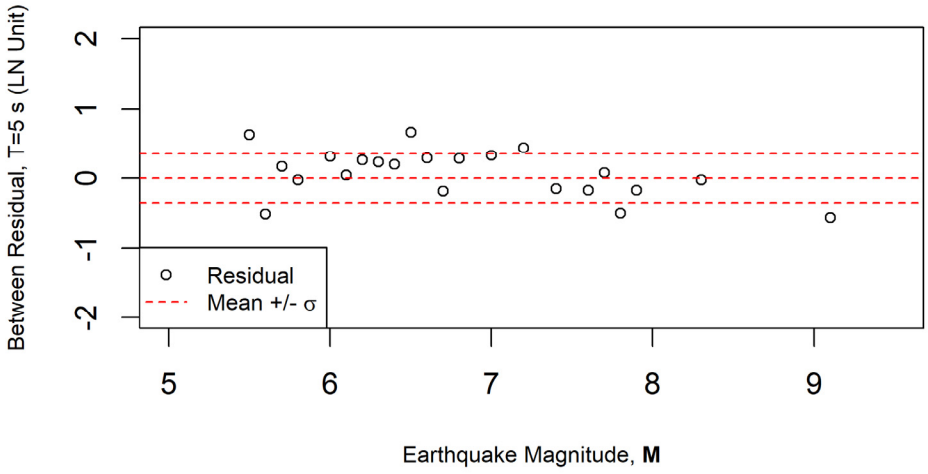

(e)

Figure 3.28 (continued).

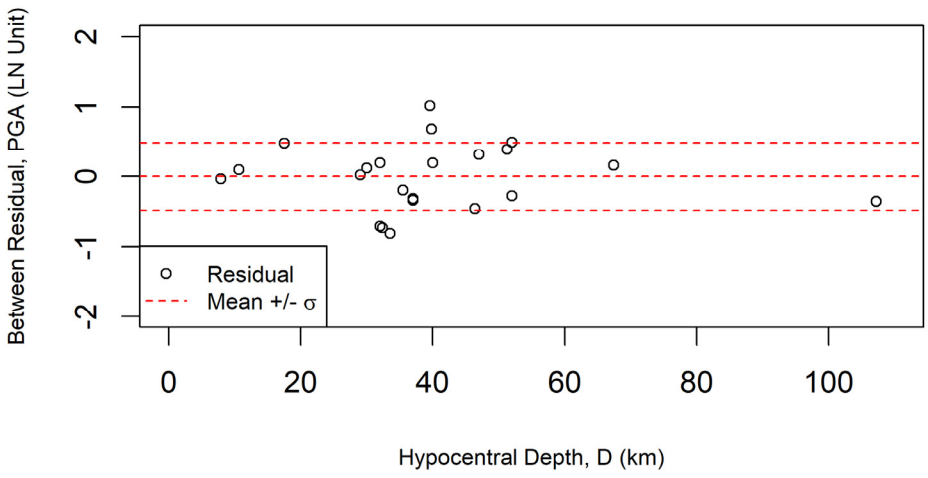

(a)

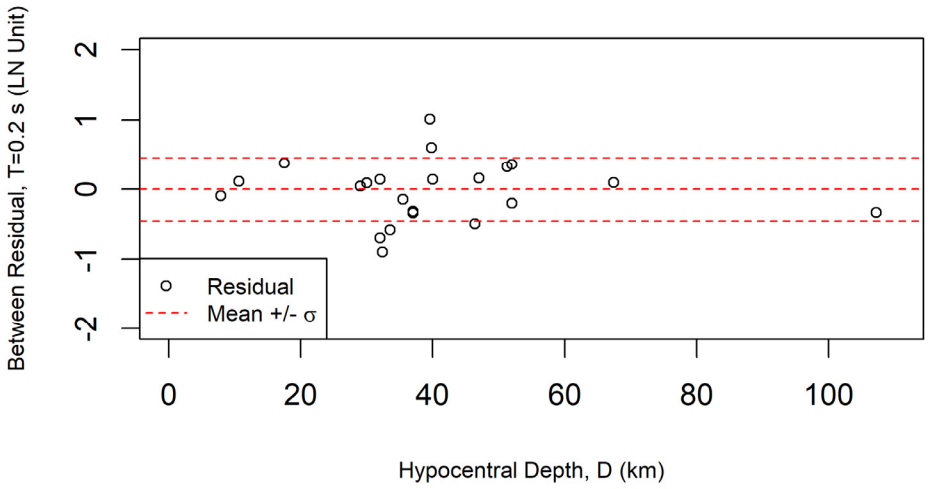

(b)

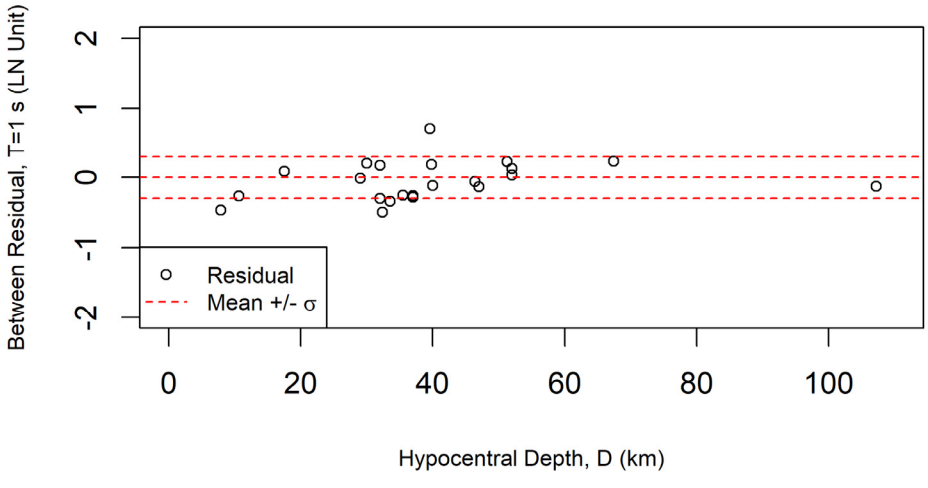

(c)

Figure 3.29 **Between-event residuals of PSA vs hypocentral depth, *D* (km): (a) PGA; (b) *T* = 0.2 sec; (c) *T* = 1.0 sec; (d) *T* = 3.0 sec; and (e) *T* = 5.0 sec.**

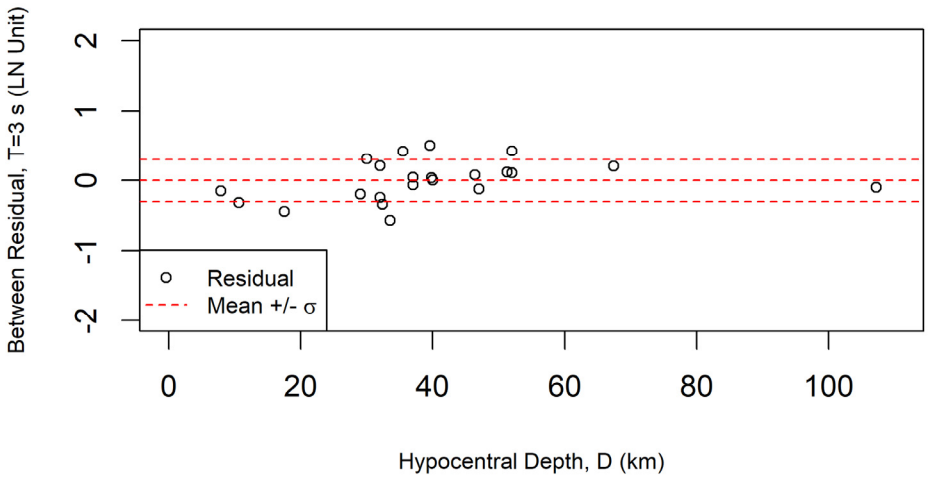

(d)

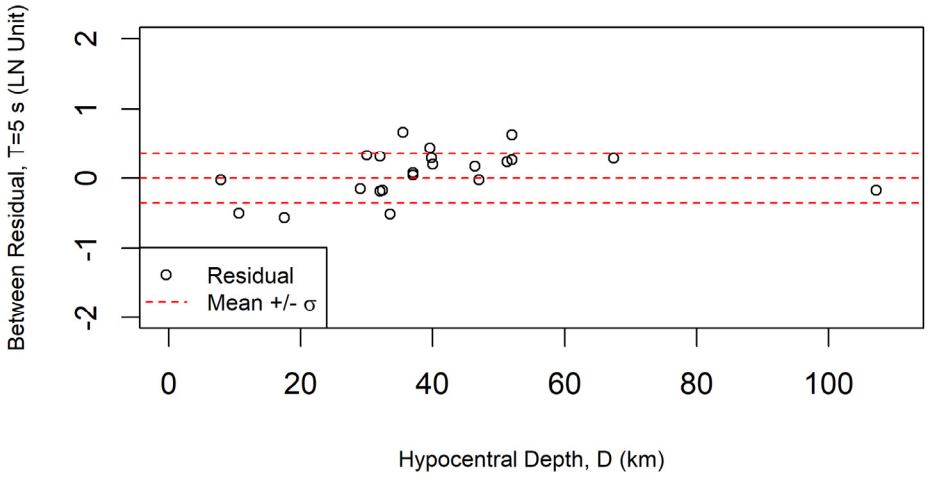

(e)

Figure 3.29 (continued).

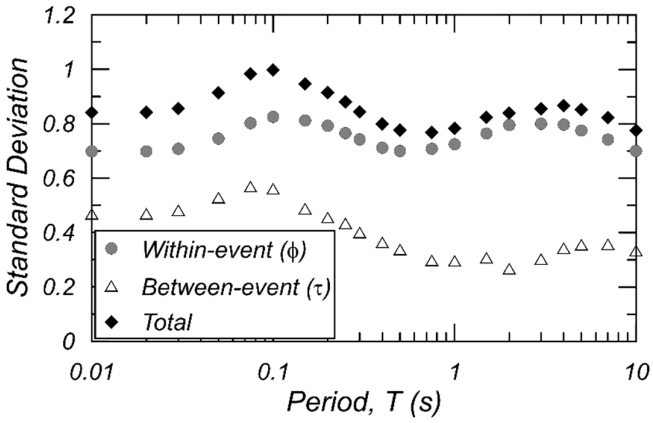

Figure 3.30 **Variation in within-event, between-event and total standard deviations of PSA against *T*.**

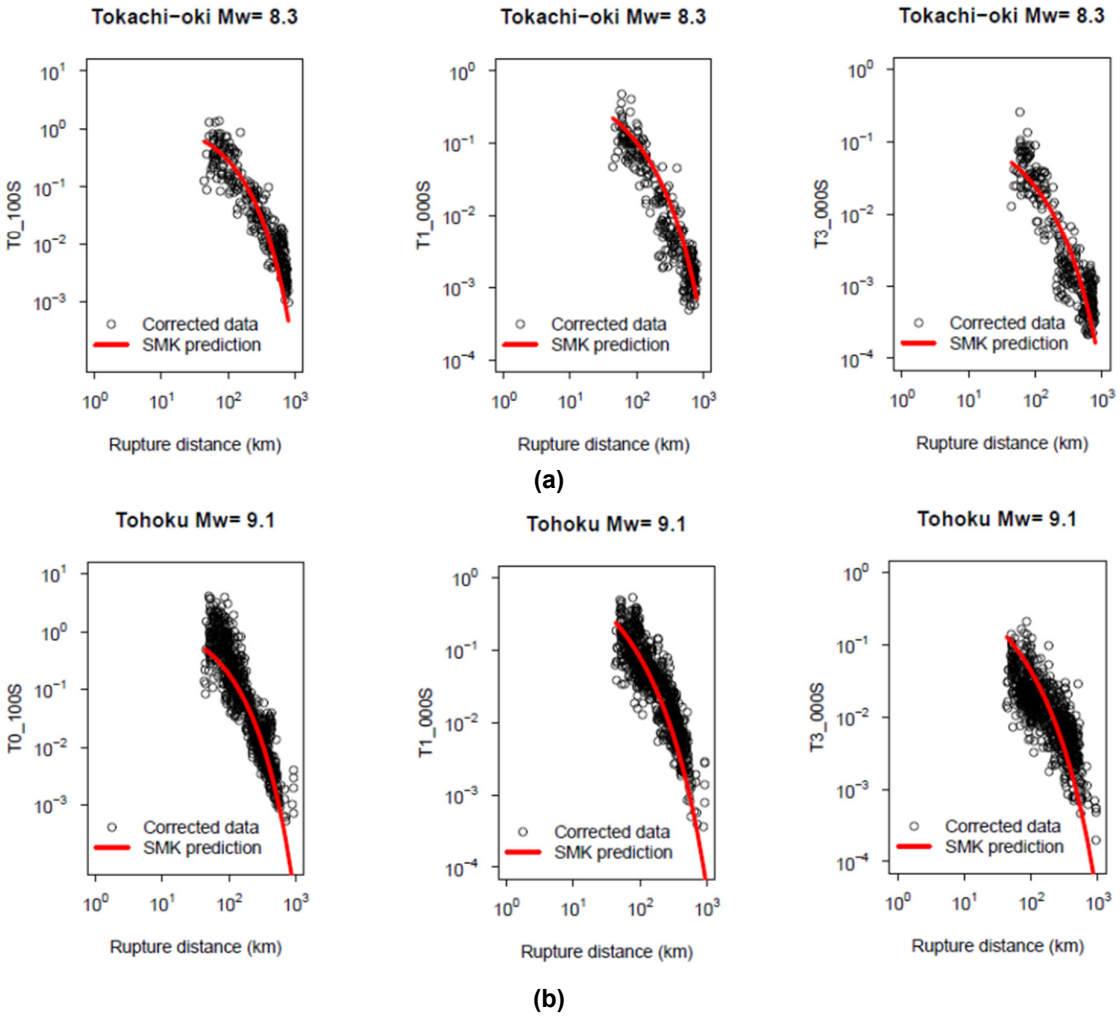

Figure 3.31 **Comparison of SMK model and the observed PSA corrected to engineering bedrock with V_{S30} = 760 m/sec at periods of 0.1 sec, 1.0 sec, and 3.0 sec for two well recorded inter-plate earthquakes: (a) the 2003 Tokachi-Oki earthquake; and (b) the 2011 Tohoku earthquake, respectively.**

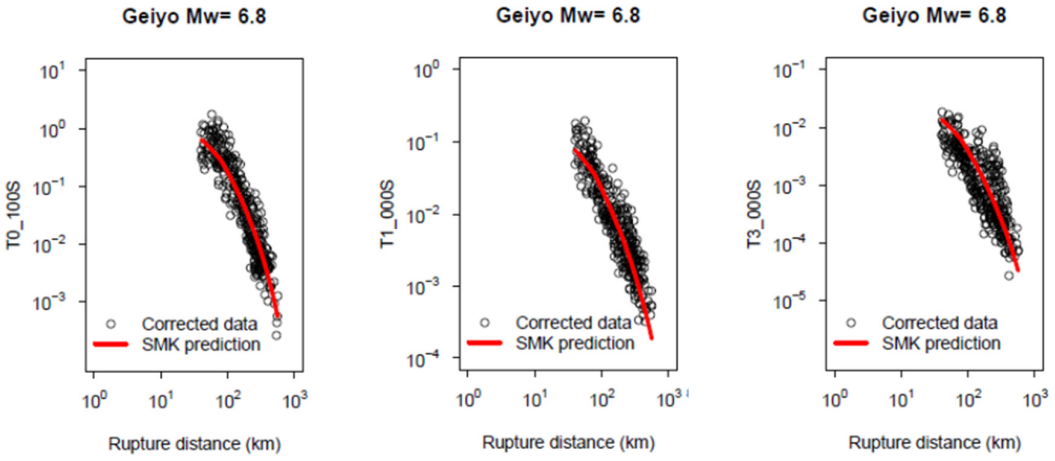

(a)

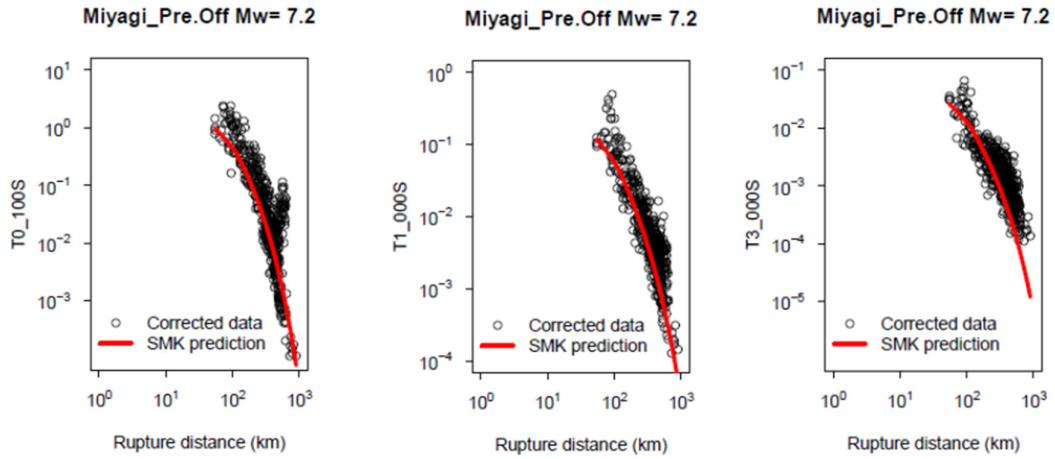

(b)

Figure 3.32 **Comparison of SMK model and the observed PSA corrected to engineering bedrock with V_{S30} = 760 m/sec at periods of 0.1 sec, 1.0 sec, and 3.0 sec for two well recorded intra-plate earthquakes: (a) the 2001 Geiyo earthquake; and (b) the 2011 Miyagi Pref. Off earthquake, respectively.**

4 Summary

Presented herein is a GMPE developed for interplate and intraplate subduction-zone earthquakes in Japan based on the NGA-Sub database. These equations will be useful for many seismic hazard analyses since the adopted formula and predictor variables are relatively simple. Because the amount of recorded data increases continuously, future equations could include revised and additional terms if there is a clear observation with supported physical understanding.

The report presented amplification models for shallow soils. A semi-empirical model by Seyhan and Stewart [2014] was modified for nonlinear terms based on strong-motion observations [Midorikawa and Hori 2018] of Japanese earthquakes. Basin amplification models were successively derived from the strong-motion records after removing the shallow-soil response terms and path effects [Midorikawa and Ohtake 2004]. The source effects were modeled—such as magnitude scaling, earthquake-type and hypocentral-depth dependencies—using ground-motion parameters at reference-rock sites after removing the path effects per Si et al. [2016] and Ibrahim et al. [2016]. Finally, this GMPE combines site terms, path terms, and source terms.

The proposed GMPE shows that intraplate earthquakes have a larger amplitude of PSA compared to interplate earthquakes. The amplitudes increase as magnitude increases—especially for longer periods—and its influence saturates when **M** is larger than 8. Deeper earthquakes have larger amplitudes than shallower ones at the same C_{IstD}, and its trend is stronger at shorter periods. Attenuation of PSA against C_{IstD} becomes stronger as magnitude decreases at short distances and as hypocentral depth increases. Therefore, the proposed model considers the dependency of PSA on nonlinear magnitude scaling and hypocentral depth for interplate and intraplate earthquakes, with a different attenuation decay for shallower and deeper earthquakes for different periods.

REFERENCES

Boore D.M., Stewart J.P., Seyhan E., Atkinson G.M. (2014). NGA-West 2 equations for predicting PGA, PGV, and 5%-damped PSA for shallow crustal earthquakes, *Earthq. Spectra*, 30(3): 1057–1085.

Douglas J. (2003). Earthquake ground motion estimation using strong motion records: A review of equations for the estimation of peak ground acceleration and response spectral ordinates, *Earth-Science Reviews,* 61(1/2): 43–104.

Ibrahim R., Si H., Koketsu K., Miyake H. (2016). Long-period ground-motion prediction equations for moment magnitude estimation of large earthquakes in Japan, *Bull. Seismol. Soc. Am*., 106: 54–72, doi:10.1785/0120140244.

Joshi A., Midorikawa S. (2005). Attenuation characteristics of ground motion intensity from earthquakes with intermediate depth, *J. Seismol*., 9(1): 23–37.

Kanai K. (1961). An empirical formula for the spectrum of strong earthquake motion, *Bull. Earthq. Res. Inst*., University of Tokyo, 39(1): 8595.

Kishida T., Contreras V, Bozorgnia Y, Abrahamson N.A., Ahdi S.K., Ancheta T.D., Boore D.M., Campbell K.W., Chiou B.S.-J., Darragh R.B., Gregor N., Kuehn N., Kwak D.Y., Kwok A.O., Lin P., Magistrale H., Mazzoni S., Muin S., Midorikawa S., Si H., Silva W.J., Stewart J.P.; Wooddell K.E., Youngs, R.R. (2018). NGA-Sub ground motion database, *Proceedings, Eleventh U.S. National Conference on Earthquake Engineering*, Paper No. 001402, 10 pgs., Los Angeles, CA.

Midorikawa S., Hori A. (2018). Nonlinear site amplification model derived from strong motion records including records of the 2011 Tohoku, Japan, earthquake, *Proceedings, 16th European Conference on Earthquake Engineering*, Paper No. 3452, 7 pgs., Thessaloniki, Greece.

Midorikawa S., Ohtake Y. (2004). Variance of peak ground acceleration and velocity in attenuation relationships, *Proceedings, Thirteenth World Conference on Earthquake Engineering*, Paper No. 325, 10 pgs, Vancouver, B.C., Canada.

Seyhan E., Stewart J. (2014). Semi-empirical nonlinear site amplification from NGA-West2 data and simulations, *Earthq. Spectra*, 30(3): 12411256.

Si H., Koketsu K., Miyake H. (2016). Attenuation characteristics of strong ground motion from megathrust earthquakes in subduction zone—On the pass effects, *J. Japan Assoc. Earthq. Eng.*, 16(1): 96–105, doi:10.5610/jaee.16.1_96 (in Japanese with English abstract).

Si H., Midorikawa S. (2000). Attenuation relationships of peak ground acceleration and velocity considering effects of fault type and site condition, *Proceedings. Twelfth World Conference on Earthquake Engineering,* New Zealand Society for Earthquake Engineering, Paper No. 532, 6 pgs., Auckland, NZ.

APPENDIX A R-code: Proposed Ground Motion Prediction Model

Table A.1 Coefficients of the proposed ground motion prediction model.

T	e	a_1	d_0	d_1	a_2	h	C_d	D_d
0.010	-2.68998	0.498552	0	0.216458	0.000000	0.007288	0.000	0.000
0.020	-2.68899	0.500247	0	0.223950	0.000000	0.007439	0.000	0.000
0.030	-2.66892	0.501942	0	0.231442	0.000000	0.007589	0.000	0.000
0.050	-2.59009	0.505332	0	0.241116	0.000000	0.007853	0.000	0.000
0.075	-2.50409	0.509569	0	0.250082	0.000000	0.008122	0.000	0.000
0.100	-2.46809	0.513807	0	0.255437	0.000000	0.008257	0.000	0.000
0.150	-2.50263	0.522281	0	0.255227	0.000000	0.008109	0.000	0.000
0.200	-2.59464	0.530749	0	0.250353	0.000000	0.007767	0.000	0.000
0.250	-2.70833	0.539207	0	0.245524	0.000000	0.007413	0.000	0.000
0.300	-2.82381	0.547649	0	0.235807	0.000000	0.006936	0.000	0.000
0.400	-3.08718	0.564470	0	0.221383	0.000000	0.006315	0.000	0.000
0.500	-3.34239	0.581188	0	0.208055	0.000000	0.005913	0.000	0.000
0.750	-3.84426	0.622416	0	0.191215	0.111810	0.005148	0.000	0.000
1.000	-4.26100	0.662623	0	0.180722	0.133992	0.004684	-0.001	0.085
1.500	-5.05203	0.738788	0	0.177385	0.255782	0.004415	0.020	0.100
2.000	-5.70886	0.807386	0	0.180866	0.516818	0.004411	0.026	0.117
3.000	-6.73173	0.915403	0	0.179712	0.590622	0.004659	0.021	0.138
4.000	-7.43243	0.985113	0	0.176581	0.624361	0.004797	-0.013	0.168
5.000	-7.87188	1.025265	0	0.174349	0.660155	0.004726	-0.053	0.201
7.000	-8.27432	1.056000	0	0.167460	0.702621	0.003719	-0.084	0.210
10.000	-8.49984	1.071204	0	0.157127	0.617846	0.002209	-0.107	0.196
PGA	-2.73196	0.491752	0	0.211431	0.000000	0.007203	0.000	0.000
PGV	-1.93773	0.644909	0	0.181808	0.000000	0.005427	0.000	0.000

PEER REPORTS

PEER reports are available as a free PDF download from https://peer.berkeley.edu/peer-reports. In addition, printed hard copies of PEER reports can be ordered directly from our printer by following the instructions at https://peer.berkeley.edu/peer-reports. For other related questions about the PEER Report Series, contact the Pacific Earthquake Engineering Research Center, 325 Davis Hall, Mail Code 1792, Berkeley, CA 94720. Tel.: (510) 642-3437; and Email: peer_center@berkeley.edu.

PEER 2020/05 *Conditional Ground-Motion Model for Peak Ground Velocity for Active Crustal Regions.* Norman A. Abrahamson and Sarabjot Bhasin. October 2020.

PEER 2020/04 *Partially Non-Ergodic Ground-Motion Model for Subduction Regions using the NGA-Subduction Database.* Nicolas Kuehn, Yousef Bozognia, Kenneth W. Campbell, and Nicholas Gregor. September 2020.

PEER 2020/03 *NGA-Subduction Global Ground-Motion Models with Regional Adjustment Factors.* Grace A. Parker, Jonathan P. Stewart, David M. Boore, Gail M. Atkinson, and Behzad Hassani. September 2020.

PEER 2020/02 *Data Resources for NGA-Subduction Project.* Yousef Bozorgnia (PI) and Jonathan P. Stewart (Editor). March 2020.

PEER 2020/01 *Modeling Viscous Damping in Nonlinear Response History Analysis for Steel Moment-Frame Buildings.* Xin Qian, Anil K. Chopra, and Frank McKenna. June 2020.

PEER 2019/09 Seismic Behavior of Special Concentric Braced Frames under Short- and Long-Duration Ground Motions. Ali Hammad and Mohamed A. Moustafa. December 2019.

PEER 2019/08 Influence of Vertical Ground Motion on Bridges Isolated with Spherical Sliding Bearings. Rushil Mojidra and Keri L. Ryan. December 2019.

PEER 2019/07 *PEER Hub ImageNet* (ϕ-Net): *A Large-Scale Multi-Attribute Benchmark Dataset of Structural Images*. Yuqing Gao, and Khalid. M. Mosalam. November 2019.

PEER 2019/06 *Fluid-Structure Interaction and Python-Scripting Capabilities in OpenSees*. Minjie Zhu and Michael H. Scott. August 2019.

PEER 2019/05 *Expected Earthquake Performance of Buildings Designed to the California Building Code (California Alfred E. Alquist Seismic Safety Publication 19-01).* Grace S. Kang, Sifat Muin, Jorge Archbold, Bitanoosh Woods, and Khalid Mosalam. July 2019.

PEER 2019/04 *Aftershock Seismic Vulnerability and Time-Dependent Risk Assessment of Bridges*. Sujith Mangalathu, Mehrdad Shokrabadi, and Henry V. Burton. May 2019.

PEER 2019/03 *Ground-Motion Directivity Modeling for Seismic Hazard Applications*. Jennifer L. Donahue, Jonathan P. Stewart, Nicolas Gregor, and Yousef Bozorgnia. Review Panel: Jonathan D. Bray, Stephen A. Mahin, I. M. Idriss, Robert W. Graves, and Tom Shantz. May 2019.

PEER 2019/02 *Direct-Finite-Element Method for Nonlinear Earthquake Analysis of Concrete Dams Including Dam–Water–Foundation Rock Interaction.* Arnkjell Løkke and Anil K. Chopra. March 2019.

PEER 2019/01 *Flow-Failure Case History of the Las Palmas, Chile, Tailings Dam.* R. E. S. Moss, T. R. Gebhart, D. J. Frost, and C. Ledezma. January 2019.

PEER 2018/08 *Central and Eastern North America Ground-Motion Characterization: NGA-East Final Report*. Christine Goulet, Yousef Bozorgnia, Norman Abrahamson, Nicolas Kuehn, Linda Al Atik, Robert Youngs, Robert Graves, and Gail Atkinson. December 2018.

PEER 2018/07 *An Empirical Model for Fourier Amplitude Spectra using the NGA-West2 Database*. Jeff Bayless, and Norman A. Abrahamson. December 2018.

PEER 2018/06 *Estimation of Shear Demands on Rock-Socketed Drilled Shafts subjected to Lateral Loading*. Pedro Arduino, Long Chen, and Christopher R. McGann. December 2018.

PEER 2018/05 *Selection of Random Vibration Procedures for the NGA-East Project*. Albert Kottke, Norman A. Abrahamson, David M. Boore, Yousef Bozorgnia, Christine Goulet, Justin Hollenback, Tadahiro Kishida, Armen Der Kiureghian, Olga-Joan Ktenidou, Nicolas Kuehn, Ellen M. Rathje, Walter J. Silva, Eric Thompson, and Xiaoyue Wang. December 2018.

PEER 2018/04 *Capturing Directivity Effects in the Mean and Aleatory Variability of the NGA-West 2 Ground Motion Prediction Equations.* Jennie A. Watson-Lamprey. November 2018.

PEER 2018/03 *Probabilistic Seismic Hazard Analysis Code Verification*. Christie Hale, Norman Abrahamson, and Yousef Bozorgnia. July 2018.

PEER 2018/02 *Update of the BCHydro Subduction Ground-Motion Model using the NGA-Subduction Dataset.* Norman Abrahamson, Nicolas Kuehn, Zeynep Gulerce, Nicholas Gregor, Yousef Bozorgnia, Grace Parker, Jonathan Stewart, Brian Chiou, I. M. Idriss, Kenneth Campbell, and Robert Youngs. June 2018.

PEER 2018/01 *PEER Annual Report 2017–2018*. Khalid Mosalam, Amarnath Kasalanati, and Selim Günay. June 2018.

PEER 2017/12 *Experimental Investigation of the Behavior of Vintage and Retrofit Concentrically Braced Steel Frames under Cyclic Loading*. Barbara G. Simpson, Stephen A. Mahin, and Jiun-Wei Lai, December 2017.

PEER 2017/11 *Preliminary Studies on the Dynamic Response of a Seismically Isolated Prototype Gen-IV Sodium-Cooled Fast Reactor* (*PGSFR*). Benshun Shao, Andreas H. Schellenberg, Matthew J. Schoettler, and Stephen A. Mahin. December 2017.

PEER 2017/10 *Development of Time Histories for IEEE693 Testing and Analysis (including Seismically Isolated Equipment).* Shakhzod M. Takhirov, Eric Fujisaki, Leon Kempner, Michael Riley, and Brian Low. December 2017.

PEER 2017/09 *""R" Package for Computation of Earthquake Ground-Motion Response Spectra.* Pengfei Wang, Jonathan P. Stewart, Yousef Bozorgnia, David M. Boore, and Tadahiro Kishida. December 2017.

PEER 2017/08 *Influence of Kinematic SSI on Foundation Input Motions for Bridges on Deep Foundations*. Benjamin J. Turner, Scott J. Brandenberg, and Jonathan P. Stewart. November 2017.

PEER 2017/07 *A Nonlinear Kinetic Model for Multi-Stage Friction Pendulum Systems*. Paul L. Drazin and Sanjay Govindjee. September 2017.

PEER 2017/06 *Guidelines for Performance-Based Seismic Design of Tall Buildings, Version 2.02*. TBI Working Group led by co-chairs Ron Hamburger and Jack Moehle: Jack Baker, Jonathan Bray, C.B. Crouse, Greg Deierlein, John Hooper, Marshall Lew, Joe Maffei, Stephen Mahin, James Malley, Farzad Naeim, Jonathan Stewart, and John Wallace. May 2017.

PEER 2017/05 *Recommendations for Ergodic Nonlinear Site Amplification in Central and Eastern North America*. Youssef M.A. Hashash, Joseph A. Harmon, Okan Ilhan, Grace A. Parker, and Jonathan P. Stewart. March 2017.

PEER 2017/04 *Expert Panel Recommendations for Ergodic Site Amplification in Central and Eastern North America*. Jonathan P. Stewart, Grace A. Parker, Joseph P. Harmon, Gail M. Atkinson, David M. Boore, Robert B. Darragh, Walter J. Silva, and Youssef M.A. Hashash. March 2017.

PEER 2017/03 *NGA-East Ground-Motion Models for the U.S. Geological Survey National Seismic Hazard Maps*. Christine A. Goulet, Yousef Bozorgnia, Nicolas Kuehn, Linda Al Atik, Robert R. Youngs, Robert W. Graves, and Gail M. Atkinson. March 2017.

PEER 2017/02 *U.S.–New Zealand–Japan Workshop: Liquefaction-Induced Ground Movements Effects, University of California, Berkeley, California, 2–4 November 2016.* Jonathan D. Bray, Ross W. Boulanger, Misko Cubrinovski, Kohji Tokimatsu, Steven L. Kramer, Thomas O'Rourke, Ellen Rathje, Russell A. Green, Peter K. Robinson, and Christine Z. Beyzaei. March 2017.

PEER 2017/01 *2016 PEER Annual Report*. Khalid M. Mosalam, Amarnath Kasalanati, and Grace Kang. March 2017.

PEER 2016/10 *Performance-Based Robust Nonlinear Seismic Analysis with Application to Reinforced Concrete Bridge Systems*. Xiao Ling and Khalid M. Mosalam. December 2016.

PEER 2017/09 *Detailing Requirements for Column Plastic Hinges subjected to Combined Flexural, Axial, and Torsional Seismic Loading.* Gabriel Hurtado and Jack P. Moehle. December 2016.

PEER 2016/08 *Resilience of Critical Structures, Infrastructure, and Communities*. Gian Paolo Cimellaro, Ali Zamani-Noori, Omar Kamouh, Vesna Terzic, and Stephen A. Mahin. December 2016.

PEER 2016/07 *Hybrid Simulation Theory for a Classical Nonlinear Dynamical System*. Paul L. Drazin and Sanjay Govindjee. September 2016.

PEER 2016/06 *California Earthquake Early Warning System Benefit Study*. Laurie A. Johnson, Sharyl Rabinovici, Grace S. Kang, and Stephen A. Mahin. July 2006.

PEER 2016/05 *Ground-Motion Prediction Equations for Arias Intensity Consistent with the NGA-West2 Ground-Motion Models.* Charlotte Abrahamson, Hao-Jun Michael Shi, and Brian Yang. July 2016.

PEER 2016/04 *The M_W 6.0 South Napa Earthquake of August 24, 2014: A Wake-Up Call for Renewed Investment in Seismic Resilience Across California.* Prepared for the California Seismic Safety Commission, Laurie A. Johnson and Stephen A. Mahin. May 2016.

PEER 2016/03 *Simulation Confidence in Tsunami-Driven Overland Flow.* Patrick Lynett. May 2016.

PEER 2016/02 *Semi-Automated Procedure for Windowing time Series and Computing Fourier Amplitude Spectra for the NGA-West2 Database.* Tadahiro Kishida, Olga-Joan Ktenidou, Robert B. Darragh, and Walter J. Silva. May 2016.

PEER 2016/01 *A Methodology for the Estimation of Kappa (κ) from Large Datasets: Example Application to Rock Sites in the NGA-East Database and Implications on Design Motions*. Olga-Joan Ktenidou, Norman A. Abrahamson, Robert B. Darragh, and Walter J. Silva. April 2016.

PEER 2015/13 *Self-Centering Precast Concrete Dual-Steel-Shell Columns for Accelerated Bridge Construction: Seismic Performance, Analysis, and Design*. Gabriele Guerrini, José I. Restrepo, Athanassios Vervelidis, and Milena Massari. December 2015.

PEER 2015/12 *Shear-Flexure Interaction Modeling for Reinforced Concrete Structural Walls and Columns under Reversed Cyclic Loading*. Kristijan Kolozvari, Kutay Orakcal, and John Wallace. December 2015.

PEER 2015/11 *Selection and Scaling of Ground Motions for Nonlinear Response History Analysis of Buildings in Performance-Based Earthquake Engineering*. N. Simon Kwong and Anil K. Chopra. December 2015.

PEER 2015/10 *Structural Behavior of Column-Bent Cap Beam-Box Girder Systems in Reinforced Concrete Bridges Subjected to Gravity and Seismic Loads. Part II: Hybrid Simulation and Post-Test Analysis*. Mohamed A. Moustafa and Khalid M. Mosalam. November 2015.

PEER 2015/09 *Structural Behavior of Column-Bent Cap Beam-Box Girder Systems in Reinforced Concrete Bridges Subjected to Gravity and Seismic Loads. Part I: Pre-Test Analysis and Quasi-Static Experiments*. Mohamed A. Moustafa and Khalid M. Mosalam. September 2015.

PEER 2015/08 *NGA-East: Adjustments to Median Ground-Motion Models for Center and Eastern North America*. August 2015.

PEER 2015/07 *NGA-East: Ground-Motion Standard-Deviation Models for Central and Eastern North America*. Linda Al Atik. June 2015.

PEER 2015/06 *Adjusting Ground-Motion Intensity Measures to a Reference Site for which V_{S30} = 3000 m/sec*. David M. Boore. May 2015.

PEER 2015/05 *Hybrid Simulation of Seismic Isolation Systems Applied to an APR-1400 Nuclear Power Plant.* Andreas H. Schellenberg, Alireza Sarebanha, Matthew J. Schoettler, Gilberto Mosqueda, Gianmario Benzoni, and Stephen A. Mahin. April 2015.

PEER 2015/04 *NGA-East: Median Ground-Motion Models for the Central and Eastern North America Region*. April 2015.

PEER 2015/03 *Single Series Solution for the Rectangular Fiber-Reinforced Elastomeric Isolator Compression Modulus*. James M. Kelly and Niel C. Van Engelen. March 2015.

PEER 2015/02 *A Full-Scale, Single-Column Bridge Bent Tested by Shake-Table Excitation.* Matthew J. Schoettler, José I. Restrepo, Gabriele Guerrini, David E. Duck, and Francesco Carrea. March 2015.

PEER 2015/01 *Concrete Column Blind Prediction Contest 2010: Outcomes and Observations.* Vesna Terzic, Matthew J. Schoettler, José I. Restrepo, and Stephen A Mahin. March 2015.

PEER 2014/20 *Stochastic Modeling and Simulation of Near-Fault Ground Motions for Performance-Based Earthquake Engineering*. Mayssa Dabaghi and Armen Der Kiureghian. December 2014.

PEER 2014/19 *Seismic Response of a Hybrid Fiber-Reinforced Concrete Bridge Column Detailed for Accelerated Bridge Construction*. Wilson Nguyen, William Trono, Marios Panagiotou, and Claudia P. Ostertag. December 2014.

PEER 2014/18 *Three-Dimensional Beam-Truss Model for Reinforced Concrete Walls and Slabs Subjected to Cyclic Static or Dynamic Loading*. Yuan Lu, Marios Panagiotou, and Ioannis Koutromanos. December 2014.

PEER 2014/17 *PEER NGA-East Database*. Christine A. Goulet, Tadahiro Kishida, Timothy D. Ancheta, Chris H. Cramer, Robert B. Darragh, Walter J. Silva, Youssef M.A. Hashash, Joseph Harmon, Jonathan P. Stewart, Katie E. Wooddell, and Robert R. Youngs. October 2014.

PEER 2014/16 *Guidelines for Performing Hazard-Consistent One-Dimensional Ground Response Analysis for Ground Motion Prediction*. Jonathan P. Stewart, Kioumars Afshari, and Youssef M.A. Hashash. October 2014.

PEER 2014/15 *NGA-East Regionalization Report: Comparison of Four Crustal Regions within Central and Eastern North America using Waveform Modeling and 5%-Damped Pseudo-Spectral Acceleration Response*. Jennifer Dreiling, Marius P. Isken, Walter D. Mooney, Martin C. Chapman, and Richard W. Godbee. October 2014.

PEER 2014/14 *Scaling Relations between Seismic Moment and Rupture Area of Earthquakes in Stable Continental Regions*. Paul Somerville. August 2014.

PEER 2014/13 *PEER Preliminary Notes and Observations on the August 24, 2014, South Napa Earthquake*. Grace S. Kang and Stephen A. Mahin, Editors. September 2014.

PEER 2014/12 *Reference-Rock Site Conditions for Central and Eastern North America: Part II – Attenuation (Kappa) Definition*. Kenneth W. Campbell, Youssef M.A. Hashash, Byungmin Kim, Albert R. Kottke, Ellen M. Rathje, Walter J. Silva, and Jonathan P. Stewart. August 2014.

PEER 2014/11 *Reference-Rock Site Conditions for Central and Eastern North America: Part I - Velocity Definition*. Youssef M.A. Hashash, Albert R. Kottke, Jonathan P. Stewart, Kenneth W. Campbell, Byungmin Kim, Ellen M. Rathje, Walter J. Silva, Sissy Nikolaou, and Cheryl Moss. August 2014.

PEER 2014/10 *Evaluation of Collapse and Non-Collapse of Parallel Bridges Affected by Liquefaction and Lateral Spreading*. Benjamin Turner, Scott J. Brandenberg, and Jonathan P. Stewart. August 2014.

PEER 2014/09 *PEER Arizona Strong-Motion Database and GMPEs Evaluation*. Tadahiro Kishida, Robert E. Kayen, Olga-Joan Ktenidou, Walter J. Silva, Robert B. Darragh, and Jennie Watson-Lamprey. June 2014.

PEER 2014/08 *Unbonded Pretensioned Bridge Columns with Rocking Detail*. Jeffrey A. Schaefer, Bryan Kennedy, Marc O. Eberhard, and John F. Stanton. June 2014.

PEER 2014/07 *Northridge 20 Symposium Summary Report: Impacts, Outcomes, and Next Steps*. May 2014.

PEER 2014/06 *Report of the Tenth Planning Meeting of NEES/E-Defense Collaborative Research on Earthquake Engineering*. December 2013.

PEER 2014/05 *Seismic Velocity Site Characterization of Thirty-One Chilean Seismometer Stations by Spectral Analysis of Surface Wave Dispersion*. Robert Kayen, Brad D. Carkin, Skye Corbet, Camilo Pinilla, Allan Ng, Edward Gorbis, and Christine Truong. April 2014.

PEER 2014/04 Effect of Vertical Acceleration on Shear Strength of Reinforced Concrete Columns. Hyerin Lee and Khalid M. Mosalam. April 2014.

PEER 2014/03 *Retest of Thirty-Year-Old Neoprene Isolation Bearings.* James M. Kelly and Niel C. Van Engelen. March 2014.

PEER 2014/02 *Theoretical Development of Hybrid Simulation Applied to Plate Structures.* Ahmed A. Bakhaty, Khalid M. Mosalam, and Sanjay Govindjee. January 2014.

PEER 2014/01 *Performance-Based Seismic Assessment of Skewed Bridges.* Peyman Kaviani, Farzin Zareian, and Ertugrul Taciroglu. January 2014.

PEER 2013/26 *Urban Earthquake Engineerin*g. Proceedings of the U.S.-Iran Seismic Workshop. December 2013.

PEER 2013/25 *Earthquake Engineering for Resilient Communities: 2013 PEER Internship Program Research Report Collection.* Heidi Tremayne (Editor), Stephen A. Mahin (Editor), Jorge Archbold Monterossa, Matt Brosman, Shelly Dean, Katherine deLaveaga, Curtis Fong, Donovan Holder, Rakeeb Khan, Elizabeth Jachens, David Lam, Daniela Martinez Lopez, Mara Minner, Geffen Oren, Julia Pavicic, Melissa Quinonez, Lorena Rodriguez, Sean Salazar, Kelli Slaven, Vivian Steyert, Jenny Taing, and Salvador Tena. December 2013.

PEER 2013/24 *NGA-West2 Ground Motion Prediction Equations for Vertical Ground Motions*. September 2013.

PEER 2013/23 *Coordinated Planning and Preparedness for Fire Following Major Earthquakes*. Charles Scawthorn. November 2013.

PEER 2013/22 *GEM-PEER Task 3 Project: Selection of a Global Set of Ground Motion Prediction Equations.* Jonathan P. Stewart, John Douglas, Mohammad B. Javanbarg, Carola Di Alessandro, Yousef Bozorgnia, Norman A. Abrahamson, David M. Boore, Kenneth W. Campbell, Elise Delavaud, Mustafa Erdik, and Peter J. Stafford. December 2013.

PEER 2013/21 *Seismic Design and Performance of Bridges with Columns on Rocking Foundations*. Grigorios Antonellis and Marios Panagiotou. September 2013.

PEER 2013/20 *Experimental and Analytical Studies on the Seismic Behavior of Conventional and Hybrid Braced Frames*. Jiun-Wei Lai and Stephen A. Mahin. September 2013.

PEER 2013/19 *Toward Resilient Communities: A Performance-Based Engineering Framework for Design and Evaluation of the Built Environment.* Michael William Mieler, Bozidar Stojadinovic, Robert J. Budnitz, Stephen A. Mahin, and Mary C. Comerio. September 2013.

PEER 2013/18 *Identification of Site Parameters that Improve Predictions of Site Amplification*. Ellen M. Rathje and Sara Navidi. July 2013.

PEER 2013/17 *Response Spectrum Analysis of Concrete Gravity Dams Including Dam-Water-Foundation Interaction*. Arnkjell Løkke and Anil K. Chopra. July 2013.

PEER 2013/16 *Effect of Hoop Reinforcement Spacing on the Cyclic Response of Large Reinforced Concrete Special Moment Frame Beams.* Marios Panagiotou, Tea Visnjic, Grigorios Antonellis, Panagiotis Galanis, and Jack P. Moehle. June 2013.

PEER 2013/15 *A Probabilistic Framework to Include the Effects of Near-Fault Directivity in Seismic Hazard Assessment*. Shrey Kumar Shahi, Jack W. Baker. October 2013.

PEER 2013/14 *Hanging-Wall Scaling using Finite-Fault Simulations.* Jennifer L. Donahue and Norman A. Abrahamson. September 2013.

PEER 2013/13 *Semi-Empirical Nonlinear Site Amplification and its Application in NEHRP Site Factors*. Jonathan P. Stewart and Emel Seyhan. November 2013.

PEER 2013/12 *Nonlinear Horizontal Site Response for the NGA-West2 Project.* Ronnie Kamai, Norman A. Abramson, Walter J. Silva. May 2013.

PEER 2013/11 *Epistemic Uncertainty for NGA-West2 Models.* Linda Al Atik and Robert R. Youngs. May 2013.

PEER 2013/10 *NGA-West 2 Models for Ground-Motion Directionality*. Shrey K. Shahi and Jack W. Baker. May 2013.

PEER 2013/09 *Final Report of the NGA-West2 Directivity Working Group.* Paul Spudich, Jeffrey R. Bayless, Jack W. Baker, Brian S.J. Chiou, Badie Rowshandel, Shrey Shahi, and Paul Somerville. May 2013.

PEER 2013/08 *NGA-West2 Model for Estimating Average Horizontal Values of Pseudo-Absolute Spectral Accelerations Generated by Crustal Earthquakes*. I. M. Idriss. May 2013.

PEER 2013/07 *Update of the Chiou and Youngs NGA Ground Motion Model for Average Horizontal Component of Peak Ground Motion and Response Spectra*. Brian Chiou and Robert Youngs. May 2013.

PEER 2013/06 *NGA-West2 Campbell-Bozorgnia Ground Motion Model for the Horizontal Components of PGA, PGV, and 5%-Damped Elastic Pseudo-Acceleration Response Spectra for Periods Ranging from 0.01 to 10 sec.* Kenneth W. Campbell and Yousef Bozorgnia. May 2013.

PEER 2013/05 *NGA-West 2 Equations for Predicting Response Spectral Accelerations for Shallow Crustal Earthquakes*. David M. Boore, Jonathan P. Stewart, Emel Seyhan, and Gail M. Atkinson. May 2013.

PEER 2013/04 *Update of the AS08 Ground-Motion Prediction Equations Based on the NGA-West2 Data Set*. Norman Abrahamson, Walter Silva, and Ronnie Kamai. May 2013.

PEER 2013/03 *PEER NGA-West2 Database.* Timothy D. Ancheta, Robert B. Darragh, Jonathan P. Stewart, Emel Seyhan, Walter J. Silva, Brian S.J. Chiou, Katie E. Wooddell, Robert W. Graves, Albert R. Kottke, David M. Boore, Tadahiro Kishida, and Jennifer L. Donahue. May 2013.

PEER 2013/02 *Hybrid Simulation of the Seismic Response of Squat Reinforced Concrete Shear Walls*. Catherine A. Whyte and Bozidar Stojadinovic. May 2013.

PEER 2013/01 *Housing Recovery in Chile: A Qualitative Mid-program Review*. Mary C. Comerio. February 2013.

PEER 2012/08 *Guidelines for Estimation of Shear Wave Velocity.* Bernard R. Wair, Jason T. DeJong, and Thomas Shantz. December 2012.

PEER 2012/07 *Earthquake Engineering for Resilient Communities: 2012 PEER Internship Program Research Report Collection.* Heidi Tremayne (Editor), Stephen A. Mahin (Editor), Collin Anderson, Dustin Cook, Michael Erceg, Carlos Esparza, Jose Jimenez, Dorian Krausz, Andrew Lo, Stephanie Lopez, Nicole McCurdy, Paul Shipman, Alexander Strum, Eduardo Vega. December 2012.

PEER 2012/06 *Fragilities for Precarious Rocks at Yucca Mountain.* Matthew D. Purvance, Rasool Anooshehpoor, and James N. Brune. December 2012.

PEER 2012/05 *Development of Simplified Analysis Procedure for Piles in Laterally Spreading Layered Soils.* Christopher R. McGann, Pedro Arduino, and Peter Mackenzie–Helnwein. December 2012.

PEER 2012/04 *Unbonded Pre-Tensioned Columns for Bridges in Seismic Regions.* Phillip M. Davis, Todd M. Janes, Marc O. Eberhard, and John F. Stanton. December 2012.

PEER 2012/03 *Experimental and Analytical Studies on Reinforced Concrete Buildings with Seismically Vulnerable Beam-Column Joints*. Sangjoon Park and Khalid M. Mosalam. October 2012.

PEER 2012/02 *Seismic Performance of Reinforced Concrete Bridges Allowed to Uplift during Multi-Directional Excitation*. Andres Oscar Espinoza and Stephen A. Mahin. July 2012.

PEER 2012/01 *Spectral Damping Scaling Factors for Shallow Crustal Earthquakes in Active Tectonic Regions.* Sanaz Rezaeian, Yousef Bozorgnia, I. M. Idriss, Kenneth Campbell, Norman Abrahamson, and Walter Silva. July 2012.

PEER 2011/10 *Earthquake Engineering for Resilient Communities: 2011 PEER Internship Program Research Report Collection*. Heidi Faison and Stephen A. Mahin, Editors. December 2011.

PEER 2011/09 *Calibration of Semi-Stochastic Procedure for Simulating High-Frequency Ground Motions*. Jonathan P. Stewart, Emel Seyhan, and Robert W. Graves. December 2011.

PEER 2011/08 *Water Supply in regard to Fire Following Earthquake*. Charles Scawthorn. November 2011.

PEER 2011/07 *Seismic Risk Management in Urban Areas*. Proceedings of a U.S.-Iran-Turkey Seismic Workshop. September 2011.

PEER 2011/06 *The Use of Base Isolation Systems to Achieve Complex Seismic Performance Objectives*. Troy A. Morgan and Stephen A. Mahin. July 2011.

PEER 2011/05 *Case Studies of the Seismic Performance of Tall Buildings Designed by Alternative Means.* Task 12 Report for the Tall Buildings Initiative. Jack Moehle, Yousef Bozorgnia, Nirmal Jayaram, Pierson Jones, Mohsen Rahnama, Nilesh Shome, Zeynep Tuna, John Wallace, Tony Yang, and Farzin Zareian. July 2011.

PEER 2011/04 *Recommended Design Practice for Pile Foundations in Laterally Spreading Ground.* Scott A. Ashford, Ross W. Boulanger, and Scott J. Brandenberg. June 2011.

PEER 2011/03 *New Ground Motion Selection Procedures and Selected Motions for the PEER Transportation Research Program*. Jack W. Baker, Ting Lin, Shrey K. Shahi, and Nirmal Jayaram. March 2011.

PEER 2011/02 *A Bayesian Network Methodology for Infrastructure Seismic Risk Assessment and Decision Support*. Michelle T. Bensi, Armen Der Kiureghian, and Daniel Straub. March 2011.

PEER 2011/01 *Demand Fragility Surfaces for Bridges in Liquefied and Laterally Spreading Ground.* Scott J. Brandenberg, Jian Zhang, Pirooz Kashighandi, Yili Huo, and Minxing Zhao. March 2011.

PEER 2010/05 *Guidelines for Performance-Based Seismic Design of Tall Buildings.* Developed by the Tall Buildings Initiative. November 2010.

PEER 2010/04 *Application Guide for the Design of Flexible and Rigid Bus Connections between Substation Equipment Subjected to Earthquakes.* Jean-Bernard Dastous and Armen Der Kiureghian. September 2010.

PEER 2010/03 *Shear Wave Velocity as a Statistical Function of Standard Penetration Test Resistance and Vertical Effective Stress at Caltrans Bridge Sites.* Scott J. Brandenberg, Naresh Bellana, and Thomas Shantz. June 2010.

PEER 2010/02 *Stochastic Modeling and Simulation of Ground Motions for Performance-Based Earthquake Engineering.* Sanaz Rezaeian and Armen Der Kiureghian. June 2010.

PEER 2010/01 *Structural Response and Cost Characterization of Bridge Construction Using Seismic Performance Enhancement Strategies.* Ady Aviram, Božidar Stojadinović, Gustavo J. Parra-Montesinos, and Kevin R. Mackie. March 2010.

PEER 2009/03 *The Integration of Experimental and Simulation Data in the Study of Reinforced Concrete Bridge Systems Including Soil-Foundation-Structure Interaction.* Matthew Dryden and Gregory L. Fenves. November 2009.

PEER 2009/02 *Improving Earthquake Mitigation through Innovations and Applications in Seismic Science, Engineering, Communication, and Response*. Proceedings of a U.S.-Iran Seismic Workshop. October 2009.

PEER 2009/01 *Evaluation of Ground Motion Selection and Modification Methods: Predicting Median Interstory Drift Response of Buildings*. Curt B. Haselton, Editor. June 2009.

PEER 2008/10 *Technical Manual for Strata.* Albert R. Kottke and Ellen M. Rathje. February 2009.

PEER 2008/09 *NGA Model for Average Horizontal Component of Peak Ground Motion and Response Spectra.* Brian S.-J. Chiou and Robert R. Youngs. November 2008.

PEER 2008/08 *Toward Earthquake-Resistant Design of Concentrically Braced Steel Structures*. Patxi Uriz and Stephen A. Mahin. November 2008.

PEER 2008/07 *Using OpenSees for Performance-Based Evaluation of Bridges on Liquefiable Soils*. Stephen L. Kramer, Pedro Arduino, and HyungSuk Shin. November 2008.

PEER 2008/06 *Shaking Table Tests and Numerical Investigation of Self-Centering Reinforced Concrete Bridge Columns*. Hyung IL Jeong, Junichi Sakai, and Stephen A. Mahin. September 2008.

PEER 2008/05 *Performance-Based Earthquake Engineering Design Evaluation Procedure for Bridge Foundations Undergoing Liquefaction-Induced Lateral Ground Displacement*. Christian A. Ledezma and Jonathan D. Bray. August 2008.

PEER 2008/04 *Benchmarking of Nonlinear Geotechnical Ground Response Analysis Procedures.* Jonathan P. Stewart, Annie On-Lei Kwok, Youssef M. A. Hashash, Neven Matasovic, Robert Pyke, Zhiliang Wang, and Zhaohui Yang. August 2008.

PEER 2008/03 *Guidelines for Nonlinear Analysis of Bridge Structures in California.* Ady Aviram, Kevin R. Mackie, and Božidar Stojadinović. August 2008.

PEER 2008/02 *Treatment of Uncertainties in Seismic-Risk Analysis of Transportation Systems*. Evangelos Stergiou and Anne S. Kiremidjian. July 2008.

PEER 2008/01 *Seismic Performance Objectives for Tall Buildings.* William T. Holmes, Charles Kircher, William Petak, and Nabih Youssef. August 2008.

PEER 2007/12 *An Assessment to Benchmark the Seismic Performance of a Code-Conforming Reinforced Concrete Moment-Frame Building.* Curt Haselton, Christine A. Goulet, Judith Mitrani-Reiser, James L. Beck, Gregory G. Deierlein, Keith A. Porter, Jonathan P. Stewart, and Ertugrul Taciroglu. August 2008.

PEER 2007/11 *Bar Buckling in Reinforced Concrete Bridge Columns.* Wayne A. Brown, Dawn E. Lehman, and John F. Stanton. February 2008.

PEER 2007/10 *Computational Modeling of Progressive Collapse in Reinforced Concrete Frame Structures*. Mohamed M. Talaat and Khalid M. Mosalam. May 2008.

PEER 2007/09 *Integrated Probabilistic Performance-Based Evaluation of Benchmark Reinforced Concrete Bridges*. Kevin R. Mackie, John-Michael Wong, and Božidar Stojadinović. January 2008.

PEER 2007/08 *Assessing Seismic Collapse Safety of Modern Reinforced Concrete Moment-Frame Buildings*. Curt B. Haselton and Gregory G. Deierlein. February 2008.

PEER 2007/07 *Performance Modeling Strategies for Modern Reinforced Concrete Bridge Columns*. Michael P. Berry and Marc O. Eberhard. April 2008.

PEER 2007/06 *Development of Improved Procedures for Seismic Design of Buried and Partially Buried Structures*. Linda Al Atik and Nicholas Sitar. June 2007.

PEER 2007/05 *Uncertainty and Correlation in Seismic Risk Assessment of Transportation Systems*. Renee G. Lee and Anne S. Kiremidjian. July 2007.

PEER 2007/04 *Numerical Models for Analysis and Performance-Based Design of Shallow Foundations Subjected to Seismic Loading.* Sivapalan Gajan, Tara C. Hutchinson, Bruce L. Kutter, Prishati Raychowdhury, José A. Ugalde, and Jonathan P. Stewart. May 2008.

PEER 2007/03 *Beam-Column Element Model Calibrated for Predicting Flexural Response Leading to Global Collapse of RC Frame Buildings*. Curt B. Haselton, Abbie B. Liel, Sarah Taylor Lange, and Gregory G. Deierlein. May 2008.

PEER 2007/02 *Campbell-Bozorgnia NGA Ground Motion Relations for the Geometric Mean Horizontal Component of Peak and Spectral Ground Motion Parameters*. Kenneth W. Campbell and Yousef Bozorgnia. May 2007.

PEER 2007/01 *Boore-Atkinson NGA Ground Motion Relations for the Geometric Mean Horizontal Component of Peak and Spectral Ground Motion Parameters*. David M. Boore and Gail M. Atkinson. May 2007.

PEER 2006/12 Societal Implications of Performance-Based Earthquake Engineering. Peter J. May. May 2007.

PEER 2006/11 *Probabilistic Seismic Demand Analysis Using Advanced Ground Motion Intensity Measures, Attenuation Relationships, and Near-Fault Effects*. Polsak Tothong and C. Allin Cornell. March 2007.

PEER 2006/10 *Application of the PEER PBEE Methodology to the I-880 Viaduct*. Sashi Kunnath. February 2007.

PEER 2006/09 *Quantifying Economic Losses from Travel Forgone Following a Large Metropolitan Earthquake*. James Moore, Sungbin Cho, Yue Yue Fan, and Stuart Werner. November 2006.

PEER 2006/08 *Vector-Valued Ground Motion Intensity Measures for Probabilistic Seismic Demand Analysis*. Jack W. Baker and C. Allin Cornell. October 2006.

PEER 2006/07 *Analytical Modeling of Reinforced Concrete Walls for Predicting Flexural and Coupled–Shear-Flexural Responses*. Kutay Orakcal, Leonardo M. Massone, and John W. Wallace. October 2006.

PEER 2006/06 *Nonlinear Analysis of a Soil-Drilled Pier System under Static and Dynamic Axial Loading*. Gang Wang and Nicholas Sitar. November 2006.

PEER 2006/05 *Advanced Seismic Assessment Guidelines.* Paolo Bazzurro, C. Allin Cornell, Charles Menun, Maziar Motahari, and Nicolas Luco. September 2006.

PEER 2006/04 *Probabilistic Seismic Evaluation of Reinforced Concrete Structural Components and Systems*. Tae Hyung Lee and Khalid M. Mosalam. August 2006.

PEER 2006/03 *Performance of Lifelines Subjected to Lateral Spreading.* Scott A. Ashford and Teerawut Juirnarongrit. July 2006.

PEER 2006/02 *Pacific Earthquake Engineering Research Center Highway Demonstration Project.* Anne Kiremidjian, James Moore, Yue Yue Fan, Nesrin Basoz, Ozgur Yazali, and Meredith Williams. April 2006.

PEER 2006/01 *Bracing Berkeley. A Guide to Seismic Safety on the UC Berkeley Campus.* Mary C. Comerio, Stephen Tobriner, and Ariane Fehrenkamp. January 2006.

PEER 2005/17 *Earthquake Simulation Tests on Reducing Residual Displacements of Reinforced Concrete Bridges.* Junichi Sakai, Stephen A Mahin, and Andres Espinoza. December 2005.

PEER 2005/16 *Seismic Response and Reliability of Electrical Substation Equipment and Systems.* Junho Song, Armen Der Kiureghian, and Jerome L. Sackman. April 2006.

PEER 2005/15 *CPT-Based Probabilistic Assessment of Seismic Soil Liquefaction Initiation.* R. E. S. Moss, R. B. Seed, R. E. Kayen, J. P. Stewart, and A. Der Kiureghian. April 2006.

PEER 2005/14 *Workshop on Modeling of Nonlinear Cyclic Load-Deformation Behavior of Shallow Foundations.* Bruce L. Kutter, Geoffrey Martin, Tara Hutchinson, Chad Harden, Sivapalan Gajan, and Justin Phalen. March 2006.

PEER 2005/13 *Stochastic Characterization and Decision Bases under Time-Dependent Aftershock Risk in Performance-Based Earthquake Engineering*. Gee Liek Yeo and C. Allin Cornell. July 2005.

PEER 2005/12 *PEER Testbed Study on a Laboratory Building: Exercising Seismic Performance Assessment.* Mary C. Comerio, Editor. November 2005.

PEER 2005/11 *Van Nuys Hotel Building Testbed Report: Exercising Seismic Performance Assessment.* Helmut Krawinkler, Editor. October 2005.

PEER 2005/10 *First NEES/E-Defense Workshop on Collapse Simulation of Reinforced Concrete Building Structures.* September 2005.

PEER 2005/09 *Test Applications of Advanced Seismic Assessment Guidelines.* Joe Maffei, Karl Telleen, Danya Mohr, William Holmes, and Yuki Nakayama. August 2006.

PEER 2005/08 *Damage Accumulation in Lightly Confined Reinforced Concrete Bridge Columns.* R. Tyler Ranf, Jared M. Nelson, Zach Price, Marc O. Eberhard, and John F. Stanton. April 2006.

PEER 2005/07 *Experimental and Analytical Studies on the Seismic Response of Freestanding and Anchored Laboratory Equipment.* Dimitrios Konstantinidis and Nicos Makris. January 2005.

PEER 2005/06 *Global Collapse of Frame Structures under Seismic Excitations*. Luis F. Ibarra and Helmut Krawinkler. September 2005.

PEER 2005//05 *Performance Characterization of Bench- and Shelf-Mounted Equipment.* Samit Ray Chaudhuri and Tara C. Hutchinson. May 2006.

PEER 2005/04 *Numerical Modeling of the Nonlinear Cyclic Response of Shallow Foundations.* Chad Harden, Tara Hutchinson, Geoffrey R. Martin, and Bruce L. Kutter. August 2005.

PEER 2005/03 *A Taxonomy of Building Components for Performance-Based Earthquake Engineering.* Keith A. Porter. September 2005.

PEER 2005/02 *Fragility Basis for California Highway Overpass Bridge Seismic Decision Making*. Kevin R. Mackie and Božidar Stojadinović. June 2005.

PEER 2005/01 *Empirical Characterization of Site Conditions on Strong Ground Motion.* Jonathan P. Stewart, Yoojoong Choi, and Robert W. Graves. June 2005.

PEER 2004/09 *Electrical Substation Equipment Interaction: Experimental Rigid Conductor Studies.* Christopher Stearns and André Filiatrault. February 2005.

PEER 2004/08 *Seismic Qualification and Fragility Testing of Line Break 550-kV Disconnect Switches.* Shakhzod M. Takhirov, Gregory L. Fenves, and Eric Fujisaki. January 2005.

PEER 2004/07 *Ground Motions for Earthquake Simulator Qualification of Electrical Substation Equipment.* Shakhzod M. Takhirov, Gregory L. Fenves, Eric Fujisaki, and Don Clyde. January 2005.

PEER 2004/06 *Performance-Based Regulation and Regulatory Regimes.* Peter J. May and Chris Koski. September 2004.

PEER 2004/05 *Performance-Based Seismic Design Concepts and Implementation: Proceedings of an International Workshop.* Peter Fajfar and Helmut Krawinkler, Editors. September 2004.

PEER 2004/04 *Seismic Performance of an Instrumented Tilt-up Wall Building.* James C. Anderson and Vitelmo V. Bertero. July 2004.

PEER 2004/03 *Evaluation and Application of Concrete Tilt-up Assessment Methodologies.* Timothy Graf and James O. Malley. October 2004.

PEER 2004/02 *Analytical Investigations of New Methods for Reducing Residual Displacements of Reinforced Concrete Bridge Columns.* Junichi Sakai and Stephen A. Mahin. August 2004.

PEER 2004/01 *Seismic Performance of Masonry Buildings and Design Implications.* Kerri Anne Taeko Tokoro, James C. Anderson, and Vitelmo V. Bertero. February 2004.

PEER 2003/18 *Performance Models for Flexural Damage in Reinforced Concrete Columns.* Michael Berry and Marc Eberhard. August 2003.

PEER 2003/17 *Predicting Earthquake Damage in Older Reinforced Concrete Beam-Column Joints.* Catherine Pagni and Laura Lowes. October 2004.

PEER 2003/16 *Seismic Demands for Performance-Based Design of Bridges.* Kevin Mackie and Božidar Stojadinović. August 2003.

PEER 2003/15 *Seismic Demands for Nondeteriorating Frame Structures and Their Dependence on Ground Motions.* Ricardo Antonio Medina and Helmut Krawinkler. May 2004.

PEER 2003/14 *Finite Element Reliability and Sensitivity Methods for Performance-Based Earthquake Engineering*. Terje Haukaas and Armen Der Kiureghian. April 2004.

PEER 2003/13 *Effects of Connection Hysteretic Degradation on the Seismic Behavior of Steel Moment-Resisting Frames.* Janise E. Rodgers and Stephen A. Mahin. March 2004.

PEER 2003/12 *Implementation Manual for the Seismic Protection of Laboratory Contents: Format and Case Studies*. William T. Holmes and Mary C. Comerio. October 2003.

PEER 2003/11 *Fifth U.S.-Japan Workshop on Performance-Based Earthquake Engineering Methodology for Reinforced Concrete Building Structures*. February 2004.

PEER 2003/10 *A Beam-Column Joint Model for Simulating the Earthquake Response of Reinforced Concrete Frames.* Laura N. Lowes, Nilanjan Mitra, and Arash Altoontash. February 2004.

PEER 2003/09 *Sequencing Repairs after an Earthquake: An Economic Approach.* Marco Casari and Simon J. Wilkie. April 2004.

PEER 2003/08 *A Technical Framework for Probability-Based Demand and Capacity Factor Design (DCFD) Seismic Formats*. Fatemeh Jalayer and C. Allin Cornell. November 2003.

PEER 2003/07 *Uncertainty Specification and Propagation for Loss Estimation Using FOSM Methods.* Jack W. Baker and C. Allin Cornell. September 2003.

PEER 2003/06 *Performance of Circular Reinforced Concrete Bridge Columns under Bidirectional Earthquake Loading*. Mahmoud M. Hachem, Stephen A. Mahin, and Jack P. Moehle. February 2003.

PEER 2003/05 *Response Assessment for Building-Specific Loss Estimation.* Eduardo Miranda and Shahram Taghavi. September 2003.

PEER 2003/04 *Experimental Assessment of Columns with Short Lap Splices Subjected to Cyclic Loads*. Murat Melek, John W. Wallace, and Joel Conte. April 2003.

PEER 2003/03 *Probabilistic Response Assessment for Building-Specific Loss Estimation*. Eduardo Miranda and Hesameddin Aslani. September 2003.

PEER 2003/02 *Software Framework for Collaborative Development of Nonlinear Dynamic Analysis Program*. Jun Peng and Kincho H. Law. September 2003.

PEER 2003/01 *Shake Table Tests and Analytical Studies on the Gravity Load Collapse of Reinforced Concrete Frames.* Kenneth John Elwood and Jack P. Moehle. November 2003.

PEER 2002/24 *Performance of Beam to Column Bridge Joints Subjected to a Large Velocity Pulse.* Natalie Gibson, André Filiatrault, and Scott A. Ashford. April 2002.

PEER 2002/23 *Effects of Large Velocity Pulses on Reinforced Concrete Bridge Columns.* Greg L. Orozco and Scott A. Ashford. April 2002.

PEER 2002/22 *Characterization of Large Velocity Pulses for Laboratory Testing.* Kenneth E. Cox and Scott A. Ashford. April 2002.

PEER 2002/21 *Fourth U.S.-Japan Workshop on Performance-Based Earthquake Engineering Methodology for Reinforced Concrete Building Structures*. December 2002.

PEER 2002/20 *Barriers to Adoption and Implementation of PBEE Innovations.* Peter J. May. August 2002.

PEER 2002/19 *Economic-Engineered Integrated Models for Earthquakes: Socioeconomic Impacts.* Peter Gordon, James E. Moore II, and Harry W. Richardson. July 2002.

PEER 2002/18 *Assessment of Reinforced Concrete Building Exterior Joints with Substandard Details.* Chris P. Pantelides, Jon Hansen, Justin Nadauld, and Lawrence D. Reaveley. May 2002.

PEER 2002/17 *Structural Characterization and Seismic Response Analysis of a Highway Overcrossing Equipped with Elastomeric Bearings and Fluid Dampers: A Case Study*. Nicos Makris and Jian Zhang. November 2002.

PEER 2002/16 *Estimation of Uncertainty in Geotechnical Properties for Performance-Based Earthquake Engineering*. Allen L. Jones, Steven L. Kramer, and Pedro Arduino. December 2002.

PEER 2002/15 *Seismic Behavior of Bridge Columns Subjected to Various Loading Patterns*. Asadollah Esmaeily-Gh. and Yan Xiao. December 2002.

PEER 2002/14 *Inelastic Seismic Response of Extended Pile Shaft Supported Bridge Structures.* T.C. Hutchinson, R.W. Boulanger, Y.H. Chai, and I.M. Idriss. December 2002.

PEER 2002/13 *Probabilistic Models and Fragility Estimates for Bridge Components and Systems*. Paolo Gardoni, Armen Der Kiureghian, and Khalid M. Mosalam. June 2002.

PEER 2002/12 *Effects of Fault Dip and Slip Rake on Near-Source Ground Motions: Why Chi-Chi Was a Relatively Mild M7.6 Earthquake*. Brad T. Aagaard, John F. Hall, and Thomas H. Heaton. December 2002.

PEER 2002/11 *Analytical and Experimental Study of Fiber-Reinforced Strip Isolators*. James M. Kelly and Shakhzod M. Takhirov. September 2002.

PEER 2002/10 *Centrifuge Modeling of Settlement and Lateral Spreading with Comparisons to Numerical Analyses***.** Sivapalan Gajan and Bruce L. Kutter. January 2003.

PEER 2002/09 *Documentation and Analysis of Field Case Histories of Seismic Compression during the 1994 Northridge, California, Earthquake*. Jonathan P. Stewart, Patrick M. Smith, Daniel H. Whang, and Jonathan D. Bray. October 2002.

PEER 2002/08 *Component Testing, Stability Analysis and Characterization of Buckling-Restrained Unbonded Braces™*. Cameron Black, Nicos Makris, and Ian Aiken. September 2002.

PEER 2002/07 *Seismic Performance of Pile-Wharf Connections.* Charles W. Roeder, Robert Graff, Jennifer Soderstrom, and Jun Han Yoo. December 2001.

PEER 2002/06 *The Use of Benefit-Cost Analysis for Evaluation of Performance-Based Earthquake Engineering Decisions*. Richard O. Zerbe and Anthony Falit-Baiamonte. September 2001.

PEER 2002/05 *Guidelines, Specifications, and Seismic Performance Characterization of Nonstructural Building Components and Equipment*. André Filiatrault, Constantin Christopoulos, and Christopher Stearns. September 2001.

PEER 2002/04 *Consortium of Organizations for Strong-Motion Observation Systems and the Pacific Earthquake Engineering Research Center Lifelines Program: Invited Workshop on Archiving and Web Dissemination of Geotechnical Data, 4–5 October 2001*. September 2002.

PEER 2002/03 *Investigation of Sensitivity of Building Loss Estimates to Major Uncertain Variables for the Van Nuys Testbed*. Keith A. Porter, James L. Beck, and Rustem V. Shaikhutdinov. August 2002.

PEER 2002/02 *The Third U.S.-Japan Workshop on Performance-Based Earthquake Engineering Methodology for Reinforced Concrete Building Structures*. July 2002.

PEER 2002/01 *Nonstructural Loss Estimation: The UC Berkeley Case Study.* Mary C. Comerio and John C. Stallmeyer. December 2001.

PEER 2001/16 *Statistics of SDF-System Estimate of Roof Displacement for Pushover Analysis of Buildings.* Anil K. Chopra, Rakesh K. Goel, and Chatpan Chintanapakdee. December 2001.

PEER 2001/15 *Damage to Bridges during the 2001 Nisqually Earthquake.* R. Tyler Ranf, Marc O. Eberhard, and Michael P. Berry. November 2001.

PEER 2001/14 *Rocking Response of Equipment Anchored to a Base Foundation.* Nicos Makris and Cameron J. Black. September 2001.

PEER 2001/13 *Modeling Soil Liquefaction Hazards for Performance-Based Earthquake Engineering*. Steven L. Kramer and Ahmed-W. Elgamal. February 2001.

PEER 2001/12 *Development of Geotechnical Capabilities in OpenSees*. Boris Jeremić. September 2001.

PEER 2001/11 *Analytical and Experimental Study of Fiber-Reinforced Elastomeric Isolators*. James M. Kelly and Shakhzod M. Takhirov. September 2001.

PEER 2001/10 *Amplification Factors for Spectral Acceleration in Active Regions.* Jonathan P. Stewart, Andrew H. Liu, Yoojoong Choi, and Mehmet B. Baturay. December 2001.

PEER 2001/09 *Ground Motion Evaluation Procedures for Performance-Based Design.* Jonathan P. Stewart, Shyh-Jeng Chiou, Jonathan D. Bray, Robert W. Graves, Paul G. Somerville, and Norman A. Abrahamson. September 2001.

PEER 2001/08 *Experimental and Computational Evaluation of Reinforced Concrete Bridge Beam-Column Connections for Seismic Performance*. Clay J. Naito, Jack P. Moehle, and Khalid M. Mosalam. November 2001.

PEER 2001/07 *The Rocking Spectrum and the Shortcomings of Design Guidelines.* Nicos Makris and Dimitrios Konstantinidis. August 2001.

PEER 2001/06 *Development of an Electrical Substation Equipment Performance Database for Evaluation of Equipment Fragilities*. Thalia Agnanos. April 1999.

PEER 2001/05 *Stiffness Analysis of Fiber-Reinforced Elastomeric Isolators.* Hsiang-Chuan Tsai and James M. Kelly. May 2001.

PEER 2001/04 *Organizational and Societal Considerations for Performance-Based Earthquake Engineering*. Peter J. May. April 2001.

PEER 2001/03 *A Modal Pushover Analysis Procedure to Estimate Seismic Demands for Buildings: Theory and Preliminary Evaluation*. Anil K. Chopra and Rakesh K. Goel. January 2001.

PEER 2001/02 *Seismic Response Analysis of Highway Overcrossings Including Soil-Structure Interaction*. Jian Zhang and Nicos Makris. March 2001.

PEER 2001/01 *Experimental Study of Large Seismic Steel Beam-to-Column Connections.* Egor P. Popov and Shakhzod M. Takhirov. November 2000.

PEER 2000/10 *The Second U.S.-Japan Workshop on Performance-Based Earthquake Engineering Methodology for Reinforced Concrete Building Structures*. March 2000.

PEER 2000/09 *Structural Engineering Reconnaissance of the August 17, 1999 Earthquake: Kocaeli (Izmit), Turkey*. Halil Sezen, Kenneth J. Elwood, Andrew S. Whittaker, Khalid Mosalam, John J. Wallace, and John F. Stanton. December 2000.

PEER 2000/08 *Behavior of Reinforced Concrete Bridge Columns Having Varying Aspect Ratios and Varying Lengths of Confinement*. Anthony J. Calderone, Dawn E. Lehman, and Jack P. Moehle. January 2001.

PEER 2000/07 *Cover-Plate and Flange-Plate Reinforced Steel Moment-Resisting Connections.* Taejin Kim, Andrew S. Whittaker, Amir S. Gilani, Vitelmo V. Bertero, and Shakhzod M. Takhirov. September 2000.

PEER 2000/06 *Seismic Evaluation and Analysis of 230-kV Disconnect Switches.* Amir S. J. Gilani, Andrew S. Whittaker, Gregory L. Fenves, Chun-Hao Chen, Henry Ho, and Eric Fujisaki. July 2000.

PEER 2000/05 *Performance-Based Evaluation of Exterior Reinforced Concrete Building Joints for Seismic Excitation*. Chandra Clyde, Chris P. Pantelides, and Lawrence D. Reaveley. July 2000.

PEER 2000/04 *An Evaluation of Seismic Energy Demand: An Attenuation Approach*. Chung-Che Chou and Chia-Ming Uang. July 1999.

PEER 2000/03 *Framing Earthquake Retrofitting Decisions: The Case of Hillside Homes in Los Angeles.* Detlof von Winterfeldt, Nels Roselund, and Alicia Kitsuse. March 2000.

PEER 2000/02 *U.S.-Japan Workshop on the Effects of Near-Field Earthquake Shaking*. Andrew Whittaker, Editor. July 2000.

PEER 2000/01 *Further Studies on Seismic Interaction in Interconnected Electrical Substation Equipment.* Armen Der Kiureghian, Kee-Jeung Hong, and Jerome L. Sackman. November 1999.

PEER 1999/14 *Seismic Evaluation and Retrofit of 230-kV Porcelain Transformer Bushings*. Amir S. Gilani, Andrew S. Whittaker, Gregory L. Fenves, and Eric Fujisaki. December 1999.

PEER 1999/13 *Building Vulnerability Studies: Modeling and Evaluation of Tilt-up and Steel Reinforced Concrete Buildings*. John W. Wallace, Jonathan P. Stewart, and Andrew S. Whittaker, Editors. December 1999.

PEER 1999/12 *Rehabilitation of Nonductile RC Frame Building Using Encasement Plates and Energy-Dissipating Devices*. Mehrdad Sasani, Vitelmo V. Bertero, James C. Anderson. December 1999.

PEER 1999/11 *Performance Evaluation Database for Concrete Bridge Components and Systems under Simulated Seismic Loads*. Yael D. Hose and Frieder Seible. November 1999.

PEER 1999/10 *U.S.-Japan Workshop on Performance-Based Earthquake Engineering Methodology for Reinforced Concrete Building Structures*. December 1999.

PEER 1999/09 *Performance Improvement of Long Period Building Structures Subjected to Severe Pulse-Type Ground Motions*. James C. Anderson, Vitelmo V. Bertero, and Raul Bertero. October 1999.

PEER 1999/08 *Envelopes for Seismic Response Vectors.* Charles Menun and Armen Der Kiureghian. July 1999.

PEER 1999/07 *Documentation of Strengths and Weaknesses of Current Computer Analysis Methods for Seismic Performance of Reinforced Concrete Members*. William F. Cofer. November 1999.

PEER 1999/06 *Rocking Response and Overturning of Anchored Equipment under Seismic Excitations*. Nicos Makris and Jian Zhang. November 1999.

PEER 1999/05 *Seismic Evaluation of 550 kV Porcelain Transformer Bushings.* Amir S. Gilani, Andrew S. Whittaker, Gregory L. Fenves, and Eric Fujisaki. October 1999.

PEER 1999/04 *Adoption and Enforcement of Earthquake Risk-Reduction Measures.* Peter J. May, Raymond J. Burby, T. Jens Feeley, and Robert Wood. August 1999.

PEER 1999/03 *Task 3 Characterization of Site Response General Site Categories*. Adrian Rodriguez-Marek, Jonathan D. Bray and Norman Abrahamson. February 1999.

PEER 1999/02 *Capacity-Demand-Diagram Methods for Estimating Seismic Deformation of Inelastic Structures: SDF Systems*. Anil K. Chopra and Rakesh Goel. April 1999.

PEER 1999/01 *Interaction in Interconnected Electrical Substation Equipment Subjected to Earthquake Ground Motions*. Armen Der Kiureghian, Jerome L. Sackman, and Kee-Jeung Hong. February 1999.

PEER 1998/08 *Behavior and Failure Analysis of a Multiple-Frame Highway Bridge in the 1994 Northridge Earthquake*. Gregory L. Fenves and Michael Ellery. December 1998.

PEER 1998/07 *Empirical Evaluation of Inertial Soil-Structure Interaction Effects.* Jonathan P. Stewart, Raymond B. Seed, and Gregory L. Fenves. November 1998.

PEER 1998/06 *Effect of Damping Mechanisms on the Response of Seismic Isolated Structures*. Nicos Makris and Shih-Po Chang. November 1998.

PEER 1998/05 *Rocking Response and Overturning of Equipment under Horizontal Pulse-Type Motions*. Nicos Makris and Yiannis Roussos. October 1998.

PEER 1998/04 *Pacific Earthquake Engineering Research Invitational Workshop Proceedings, May 14–15, 1998: Defining the Links between Planning, Policy Analysis, Economics and Earthquake Engineering*. Mary Comerio and Peter Gordon. September 1998.

PEER 1998/03 *Repair/Upgrade Procedures for Welded Beam to Column Connections*. James C. Anderson and Xiaojing Duan. May 1998.

PEER 1998/02 *Seismic Evaluation of 196 kV Porcelain Transformer Bushings.* Amir S. Gilani, Juan W. Chavez, Gregory L. Fenves, and Andrew S. Whittaker. May 1998.

PEER 1998/01 *Seismic Performance of Well-Confined Concrete Bridge Columns.* Dawn E. Lehman and Jack P. Moehle. December 2000.

PEER REPORTS: ONE HUNDRED SERIES

PEER 2012/103 *Performance-Based Seismic Demand Assessment of Concentrically Braced Steel Frame Buildings.* Chui-Hsin Chen and Stephen A. Mahin. December 2012.

PEER 2012/102 *Procedure to Restart an Interrupted Hybrid Simulation: Addendum to PEER Report 2010/103.* Vesna Terzic and Bozidar Stojadinovic. October 2012.

PEER 2012/101 *Mechanics of Fiber Reinforced Bearings.* James M. Kelly and Andrea Calabrese. February 2012.

PEER 2011/107 *Nonlinear Site Response and Seismic Compression at Vertical Array Strongly Shaken by 2007 Niigata-ken Chuetsu-oki Earthquake.* Eric Yee, Jonathan P. Stewart, and Kohji Tokimatsu. December 2011.

PEER 2011/106 *Self Compacting Hybrid Fiber Reinforced Concrete Composites for Bridge Columns.* Pardeep Kumar, Gabriel Jen, William Trono, Marios Panagiotou, and Claudia Ostertag. September 2011.

PEER 2011/105 *Stochastic Dynamic Analysis of Bridges Subjected to Spacially Varying Ground Motions.* Katerina Konakli and Armen Der Kiureghian. August 2011.

PEER 2011/104 *Design and Instrumentation of the 2010 E-Defense Four-Story Reinforced Concrete and Post-Tensioned Concrete Buildings.* Takuya Nagae, Kenichi Tahara, Taizo Matsumori, Hitoshi Shiohara, Toshimi Kabeyasawa, Susumu Kono, Minehiro Nishiyama (Japanese Research Team) and John Wallace, Wassim Ghannoum, Jack Moehle, Richard Sause, Wesley Keller, Zeynep Tuna (U.S. Research Team). June 2011.

PEER 2011/103 *In-Situ Monitoring of the Force Output of Fluid Dampers: Experimental Investigation.* Dimitrios Konstantinidis, James M. Kelly, and Nicos Makris. April 2011.

PEER 2011/102 *Ground-Motion Prediction Equations 1964–2010.* John Douglas. April 2011.

PEER 2011/101 *Report of the Eighth Planning Meeting of NEES/E-Defense Collaborative Research on Earthquake Engineering.* Convened by the Hyogo Earthquake Engineering Research Center (NIED), NEES Consortium, Inc. February 2011.

PEER 2010/111 *Modeling and Acceptance Criteria for Seismic Design and Analysis of Tall Buildings.* Task 7 Report for the Tall Buildings Initiative - Published jointly by the Applied Technology Council. October 2010.

PEER 2010/110 *Seismic Performance Assessment and Probabilistic Repair Cost Analysis of Precast Concrete Cladding Systems for Multistory Buildlings.* Jeffrey P. Hunt and Božidar Stojadinovic. November 2010.

PEER 2010/109 *Report of the Seventh Joint Planning Meeting of NEES/E-Defense Collaboration on Earthquake Engineering. Held at the E-Defense, Miki, and Shin-Kobe, Japan, September 18–19, 2009.* August 2010.

PEER 2010/108 *Probabilistic Tsunami Hazard in California.* Hong Kie Thio, Paul Somerville, and Jascha Polet, preparers. October 2010.

PEER 2010/107 *Performance and Reliability of Exposed Column Base Plate Connections for Steel Moment-Resisting Frames.* Ady Aviram, Božidar Stojadinovic, and Armen Der Kiureghian. August 2010.

PEER 2010/106 *Verification of Probabilistic Seismic Hazard Analysis Computer Programs.* Patricia Thomas, Ivan Wong, and Norman Abrahamson. May 2010.

PEER 2010/105 *Structural Engineering Reconnaissance of the April 6, 2009, Abruzzo, Italy, Earthquake, and Lessons Learned.* M. Selim Günay and Khalid M. Mosalam. April 2010.

PEER 2010/104 *Simulating the Inelastic Seismic Behavior of Steel Braced Frames, Including the Effects of Low-Cycle Fatigue.* Yuli Huang and Stephen A. Mahin. April 2010.

PEER 2010/103 *Post-Earthquake Traffic Capacity of Modern Bridges in California.* Vesna Terzic and Božidar Stojadinović. March 2010.

PEER 2010/102 *Analysis of Cumulative Absolute Velocity (CAV) and JMA Instrumental Seismic Intensity (I_{JMA}) Using the PEER–NGA Strong Motion Database.* Kenneth W. Campbell and Yousef Bozorgnia. February 2010.

PEER 2010/101 *Rocking Response of Bridges on Shallow Foundations.* Jose A. Ugalde, Bruce L. Kutter, and Boris Jeremic. April 2010.

PEER 2009/109 *Simulation and Performance-Based Earthquake Engineering Assessment of Self-Centering Post-Tensioned Concrete Bridge Systems.* Won K. Lee and Sarah L. Billington. December 2009.

PEER 2009/108 *PEER Lifelines Geotechnical Virtual Data Center.* J. Carl Stepp, Daniel J. Ponti, Loren L. Turner, Jennifer N. Swift, Sean Devlin, Yang Zhu, Jean Benoit, and John Bobbitt. September 2009.

PEER 2009/107 *Experimental and Computational Evaluation of Current and Innovative In-Span Hinge Details in Reinforced Concrete Box-Girder Bridges: Part 2: Post-Test Analysis and Design Recommendations.* Matias A. Hube and Khalid M. Mosalam. December 2009.

PEER 2009/106 *Shear Strength Models of Exterior Beam-Column Joints without Transverse Reinforcement.* Sangjoon Park and Khalid M. Mosalam. November 2009.

PEER 2009/105 *Reduced Uncertainty of Ground Motion Prediction Equations through Bayesian Variance Analysis.* Robb Eric S. Moss. November 2009.

PEER 2009/104 *Advanced Implementation of Hybrid Simulation.* Andreas H. Schellenberg, Stephen A. Mahin, Gregory L. Fenves. November 2009.

PEER 2009/103 *Performance Evaluation of Innovative Steel Braced Frames.* T. Y. Yang, Jack P. Moehle, and Božidar Stojadinovic. August 2009.

PEER 2009/102 *Reinvestigation of Liquefaction and Nonliquefaction Case Histories from the 1976 Tangshan Earthquake.* Robb Eric Moss, Robert E. Kayen, Liyuan Tong, Songyu Liu, Guojun Cai, and Jiaer Wu. August 2009.

PEER 2009/101 *Report of the First Joint Planning Meeting for the Second Phase of NEES/E-Defense Collaborative Research on Earthquake Engineering.* Stephen A. Mahin et al. July 2009.

PEER 2008/104 *Experimental and Analytical Study of the Seismic Performance of Retaining Structures.* Linda Al Atik and Nicholas Sitar. January 2009.

PEER 2008/103 *Experimental and Computational Evaluation of Current and Innovative In-Span Hinge Details in Reinforced Concrete Box-Girder Bridges. Part 1: Experimental Findings and Pre-Test Analysis.* Matias A. Hube and Khalid M. Mosalam. January 2009.

PEER 2008/102 *Modeling of Unreinforced Masonry Infill Walls Considering In-Plane and Out-of-Plane Interaction.* Stephen Kadysiewski and Khalid M. Mosalam. January 2009.

PEER 2008/101 *Seismic Performance Objectives for Tall Buildings.* William T. Holmes, Charles Kircher, William Petak, and Nabih Youssef. August 2008.

PEER 2007/101 *Generalized Hybrid Simulation Framework for Structural Systems Subjected to Seismic Loading*. Tarek Elkhoraibi and Khalid M. Mosalam. July 2007.

PEER 2007/100 *Seismic Evaluation of Reinforced Concrete Buildings Including Effects of Masonry Infill Walls*. Alidad Hashemi and Khalid M. Mosalam. July 2007.

The Pacifi c Earthquake Engineering Research Center (PEER) is a multi-institutional research and education center with headquarters at the University of California, Berkeley. Investigators from over 20 universities, several consulting companies, and researchers at various state and federal government agencies contribute to research programs focused on performance-based earthquake engineering.

These research programs aim to identify and reduce the risks from major earthquakes to life safety and to the economy by including research in a wide variety of disciplines including structural and geotechnical engineering, geology/seismology, lifelines, transportation, architecture, economics, risk management, and public policy.

PEER is supported by federal, state, local, and regional agencies, together with industry partners.

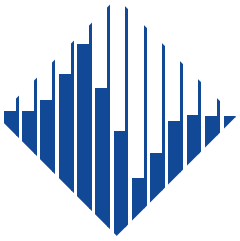

PEER Core Institutions

University of California, Berkeley (Lead Institution)
California Institute of Technology
Oregon State University
Stanford University
University of California, Davis
University of California, Irvine
University of California, Los Angeles
University of California, San Diego
University of Nevada, Reno
University of Southern California
University of Washington

PEER reports can be ordered at https://peer.berkeley.edu/peer-reports or by contacting

Pacific Earthquake Engineering Research Center
University of California, Berkeley
325 Davis Hall, Mail Code 1792
Berkeley, CA 94720-1792
Tel: 510-642-3437
Email: peer_center@berkeley.edu

ISSN 2770-8314
https://doi.org/10.55461/LIEN3652